

ANISOTROPIC SWELLING CHARACTERISTICS  
OF COMPACTED CLAY

By

VENKATRAMAN SRINIVASAN

Bachelor of Engineering  
Annamalai University  
Madras, India  
1955

Master of Science  
University of Madras  
Madras, India  
1962

Submitted to the Faculty of the Graduate College  
of the Oklahoma State University  
in partial fulfillment of the requirements  
for the Degree of  
DOCTOR OF PHILOSOPHY  
July, 1970

OKLAHOMA  
STATE UNIVERSITY  
LIBRARY  
OCT 28 1970

ANISOTROPIC SWELLING CHARACTERISTICS  
OF COMPACTED CLAY

Thesis Approved:

*J. V. Parcher*  
\_\_\_\_\_  
Thesis Adviser

*R. L. Jones*  
\_\_\_\_\_

*Arthur W. Reed*  
\_\_\_\_\_

*Mr. Donald Hardy*  
\_\_\_\_\_

*James M. Wilson*  
\_\_\_\_\_

*D. Durham*  
\_\_\_\_\_  
Dean of the Graduate College

763668

DEDICATED

TO MY PARENTS

For their guidance, understanding and sacrifice.

## ACKNOWLEDGEMENTS

The author takes this opportunity to express his sincere appreciation and gratitude to Dr. James V. Parcher, Thesis Adviser and Chairman of the Advisory Committee, for his invaluable counsel, guidance and encouragement throughout the entire progress of this research.

Sincere appreciation is extended to Drs. M. A. Hady, R. L. Janes, L. W. Reed, and J. M. Davidson, Committee Members, for their interest, advice and assistance.

The author is grateful to Mr. W. H. Batten, Jr., Tulsa, for preparing the thin sections for X-ray diffraction study; and to Mr. W. H. Bellis and Mrs. Linda Hare, both of Geology Department, University of Oklahoma, Norman Campus, for preparing the scanning electron micrographs.

The author expresses his gratitude to the Office of Engineering Research and the School of Civil Engineering for the financial support and assistance which made this study possible; and to the Watumull Foundation, Honolulu, Hawaii, for the grant-in-aid which enabled the completion of this work.

The author is grateful to Mr. D. Dakshinamurty, for his assistance in the laboratory work; Mr. C. K. Panduranga Rao, for his advice in the computer analysis; and to Mr. Samuel Ng, for his assistance in the photographic work.

The author wishes to thank his wife, Sakunthala, for her assistance in the preparation of the manuscript and encouragement during the course of this study.

Sincere appreciation is extended to Mr. Eldon Hardy for his assistance in preparing the illustrations; and to Mrs. Linda Ahsmuhs for her excellent work in typing the final manuscript.

July, 1970

V. Srinivasan

## TABLE OF CONTENTS

Chapter	Page
I. INTRODUCTION . . . . .	1
General . . . . .	1
Purpose and Scope of Study . . . . .	3
Source of Material . . . . .	5
II. LITERATURE REVIEW . . . . .	7
Origin, Composition and Structure of Clays . . . . .	7
Physico-Chemical Aspects . . . . .	13
Theories of Soil Swelling . . . . .	21
Factors Affecting Swelling . . . . .	24
Structural Damages Caused by Swelling . . . . .	47
III. EXPERIMENTAL PROCEDURES . . . . .	50
Physical Properties . . . . .	50
Triaxial Swelling Tests . . . . .	53
General . . . . .	53
Description of Apparatus . . . . .	53
Preparation of Test Specimens . . . . .	57
Preparation of Flanged Membranes . . . . .	62
Apparatus Factors . . . . .	63
Test Procedure . . . . .	69
Data and Discussion . . . . .	73
Soil Fabric Analysis . . . . .	115
General . . . . .	115
X-ray Diffraction Study . . . . .	119
Introduction . . . . .	119
Preparation of Thin Sections . . . . .	121
Test Procedure . . . . .	122
Data and Discussion . . . . .	123
Scanning Electron Microscope Study . . . . .	137
Introduction . . . . .	137
Preparation of Test Specimens . . . . .	139
Test Procedure . . . . .	140
Data and Discussion . . . . .	141

Chapter	Page
IV. GENERAL ANALYSIS . . . . .	148
Introduction . . . . .	148
Swelling Characteristics . . . . .	148
Soil Structure . . . . .	150
Effect of Soil Structure on Swelling . . . . .	151
V. CONCLUSIONS AND RECOMMENDATIONS . . . . .	154
Conclusions . . . . .	154
Recommendations for Further Research . . . . .	157
A SELECTED BIBLIOGRAPHY . . . . .	159
APPENDIX A - DERIVATION OF EXPRESSIONS FOR THE ANALYSIS OF SWELLING TEST DATA . . . . .	166
APPENDIX B - EXPRESSIONS FOR THREE-DIMENSIONAL ANISOTROPIC SWELLING . . . . .	175

LIST OF TABLES

Table	Page
I. Details of Kaolinite, Montmorillonite and Illite (Adapted after Grim, 1968 and Lambe and Whitman, 1969) . . . . .	14
II. Physical Properties of Permian Clay . . . . .	51
III. Definitions Relating to Triaxial Swelling Test . . . . .	74
IV. Details of Test Specimens - Standard AASHO Compaction . . . . .	76
V. Details of Test Specimens - Modified AASHO Compaction . . . . .	78
VI. Summary of Swelling Test Data - Standard AASHO Compaction . . . . .	87
VII. Summary of Swelling Test Data - Modified AASHO Compaction . . . . .	89
VIII. Swelling Ratios for Compacted Soil - Standard AASHO Compaction . . . . .	107
IX. Swelling Ratios for Compacted Soil - Modified AASHO Compaction . . . . .	109
X. X-ray Diffraction Peak Intensity Ratios - Standard AASHO Compaction . . . . .	133
XI. X-ray Diffraction Peak Intensity Ratios - Modified AASHO Compaction . . . . .	134



## LIST OF FIGURES

Figure	Page
1. Schematic Diagram Showing Single Units and Sheet Structures of Silica Tetrahedron and Aluminum or Magnesium Octahedron (after Grim, 1968) . . . . .	10
2. Structure of Clay Mineral Groups: (a) Kaolinite; (b) Illite; (c) Montmorillonite (after Grim, 1968) . . . . .	11
3. Variation of Ion Concentration in Solution With Distance From the Surface of a Clay Particle (after Rose, 1966) . . . . .	17
4. Theoretical Distribution of Ions at a Charged Surface: (a) Influence of Valence on Thickness of Double Layer; (b) Influence of Salt Concentration on Cation and Anion Distribution (after Yong and Warkentin, 1966) . . . . .	18
5. Curves of Repulsion, Attraction and Net Force Between two Parallel, Closely Spaced Surfaces, as a Function of Distance Between Surfaces and Electrolyte Concentration (after Scott, 1963) . . . . .	20
6. Relationship Between Percentage of Swell and Percentage of Clay Sizes for Experimental Soils (after Seed, Woodward and Lundgren, 1962) . . . . .	29
7. Orientation Versus Water Content for Boston Blue Clay (after Lambe, 1960) . . . . .	32
8. Effect of Compaction on Soil Structure (after Lambe, 1960) . . . . .	32
9. Swelling-Time Curves, Kneading Compaction, Soil B2 (after Parcher and Liu, 1965) . . . . .	35
10. Swelling-Time Curves, Kneading and Static Compaction, Soil B2 (after Parcher and Liu, 1965) . . . . .	35
11. Effect of Initial Water Content on Swelling, Soil B2 (after Parcher and Liu, 1965) . . . . .	36
12. Effect of Compaction Energy on Swelling, Soil A (after Parcher and Liu, 1965) . . . . .	37

Figure	Page
13. Swelling Ratio-Time Curves, Kneading Compaction, Soil B2 (after Parcher and Liu, 1965) . . . . .	38
14. Effect of Anisotropy on the Swelling and Swell Pressure on Compacted Clay (after Komornik and Livneh, 1967) . . . . .	39
15. Compaction-Permeability Tests on Jamaica Sandy Clay (after Lambe, 1960) . . . . .	43
16. Compaction-Permeability Tests on Siburua Clay (after Lambe, 1960) . . . . .	43
17. Sediment Structures (after Lambe, 1960) . . . . .	46
18. Swelling-Time Curves for Undisturbed and Compacted States, Soil B1 (after Parcher and Liu, 1965) . . . . .	46
19. Grain-Size Distribution Curve for Permian Clay . . . . .	52
20. Moisture-Density Curves for Permian Clay . . . . .	54
21. Details of Triaxial Swelling Apparatus (after Parcher and Liu, 1965) . . . . .	55
22. Parts of Triaxial Swelling Apparatus . . . . .	56
23. Test Assembly of Six Triaxial Swelling Apparatuses . . . . .	56
24. Location of Test Specimen in Compacted Soil Block . . . . .	59
25. Designation of Test Specimens . . . . .	60
26. Water Absorptivity Curves for Plexiglas With Smooth and Rough Surfaces . . . . .	64
27. Water Absorptivity Curves for Plexiglas (after Liu, 1964) . . . . .	66
28. Restraints to Free Swelling of Soil Specimen in Triaxial Swelling Apparatus . . . . .	68
29. Time Period Required for Swelling for Specimens With and Without Filter Strips (after Liu, 1964) . . . . .	72
30. Swelling-Time Curves for Oriented Specimens - Standard AASHO Compaction . . . . .	80
31. Swelling-Time Curves for Oriented Specimens - Modified AASHO Compaction . . . . .	81

Figure	Page
32. Swelling-Time Curves for Vertical Specimens at Different Initial Moisture Contents - Standard AASHO Compaction . . . . .	82
33. Swelling-Time Curves for Horizontal Specimens at Different Initial Moisture Contents - Standard AASHO Compaction . . . . .	83
34. Swelling-Time Curves for Vertical Specimens at Different Initial Moisture Contents - Modified AASHO Compaction . . . . .	84
35. Swelling-Time Curves for Horizontal Specimens at Different Initial Moisture Contents - Modified AASHO Compaction . . . . .	85
36. Relationship Between Volume Increase and Water Intake . . . . .	92
37. Initial and Final Degrees of Saturation for Standard AASHO Specimens . . . . .	94
38. Initial and Final Degrees of Saturation for Modified AASHO Specimens . . . . .	95
39. Effect of Compactive Energy on the Final Moisture Content After Swelling . . . . .	96
40. Relationship Between Volumetric Swelling and Initial Moisture Content - Standard and Modified AASHO Compaction . . . . .	98
41. Moisture Content Variation in Test Specimens After Swelling . . . . .	99
42. Definition Diagram for Swelling Ratio of Compacted Soil . . . . .	101
43. Particle Arrangement in Oriented Specimens in an Ideal Disperse System . . . . .	103
44. Effect of Initial Moisture Content on Unit Swelling-Standard AASHO Compaction . . . . .	105
45. Effect of Initial Moisture Content on Unit Swelling-Modified AASHO Compaction . . . . .	106
46. Effect of Initial Moisture Content on Swelling Ratio - Standard AASHO Compaction . . . . .	112
47. Effect of Initial Moisture Content on Swelling Ratio - Modified AASHO Compaction . . . . .	113

Figure	Page
48. X-ray Diffraction Pattern for Thin Section Parallel to Compaction Direction - Standard AASHO Compaction . . . . .	124
49. X-ray Diffraction Pattern for Thin Section Perpendicular to Compaction Direction - Standard AASHO Compaction . . . . .	125
50. X-ray Diffraction Pattern for Thin Section Parallel to Compaction Direction - Modified AASHO Compaction . . . . .	126
51. X-ray Diffraction Pattern for Thin Section Perpendicular to Compaction Direction - Modified AASHO Compaction . . . . .	127
52. X-ray Diffraction Pattern for a Typical Powder Sample (Minus 40 Fraction) . . . . .	129
53. X-ray Diffraction Pattern for a Typical Slurry Sample (Minus 325 Fraction) . . . . .	130
54. Relationship Between Initial Moisture Content and Peak Intensity Ratio . . . . .	136
55. Electron Micrograph for Face Inclined at 135 Degrees to Compaction Direction in Specimen B 14- 45- 1: (a) 600x; (b) 1800x . . . . .	142
56. Electron Micrograph for Specimen B 15- 0- 1; (a) Face Parallel to Compaction Direction, 540x; (b) Face Perpendicular to Compaction Direction, 1440x . . . . .	143
57. Electron Micrograph for Specimen B 17- 0- 1: (a) Face Parallel to Compaction Direction, 1800x; (b) Face Perpendicular to Compaction Direction, 1200x . . . . .	144
58. Relationship Between Swelling Ratio and Peak Intensity Ratio . . . . .	153
59. Swelling of a Cylindrical Soil Specimen . . . . .	169
60. Schematic Representation of Three-Dimensional Anisotropic Swelling of Soil . . . . .	177

## CHAPTER I

### INTRODUCTION

#### General

The detrimental effects to structures caused by the swelling of clay soils have been well documented over the years. Published literature indicate that structural damages have arisen from the swelling of both undisturbed and remolded clays. Numerous studies have been conducted in the past, to investigate the swelling characteristics of expansive soils with a view to identify those soils which are likely to possess undesirable expansive characteristics and to facilitate taking of adequate precautions in constructions where such soils are encountered (Holtz and Gibbs, 1956; Bruijin, 1961; Seed, Woodward and Lundgren, 1962 and others).

The swelling of clay soils is known to affect their engineering properties such as strength, compressibility and permeability, although the exact nature of its influence is not completely understood. Advances in the fields of colloid and crystal chemistry have greatly improved our understanding of the various electrical forces acting between atoms. It has been shown that the engineering properties of clay soils such as strength, compressibility, swelling and other phenomena, can be explained in terms of the physico-chemical interactions between the finer fractions of the soil, although complete theoretical formulations of these processes have not been successful, owing to the extreme complexity

of the problems involved.

The magnitudes of swelling and swell pressure depend on the composition of the clay, initial moisture content, compaction conditions, soil structure, chemical properties of the pore fluid, confining pressure, time allowed for swelling, curing period and temperature (Grim, 1959; Lambe, 1960; Seed, Woodward and Lundgren, 1962; Seed and Chan, 1961; Ladd, 1959; Barber, 1956 and others). Further, experience as well as experimental data indicate that there is considerable difference in the behavior of undisturbed and remolded clays. Remolding tends to produce a parallel orientation of the particles which often results in a marked difference between the undisturbed and remolded engineering properties (Mitchell, 1956 and Lambe, 1960). The molding water content and the mode of compaction have an influence on the particle arrangement of the compacted soil (Lambe, 1960). Recent advances in the techniques for studying the soil structure, using the petrographic microscope, X-ray diffractometer and electron microscope, have greatly contributed to an understanding of the fabric of clays and its relation to engineering properties (Mitchell, 1956; Pacey, 1956; Tice, 1967 and others).

Most of the reported structural damages caused by swelling were attributed to the vertical component of swelling. However, there were instances where the damage was almost certainly caused by the horizontal swelling of soil (Means, 1959). Recent studies show that the rearrangement of particles during compaction produces measurable effects on the swelling characteristics of soil. It is reported that the unit swelling in the horizontal direction of a Permian clay from Oklahoma invariably exceeds that in the vertical direction, regardless of the mode of

compaction. The full implications of this observed behavior in terms of soil structure are not clear. Also the exact relationship between the vertical and horizontal swelling of compacted soil and its correlation to the particle arrangement, have not been completely established. Recent studies have, however, demonstrated the influence of soil structure on the engineering characteristics of soil and shown that a clearer understanding of the physico-chemical interactions associated with the structural anisotropies in soils would eventually lead to new appraisals of the factors affecting strength, swelling and other properties (Mitchell, 1956; Lambe, 1960; Seed and Chan, 1961; Parcher and Liu, 1965; and others).

#### Purpose and Scope of Study

This investigation was primarily concerned with the anisotropic swelling characteristics of compacted clay and their relationship to the soil fabric.

The purpose of this study was two-fold: The first objective was to investigate the relative magnitudes of swelling of compacted Permian clay in two directions, namely parallel and perpendicular to the direction of compaction and to examine the relationship between the two, as a function of the initial water content and compactive effort. Soil blocks at different moisture contents were compacted using the Standard and Modified AASHTO procedures and test specimens were cut out of these soil blocks at the required orientations. These specimens were tested in the triaxial swelling apparatus, developed by Fost (1962) under the direction of Professor James V. Parcher of the Oklahoma State University. The unit swelling of the specimens in the vertical and horizontal

(radial) directions were determined from the swelling test data. Additional information concerning volumetric swelling and water-intake of the specimens, obtained from the swelling tests, was used to study the other characteristics associated with the swelling phenomenon. Based on the experimental data, the relationship between the magnitudes of unit swelling, parallel and perpendicular to the direction of compaction, as a function of the initial moisture content and the compactive effort, was examined.

The second objective was to study the micro-structure of the compacted soil, parallel and perpendicular to the direction of compaction, in an attempt to correlate the particle orientation with the variations in the measured swelling. To study the particle orientation in the compacted soil, the X-ray diffractometer and the scanning electron microscope were used. For X-ray diffraction studies, thin sections were prepared from the compacted soil blocks, parallel and perpendicular to the direction of compaction, using standard impregnation procedures to keep the soil fabric undisturbed during subsequent sectioning process. X-ray diffraction patterns were obtained for the oriented thin sections. From the peak intensity counts, the degree of preferred particle orientation was examined. For the scanning electron microscope study, soil specimens which were previously impregnated for making thin sections for X-ray diffraction analysis, were used. Faces parallel and perpendicular to the direction of compaction in these impregnated soil specimens were shadowed in a vacuum, using a gold-palladium alloy wire as ionizing material. Electron micrographs of these coated faces were made from which a qualitative study of the degree of preferred particle orientation with respect to the direction of compaction, was



made. Based on the X-ray diffraction data and the electron micrographs, an attempt was made to correlate the observed swelling of the compacted soil parallel and perpendicular to the direction of compaction, with the degree of particle orientation in the corresponding directions.

#### Source of Material :

The soil used in this study is the red clay occurring in extensive formations in Oklahoma and in the western parts of Kansas and Texas. These formations, comprising intermingled layers of sandstones and clays, were deposited during the Permian period in the geological history. The eastern edge of out-crop of this Permian formation runs north-south about thirty miles east of Oklahoma City. The surface soil east of this boundary consists of the older Pennsylvanian and Mississippian deposits. The red bed deposits of Permian period occurring on the surface, west of this boundary grow thicker toward the west until near the west edge of Oklahoma. Further west, these beds are covered by younger deposits of Mesozoic age and later periods.

This Permian red bed is a marine clay, formed on an inland seabed surrounded by steep mountains which were subsequently levelled off by erosion. The presence of extensive gypsum and salt deposits in this area is believed to substantiate this view. One main feature of these formations is that, unlike other marine clays, they include a good amount of coarser fractions, suggesting the possibility of a steep and short drainage path into the area during their formation.

The climatic conditions prevailing in this area consist of alternating dry and wet periods. Consequently, the surface clays are

subjected to cycles of desiccation and saturation, which result in an appreciable variation in their physical properties. Structures erected on these overconsolidated desiccated clays have suffered extensive damage because of the expansion of the clays upon increase in water content.

## CHAPTER II

### LITERATURE REVIEW

#### Origin, Composition and Structure of Clays

Soils are the products of the natural process of weathering which involves the disintegration of rocks and decomposition of organic matter through the action of physical or mechanical and chemical agents. This weathering process is controlled by many factors, each of which has a decisive influence on the nature of the soils formed. Mechanical weathering is generally considered responsible for the formation of the coarser fractions of soil. However, the finer fractions of soil are almost certainly produced by the action of chemical weathering, involving processes of solution, recombination and crystallization and hence these, unlike the products of mechanical weathering, do not possess the crystalline nature of the minerals of the parent rock. These fine particles are generally called clays and there is considerable evidence to show that these exist in size ranges less than about  $2\mu$ .

Until recently there was no consensus among soil scientists concerning the exact nature of the clay materials. Early ideas about the composition and structure of the clays ranged from a single mineral concept to a basic colloid complex of amorphous nature and to many others (Grim, 1968). Recognizing the inconsistencies involved in these approaches as revealed by the wide structural variations in the finest

fractions, many scientists, by 1920, began to think of clay materials as essentially composed of extremely small particles of a limited number of crystalline minerals. Although this formed the basis for the present day clay-mineral concept, it lacked positive evidence, and it was only in 1923 that the first X-ray diffraction data of clay materials confirmed this hypothesis. The subsequent investigations into the optical properties of clay minerals by Ross and Shannon (1926), Marshall (1930, 1931) and many others corroborated the crystalline nature of the clay minerals.

According to this concept, clays are essentially composed of very small crystalline particles of one or more members of a small group of minerals, known as clay minerals. These clay minerals are hydrous aluminum silicates with magnesium or iron proxying wholly or in part for the aluminum in some minerals and for alkalies and alkaline earths in others. The fine fraction may also include non-clay minerals like quartz, feldspar, calcite, organic matter and water-soluble salts.

There are many minerals which are ordinarily classified as clay minerals. Grim (1968) has given an elaborate discussion concerning their composition and structure. However three classes of clay minerals, namely, Kaolinite, Montmorillonite (belonging to the Smectite group, according to Grim, 1968) and Illite deserve major consideration.

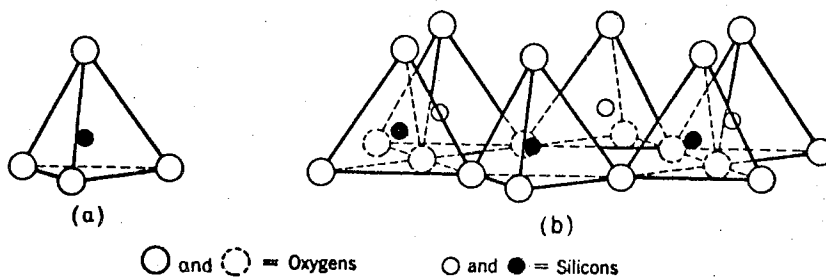
The nature of clay mineral formed, seems, in general, to depend on factors other than the chemical nature of the parent material. Provided the necessary basic minerals are present, kaolinites tend to be formed in an acid environment with good drainage conditions while the development of montmorillonites and illites depends on an alkali environment with poor drainage conditions. Other conditions favorable

for the formation of clay minerals have also been recognized.

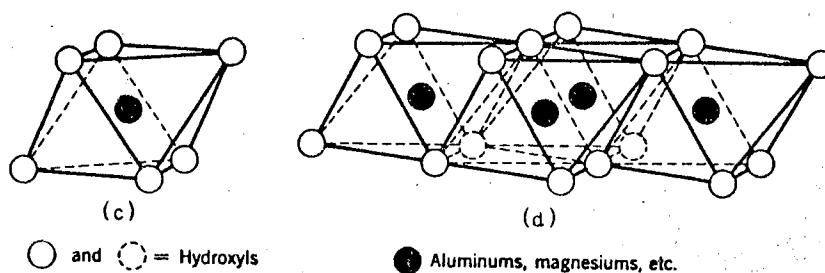
Soils occurring in nature are extremely complex and they vary widely not only in their composition and texture but also in their physical properties. Though they include particles in all size ranges, only the finer fractions which are primarily composed of clay minerals, are responsible for many of the foundation problems. In fact it is the nature and the amount of clay minerals present in a soil that largely governs its physical and engineering behavior.

Based on the generalizations of Pauling for the structure of micas and other layered minerals, the atomic structures of clay minerals have been investigated in considerable detail by many scientists and it is now known that they are mainly composed of two structural units (Figure 1). One unit consists of two sheets of closely packed oxygens or hydroxyls with aluminum, magnesium or iron atoms embedded in an octahedral coordination, equidistant from the six oxygens or hydroxyls. The other unit consists of a silicon atom surrounded by four equidistant oxygens arranged in tetrahedral coordination, with three oxygens at the corners of the base of the tetrahedron, shared by two silicons of adjacent units. These silica tetrahedral sheets are arranged in a hexagonal network which is repeated indefinitely. Although appreciable distortion of these units is possible, these constitute the fundamental building blocks of most of the clay minerals.

Kaolinites consist of repeating layers of a single alumina sheet and a single silica sheet sharing a layer of oxygen atoms between them (Figure 2). There is usually very little substitution within the crystal lattice. Variations in the crystal lattice give rise to different clay minerals with the same chemical composition. The repeating layers



- a. A SINGLE SILICA TETRAHEDRON
- b. SHEET STRUCTURE OF SILICA TETRAHEDRONS  
ARRANGED IN A HEXAGONAL NETWORK



- c. A SINGLE OCTAHEDRAL UNIT
- d. SHEET STRUCTURE OF OCTAHEDRAL UNITS

Figure 1. Schematic Diagram Showing Single Units and Sheet Structures of Silica Tetrahedron and Aluminum or Magnesium Octahedron (after Grim, 1968).

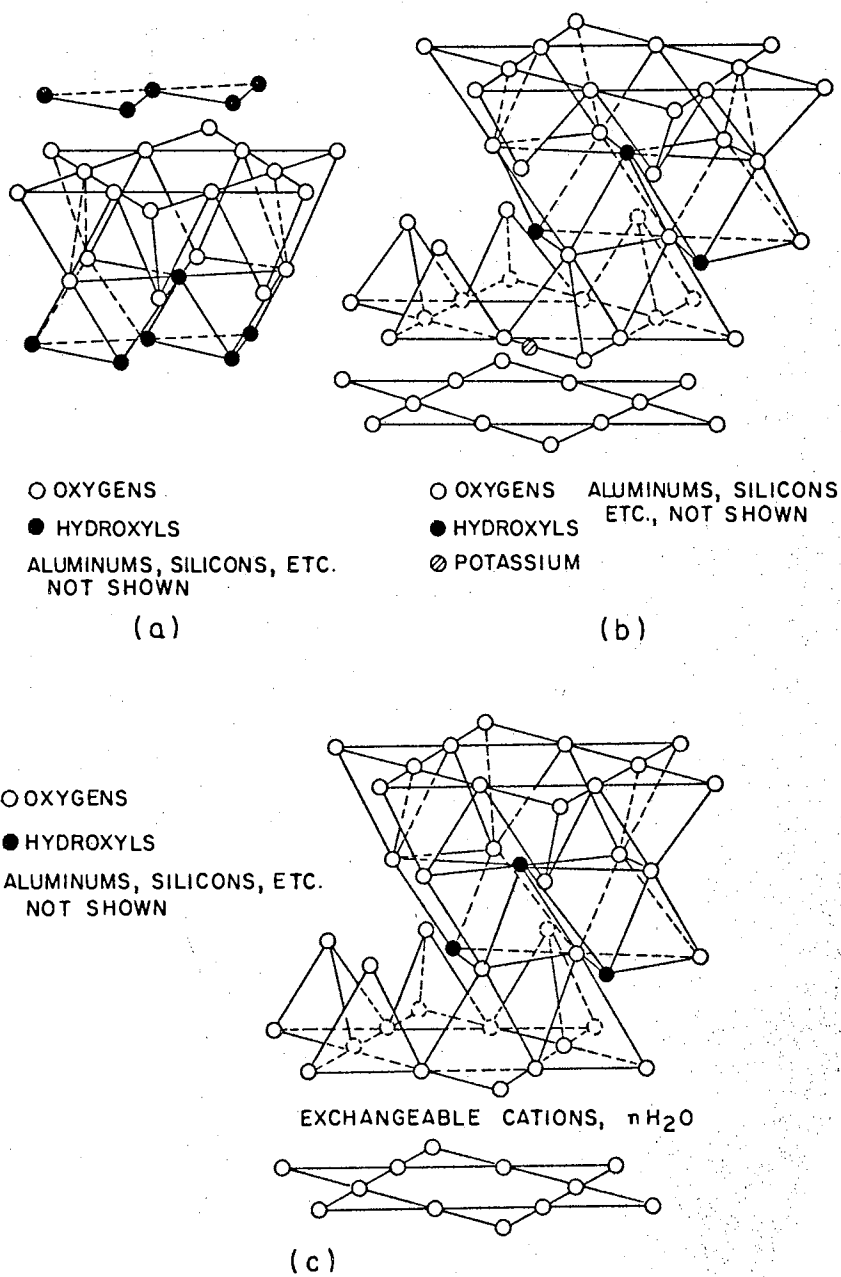


Figure 2. Structure of Clay Mineral Groups:  
 (a) Kaolinite; (b) Illite;  
 (c) Montmorillonite (after Grim,  
 1968).

are approximately 7 Å thick and are held together by hydrogen bonds. Although indefinite extension of these sheets is possible, they usually occur as hexagonal plates. Another commonly occurring mineral, halloysite, differs from kaolinite in that it occurs in a hydrated form, with a layer of water molecules between them and this results in a distorted lattice in the form of a tube-like particle, with the silica sheet on the outside.

The montmorillonite minerals are made of repeating layers of an alumina sheet sandwiched between two silica sheets. Isomorphous substitutions usually occur in the alumina sheet, with magnesium or iron substituting for aluminum. The outstanding feature of this mineral is that the bond between the unit layers is very weak and hence water and other polar molecules can easily enter between them resulting in the expansion of the lattice in the direction of the C-axis. The thickness of the unit layer is therefore not fixed and it varies from about 9.6 Å when there are no polar molecules between the unit layers to almost complete separation of the layers. This explains the marked shrinkage and swelling characteristics of clays containing an appreciable amount of montmorillonite mineral. Also the very poor bonding between adjacent layers causes disintegration into very fine particles.

Illites are similar to montmorillonites in their structure except that the silica sheets are joined by a layer of potassium ions, providing a fairly good bond. The unit layer in illite mineral is about 10 Å thick. There is considerable substitution for silicon by aluminum atoms, in the silica sheet and the resultant charge deficiency is balanced by the potassium ions. The bonds with the nonexchangeable potassium ions are weaker than the hydrogen bonds between the unit layers of



the kaolinite crystal, but they are much stronger than the ionic bonds in the montmorillonite crystal. Consequently the structural unit layers of illites are fairly stable and therefore not as susceptible to lattice expansion as are montmorillonites. However they exhibit more swelling than kaolinites.

Details of the shape, size, specific surface and the charge on the clay minerals, are summarized in Table I.

Only a very brief outline of the basic structure of the important clay minerals has been presented here. For a more complete information regarding the structure of clay minerals and their polymorphs, the reader should refer to standard texts on clay mineralogy (for example, Grim, 1968).

#### Physico - Chemical Aspects

Clays are generally composed of plate-like or tabular particles because the layer-lattice structure results in strong bonding along two axes but weak bonding between layers. The particles are usually hydrated and carry a net negative charge resulting from the substitution of one ion for another in their lattice and incomplete charge compensation arising from broken bonds at the edges. In an electrolyte solution, this net charge is neutralized by the cations and the ability of the clay particles to adsorb ions on their surface is known as the Base or Cation exchange capacity. In soils, a cation adsorbed on the surface of the soil mineral is exchanged for a cation in the pore solution and in this process the pore solution also undergoes a change in its ion concentration.

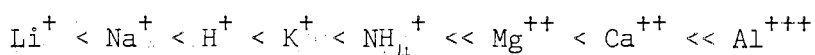
TABLE I

## DETAILS OF KAOLINITE, MONTMORILLONITE AND ILLITE

(Adapted after Grim, 1968 and Lambe and Whitman, 1969)

Clay Mineral	Isomorphous Substitutions	Bonds between Sheets	Specific Surface $m^2/g$	Exchange Capacity (pH 7) me/100g	Particle Shape and Size
Kaolinite	Al for Si 1 in 400	Hydrogen bond and secondary valence	10-20	3-15	Platy d=0.3-3 $\mu$ t=0.3-0.1 d
Montmorillonite	Mg for Al 1 in 6	Secondary valence and exchangeable ion linkage	800	80-150	Platy d=0.1-1 $\mu$ t=0.01 d
Illite	Al for Si 1 in 7 Mg, Fe for Al Fe, Al for Mg	Secondary valence and potassium linkage	80-100	10-40	Platy d=0.1-2 $\mu$ t=0.1 d

The base exchange capacity of a clay mineral is dependent on the charge deficiency resulting from substitutions within the clay lattice and also on the number of broken bonds on the surface of the particle, that is on the size of the clay particle. In soils, the predominant exchangeable cations are usually calcium and magnesium. Potassium and sodium are sometimes found in small quantities. The nature of exchangeable ions in soils is governed by geological environment and leaching conditions. For example, soils deposited in sea water will have calcium and magnesium as exchangeable ions while soils that have been subjected to considerable leaching will have aluminum and hydrogen. The valence of the cation has an important influence on the exchange capacity. The higher the valence of a cation the greater is its replacing power and generally the harder it is to replace. It is known that, in general, for ions of the same valence, increasing ion size increases its replacing power. Another factor influencing the replacing power of ions, is their geometric fit in the clay mineral structure. In general, the replacing power of cations is in the following ascending order:



The theory of soil swelling based on the physico-chemical interactions in the clay-water system is based on the diffuse double layer theory, first given by Gouy and Chapman and which was subsequently modified by Stern. According to this theory, an electric double layer forms at the interface of any phase in contact with a liquid. When a clay particle is placed in water, the electrical force between negatively charged surface and the positively charged ions attracts the cations

to the surface, but their thermal energy causes them to diffuse away. The resultant effect of the Coulomb force of attraction and the thermal diffusion produces a diffuse distribution of cations, with a high concentration of cations at the particle surface and decreasing gradually with distance (Figure 3). The above model gives rise to the Gouy-Chapman diffuse double layer concept and this was subsequently modified by Stern, who postulated a fixed adsorbed ionic layer.

The theoretical distribution of ions at a negatively charged surface was investigated by Gouy and Chapman, based on Poisson-Boltzmann equations and the resulting equation for cation is given by:

$$n_+ = n_0 (\coth 0.16 z\sqrt{c_0} x)^2$$

where

$n_+$  = number of cations per unit volume at any distance  
 $x$  from surface,

$n_0$  = number of cations per unit volume in the pore water  
away from the influence of the surface,

$z$  = valence of cations,

$c_0$  = concentration of cations in moles/liter away from  
the influence of the surface, and

$x$  = distance from surface in Angstrom.

The influence of valence on the thickness of diffuse double layer and the effect of salt concentration on cation and anion distribution are shown in Figure 4. It can be observed that lower concentration and valence would result in an extended diffuse layer and greater force of repulsion.

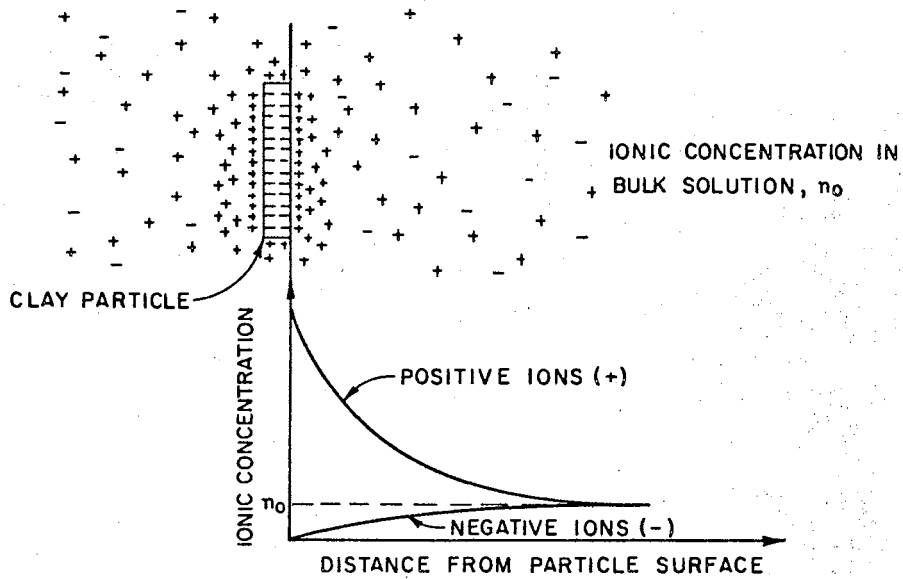


Figure 3. Variation of Ion Concentration in Solution With Distance From the Surface of a Clay Particle (after Rose, 1966).

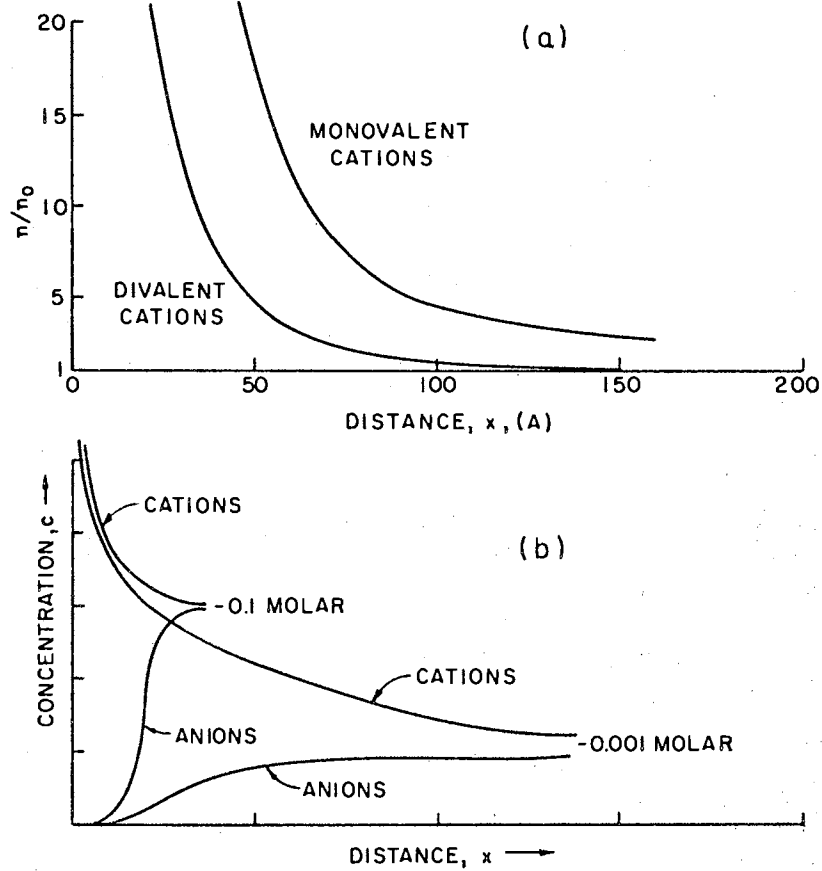


Figure 4. Theoretical Distribution of Ions at a Charged Surface: (a) Influence of Valence on Thickness of Double Layer; (b) Influence of Salt Concentration on Cation and Anion Distribution (after Yong and Warkentin, 1966).

If two clay particles in a suspension are considered with their flat surfaces parallel to each other, then diffuse double layers will be developed around each particle and they will not interfere with each other if the particles are farther apart than the thickness of the double layer. However, if the particles are very close, their diffuse double layers overlap. And as the ions in the double layers are of the same sign, interaction between them gives rise to a repulsive force between the particles. The swelling of a clay is the cumulative effect of the interaction between overlapping double layers around the clay particles and adsorption of water by the clay particles. Theoretical expression for the distribution of cations between two parallel charged plates, neglecting anion concentration, was derived by Langmuir (1938). Using similar analytical models, Yong and Warkentin (1966) and van Olphen (1963) have investigated the mechanism of swelling and this aspect is discussed further elsewhere.

The net force acting between two parallel plates is however the resultant of the repulsive force which is Coulombic in character and the Van der Waals - London attractive force existing between molecules (Figure 5). The repulsion resulting from the interpenetration of double layers will be greatest with monovalent exchangeable ions and with distilled water in the pores. The flocculation and dispersion of clay suspension are the direct consequence of the interactions between the double layers (Rose, 1966).

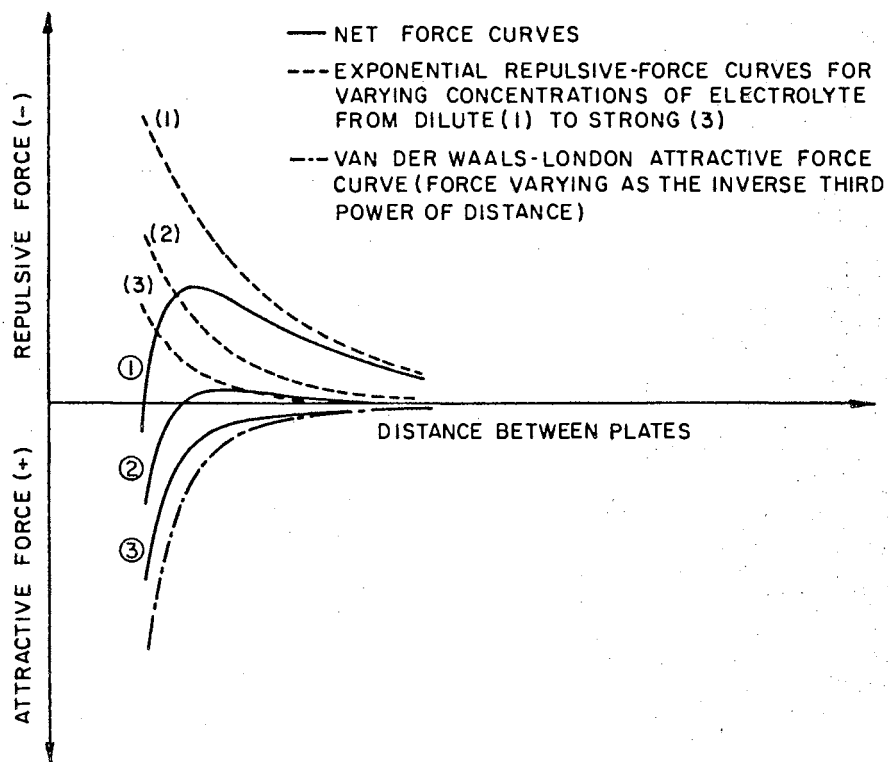


Figure 5. Curves of Repulsion, Attraction and Net Force Between two Parallel, Closely Spaced Surfaces, as a Function of Distance Between Surfaces and Electrolyte Concentration (after Scott, 1963).



## Theories of Soil Swelling

Expansive soils occur in many parts of the world and the volume changes associated with such soils have caused considerable damage to structures. It is not surprising, therefore, that the swelling characteristics of clays have been the subject of considerable investigation in the past. As a result, several theories have been advanced to explain the swelling phenomenon in soils. According to Terzaghi (1931), Katz was the first to recognize the importance of the physico-chemical factors in soil swelling. Katz investigated the relationship between swell-pressure, heat of swelling, relative vapor pressure and volume contraction and attributed the swelling entirely to physico-chemical factors. However, Terzaghi, differing from this view, pointed out that, although the importance of physico-chemical aspects is increased in fine disperse systems, purely physical factors like porosity, elasticity, capillary force, permeability and hydrostatic pressure do have a decisive influence on the swelling. He concluded that the swelling is due to elastic expansion caused by a lowering of the capillary pressure, and the physico-chemical interactions within the system influence the swelling process only by altering the elastic properties of the system. Lambe and Whitman (1959) developed physical concepts to explain the swelling in terms of the effective stress. More recently, Tsyтовich, Zaretsky and Ter-Martirosyan (1967) proposed a mathematical solution for the linear swelling of an unsaturated clay. They divided the wetting process into two stages: the first stage consisting of the water intake by the soil voids with the development of negative effective pressure and the second stage consisting of imbibition by the

mineral aggregates whose density exceeds the mean density of the soil, and they attempted to evaluate the linear swelling based on physical considerations.

Many authors attempted to explain the swelling process based on Schofield's suction-potential theory. According to this hypothesis, soil at a certain moisture content has a high capillary potential and it loses its potential energy as more water is absorbed. The moisture intake by the soil resulting from the soil suction was believed to cause the swelling. However, this theory is found to be inadequate to explain the swelling process completely since residual swell exists even at zero suction, as the water intake continues beyond that point until the hydration of the ions and the soil particles is complete (S.N. Gupta, B.N. Gupta and K.P. Shukla, 1967).

As explained earlier, the Gouy-Chapman double-layer theory attributes the swelling of clays to the osmotic pressure differentials between the midplane of adjoining particles and the external solution. According to this concept, the electric field of the clay particles causes the accumulation of ions in the interparticle spaces and thus the ion concentration in the diffuse double layer exceeds that in the external solution. This difference in the ion concentration results in the diffusion of water which forces the clay particles apart, causing the swelling. The pressure required to keep the clay from swelling, which is the swelling pressure corresponding to a constant volume condition, is equated to the osmotic pressure as given by van't Hoff's equation in physical chemistry (Yong and Warkentin, 1966). The swelling pressure is then given by the equation:

$$P = R T ( C_c - N C_o )$$

where

P = swelling pressure,

R = gas constant,

T = absolute temperature,

$C_o$  = salt concentration in the pore water, in moles  
per liter,

$C_c$  = cation concentration midway between two parallel  
clay plates, in moles per liter, and

N = number of cations and anions per molecule of  
compound.

The above expression is derived assuming only the forces of repulsion and a parallel arrangement of the clay particles. Although the predicted swelling pressures based on this theory are in reasonable agreement with the measured swelling pressures, there are many limitations to this approach and these are elaborately discussed by Bolt (1955), Lambe (1960) and Yong and Warkentin (1966).

Recently S. N. Gupta, B. N. Gupta and K. P. Shukla (1967) have investigated the physico-chemical properties of the black cotton soils of India, in relation to their engineering behavior and critically analysed the validity of the different swell pressure theories. They observed that none of the existing theories is adequate by itself to explain the residual swell even at high electrolyte concentrations, continued hydration at zero suction and the impossibility of expelling the interparticle and interlayer water by external pressure alone. Yong (1967) investigated the effect of elevated temperatures on the

swelling of a montmorillonite clay and showed that the diffuse double layer theory needs a correction for dialysate concentration, for predicting the swelling pressures under elevated temperatures.

In conclusion, it may be observed that the various theories advanced to explain the swelling phenomenon in soils have inherent deficiencies and consequently they have not been able to explain completely the actual swelling behavior of clays. Nevertheless they have greatly contributed to an understanding of the various factors involved in the swelling process. The discrepancies between the theoretical predictions and the actual behavior, only emphasize the fact that many of the complex processes involved in swelling are not yet completely understood.

#### Factors Affecting Swelling

The swelling characteristics of both undisturbed and remolded clays have been intensively studied in recent years, with a view to identify and evaluate the various factors influencing the swelling process. The results of these studies have demonstrated that the magnitudes of swelling and swell pressure are dependent on many factors and that they are different for undisturbed and remolded soils. In studying the swelling characteristics of expansive soils, it would be necessary, therefore, to recognize those factors which contribute to the variation in the behavior of undisturbed and remolded states.

#### Swelling Characteristics of Remolded Clays

The results of the previous studies indicate that the magnitude of the swelling and swell pressure of a compacted clay soil are dependent

on the following important factors:

1. Composition of the soil
2. Initial moisture content
3. Soil structure
4. Availability and properties of water
5. Confining pressure
6. Curing period
7. Time permitted for swelling
8. Temperature

The influence of each of the above factors on the swelling characteristics of clay, is briefly discussed below:

#### 1. Composition of the Soil

The type and amount of the clay minerals present in a soil largely influence its swelling characteristics. The swelling potential of clay particles results from the nature of their lattice structure and their extremely fine size. The composition and structure of the various clay minerals have been elaborately discussed by Grim (1968); and Kerr (1959) has shown that there are approximately fifteen minerals which are generally classified as clay minerals. The composition and structure of the three most common clay minerals, namely kaolinite, montmorillonite and illite, have been presented earlier.

The clay particles in soils are generally hydrated, that is, surrounded by layers of water molecules. The thickness of the adsorbed water influences the physical and engineering properties of clay soils. The main force which holds the water molecules to the surface of the particle is due to hydrogen bond, which decreases with the distance from surface. Consequently, the water layer next to the surface is

held more strongly than others, and the physical properties of this water differ significantly from those of free-water. The thickness of the strongly held water is only a few molecules thick, of the order of 10 Å. The development of a diffuse double layer around a clay particle in an electrolyte solution was described in the preceding section. The repulsion resulting from the interpenetration of the diffuse double layers of adjacent particles and from the adsorption of water on the particle surfaces, is responsible for the swelling of a clay on wetting. Kaolinite consists of repeating layers of one silica and one alumina sheet which are held together by hydrogen bonds between  $O^{2-}$  and  $(OH)^-$  ions. This hydrogen bond is weaker than the ionic and covalent bonds and consequently the kaolinite crystals tend to break into very thin sheets. There is usually very little substitution of one cation for another in the crystal lattice. The elemental sheets are very compact and stable and their inexpandible structure resists the introduction of water into their lattice. Consequently the physico-chemical interactions between particles arise largely from external surface features rather than conditions within their structure. Also water adsorption and exchange phenomenon are not well pronounced in kaolinite. The montmorillonite mineral on the other hand, consists of an alumina sheet between two silica sheets. The bond between successive silica sheets is very poor and this results in a very unstable lattice. Consequently in the presence of water, there is considerable lattice expansion in the direction of the C-axis resulting from the entry of as much as six layers of water molecules between the sheets. As water molecules happen to be the right size to fit into the structure, it requires heating upto  $200^{\circ}$  to  $300^{\circ}C$  to completely remove the water. In illite, although

the structure is similar to montmorillonite except for a layer of potassium ions between the silicia sheets, the bonds between the nonexchangeable potassium ions are weaker than the hydrogen bonds between the unit layers of kaolinite, but much stronger than the ionic bonds in the montmorillonite crystal. Consequently the lattice is much less susceptible to cleavage and exhibits less swelling than montmorillonite, although it expands more than kaolinite.

The differences in the crystal lattice, hydration and exchange characteristics of the clay minerals result in variations in the swelling behavior of the soils containing these minerals. In general, soils containing sodium montmorillonite exhibit considerable volume change. Bolt (1956) and S. N. Gupta, B. N. Gupta and K. P. Shukla (1967) have reported that swelling increases with the montmorillonite content, base exchange capacity and the specific surface. Holtz and Gibbs (1956) have made an extensive study of this problem and recommended an empirical method for both identifying and predicting the swelling characteristics of compacted clays. Seed, Woodward and Lundgren (1962), using artificial soils, studied the relationship between the clay fraction, activity of the soil and swelling potential (defined as the percentage of swell for a sample compacted at optimum moisture content to maximum dry density by Standard AASHO compaction procedure, under a surcharge of 1 psi). The empirical relationship proposed by them is of the form:

$$SP = KC^x$$

where

SP = swelling potential

C = clay content less than 2 $\mu$ , and

K and x = constants depending on the type of clay.

Their results indicate that the swelling increases with the amount of clay present in the soil (Figure 6).

Ranganatham and Satyanarayana (1965) conducted similar investigations using the black cotton soils of India and established an empirical relationship (applicable to both natural and artificial soils) between the swelling potential and shrinkage index, in the form:

$$SP = \beta(SI)^\rho$$

where

SP = swelling potential, and

SI = shrinkage index

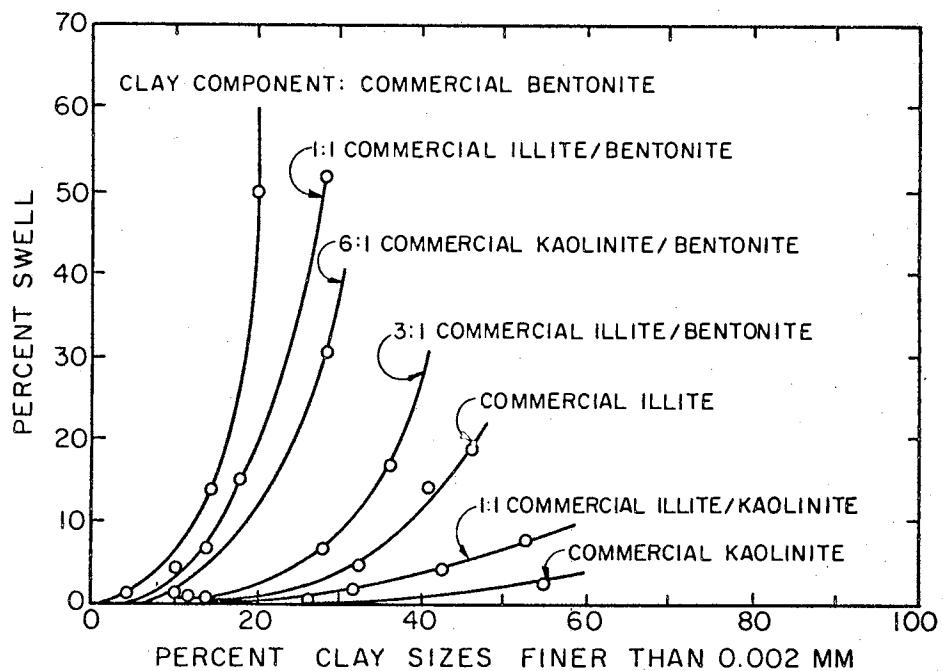
$\beta$  and  $\rho$  = constants depending upon the nature of the clay.

They reported that  $\beta = 1/256$  and  $\rho = 2.37$  for artificial soils and  $\beta = 1/6.3$  and  $\rho = 1.17$  for natural soils. They developed a classification system based solely on the shrinkage index, for predicting the degree of swell potential.

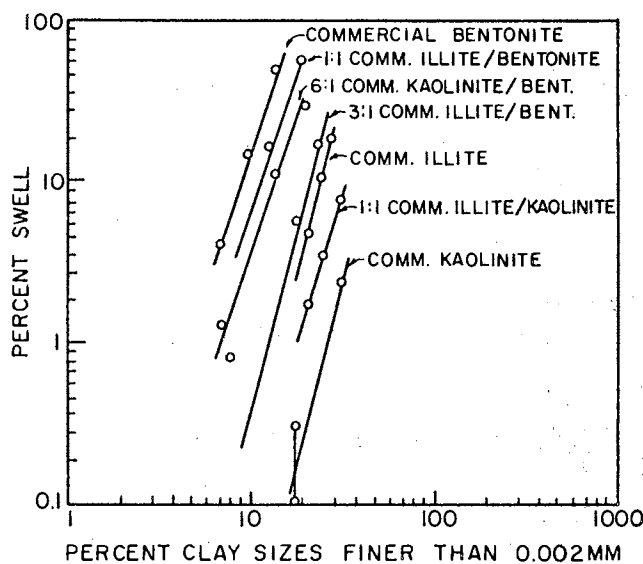
## 2. Initial Moisture Content

The initial moisture content is another important factor which governs the swelling characteristics of soil. For a given compactive effort, the dry density attained depends on the molding water content at which compaction is done. The relationships between the initial moisture content, dry density and percentage expansion for 'Porterville clays' from the Delta-Mendota Canal, were investigated by Holtz and Gibbs (1956). Ladd (1959) has given an excellent discussion on the mechanisms causing swelling and studied in detail the various factors affecting the swelling of compacted clays. His important findings are





(a) NATURAL SCALE



(b) LOGARITHMIC SCALE

NOTE: PERCENT SWELL MEASURED UNDER 1 PSI SURCHARGE FOR SAMPLE COMPACTED AT OPTIMUM WATER CONTENT TO MAXIMUM DENSITY IN STANDARD AASHO TEST.

Figure 6. Relationship Between Percentage of Swell and Percentage of Clay Sizes for Experimental Soils (after Seed, Woodward and Lundgren, 1962).

given below:

a) The thickness of the double layer is approximately proportional to the molding water content. Assuming all water to be in the double layer, the average thickness of double layer is equal to the water content divided by the specific surface area. Therefore, other things being equal, the lower the molding moisture content, the greater is the water-intake, to satisfy the double layer deficiency. For a constant molding water content, an increase in dry density results in an increase in the amount of swelling.

b) For samples compacted wet of optimum moisture content, swelling can be explained by osmotic repulsive pressures resulting from the difference in ion concentration in the diffuse double layer between clay particles and that in free pore water.

c) For samples compacted dry of optimum moisture content, swelling is influenced by factors other than osmotic pressures. These factors may be: the effect of negative electric and London - van der Waals force fields on water, cation hydration and attraction of the particle surface for water, elastic rebound of particles, a flocculated particle orientation and the presence of air.

From the results of tests on Boston blue clay, Lambe (1960) found that the pressure required to prevent the samples, compacted wet and dry of optimum, from swelling, were 0.12 and 1.01 kg. per sq. cm respectively, although the samples were compacted to the same density using the same compactive effort. The influence of molding water content on the swelling of compacted clays has also been substantiated by the work of Seed, Woodward and Lundgren (1962) and Parcher and Liu (1965).

### 3. Soil Structure

The importance of soil structure in the swelling phenomenon was first recognized by Terzaghi (1931) and was further elaborated by Casagrande (1932). Mitchell (1956), using a petrographic microscope, studied the fabric of fourteen natural clays of marine and fresh-water origin and, based on measurements of extinction of thin sections, he attempted to correlate the soil structure to the engineering properties such as strength, compressibility and permeability.

The structure of a compacted soil is influenced by the compactive energy, mode of compaction and the initial moisture content. Using the optical techniques developed by Mitchell (1956), Pacey (1956) studied the relationship between the initial moisture content and the particle arrangement and found that compaction on the dry side of optimum moisture content produces a non-parallel or flocculent structure while compaction on the wet side results in a parallel or dispersed arrangement (Figure 7). His experimental data also indicate that the degree of particle orientation increases with increasing compactive effort.

The theory of compaction proposed by Lambe (1960) attempts to explain the change in density of compacted soil based on the variations in soil structure at different moisture contents during compaction. According to this concept, soil compacted dry of optimum tends to have a flocculated structure, owing to the small amount of water which results in a very high electrolyte concentration and consequent depression of the double layers (Figure 8). An increase in water content to the optimum value, increases the electrolyte concentration and double layers around the soil particles. This results in a reduced degree of flocculation

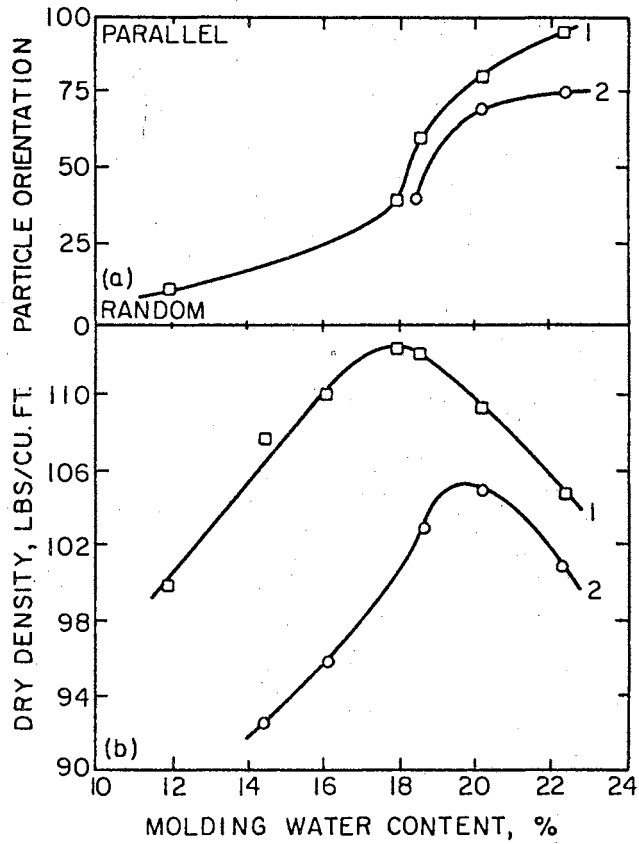


Figure 7. Orientation Versus Water Content for Boston Blue Clay (after Lambe, 1960).

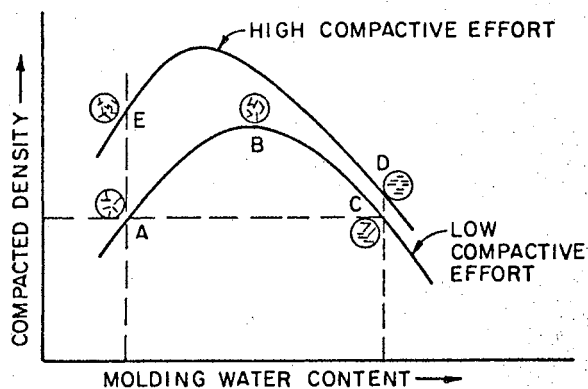


Figure 8. Effect of Compaction on Soil Structure (after Lambe, 1960).

which permits a more orderly arrangement of the particles and a higher density. Further increase of moisture from the optimum to the wet side causes further expansion of the double layers and a decrease in the net attractive forces between particles. Even though this gives rise to a more parallel arrangement of the particles, the density is reduced because the added water tends to reduce the concentration of soil particles per unit volume. The same effect was observed in a more pronounced manner in soils compacted with greater compactive effort.

The effect of particle arrangement on the swelling and other characteristics of compacted clays has been studied in considerable detail by Seed and Chan (1961) and their results corroborate the findings of Pacey (1956) concerning the influence of molding water content on particle orientation. Their main conclusions are summarized below:

a) Samples compacted dry of optimum exhibit higher swelling characteristics and swell to higher water contents than those compacted wet of optimum at the same density. This increased swell might be construed as a manifestation of the higher swelling tendency of flocculated structures than of dispersed structures.

b) Samples compacted dry of optimum (which tend to have more flocculated structures) exhibited greater swell pressures than those compacted wet of optimum (which tend to have more dispersed structures).

c) For the same initial moisture content and dry density, static compaction tends to produce a flocculent structure while kneading compaction results in a relatively more dispersed structure. Consequently samples compacted by static compaction exhibit higher swelling characteristics.

Clays with an overall orientation of particles, are generally

anisotropic with respect to shrinkage and swelling. Ward, Samuels and Butler (1959) have studied the properties of London clay and have reported a greater swelling volume and swelling pressure in the vertical direction compared to the horizontal. Liu (1964) and Parcher and Liu (1965) have investigated the swelling characteristics of compacted Permian clay, using the triaxial swelling apparatus developed by Fost (1962). Their experimental results have not only confirmed the findings of Seed and Chan (1961) but also emphasized the significance of structural anisotropy on the swelling characteristics of compacted clays. They have reported that the unit swelling in the horizontal direction exceeds that in the vertical direction, regardless of how compaction is accomplished (Figures 9 through 13). Although the full implications of this observed behavior are not clear in terms of the soil structure, their findings have clearly demonstrated the influence of soil structure on swelling. More recently the effect of anisotropy on the swelling of a montmorillonite clay was studied by Komornik and Livneh (1967). They have shown that the amount of swell parallel to the direction of compaction is greater than that in the perpendicular direction and they have attributed this to the platy structure of the montmorillonite (Figure 14). Their results also indicate that these orientational differences in lateral swelling pressure and amount of swell are larger in tests carried out at vertical pressures less than 1.0 kg. per sq. cm.

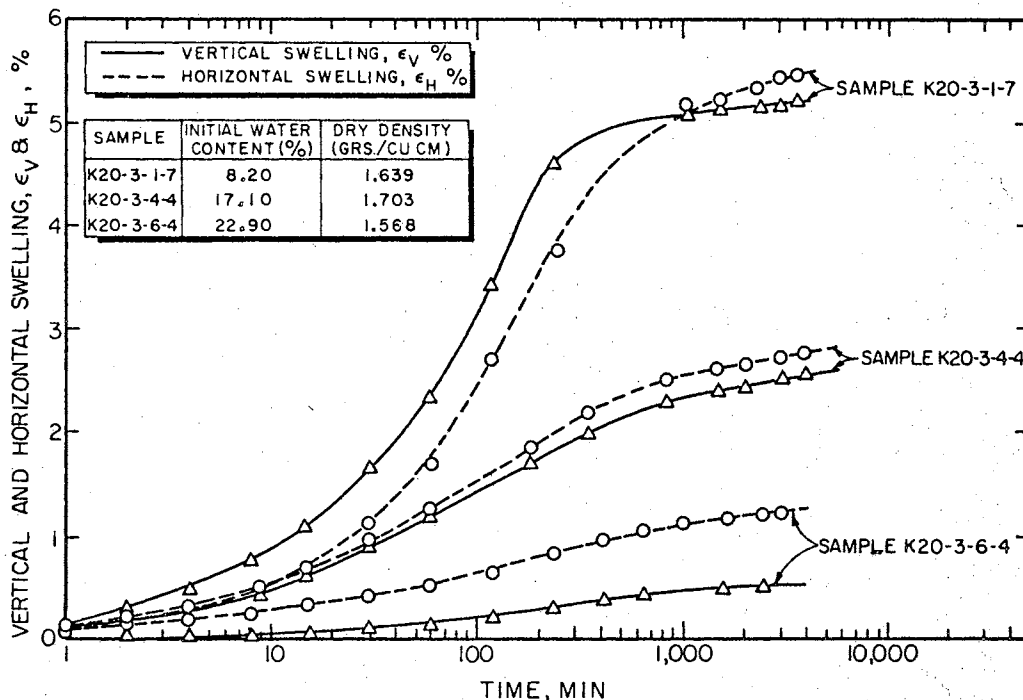


Figure 9. Swelling-Time Curves, Kneading Compaction, Soil B2 (after Parcher and Liu, 1965).

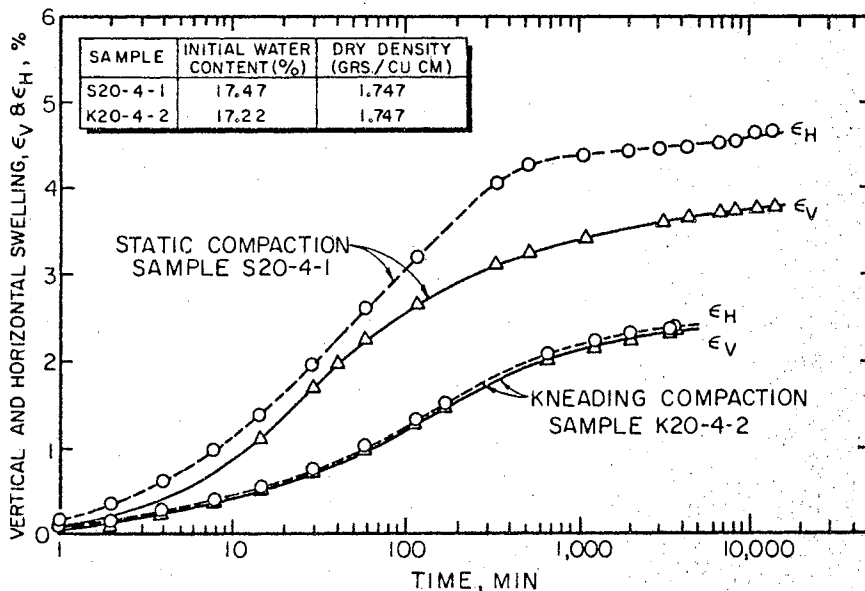
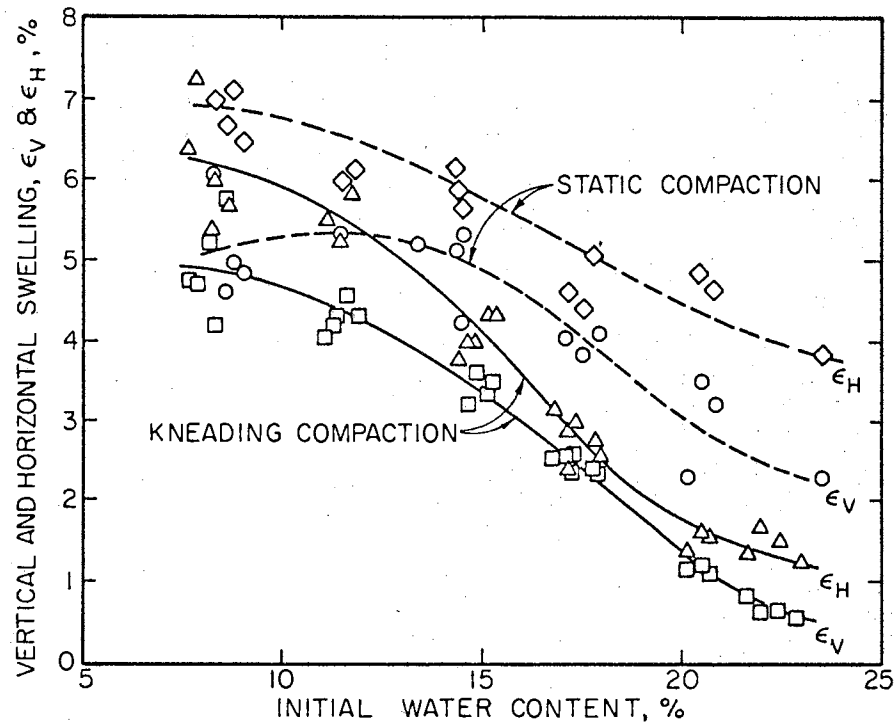
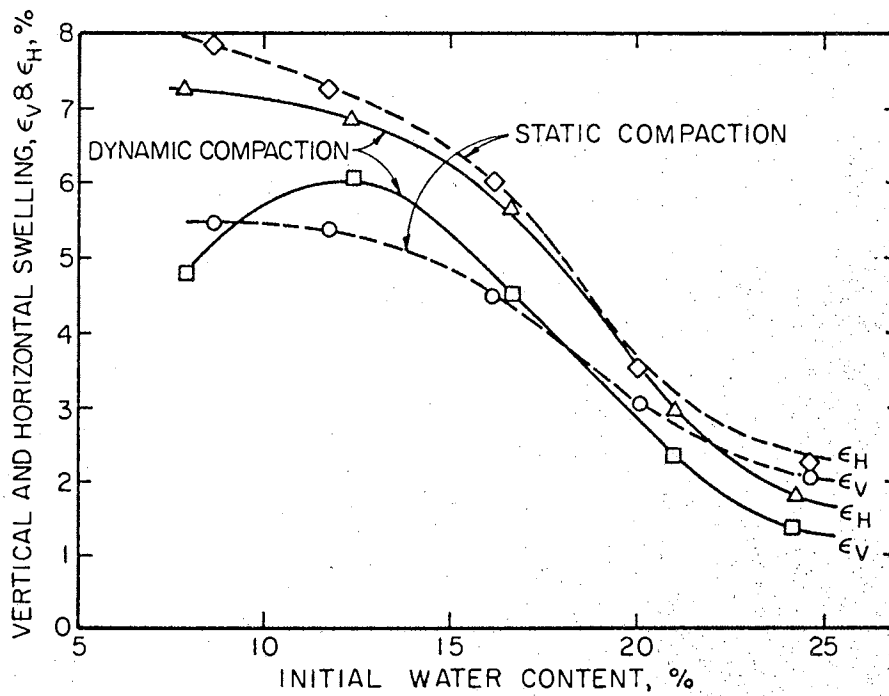


Figure 10. Swelling-Time Curves, Kneading and Static Compaction, Soil B2 (after Parcher and Liu, 1965).



(a) KNEADING AND STATIC COMPACTION



(b) DYNAMIC AND STATIC COMPACTION

Figure 11. Effect of Initial Water Content on Swelling, Soil B2 (after Parcher and Liu, 1965).



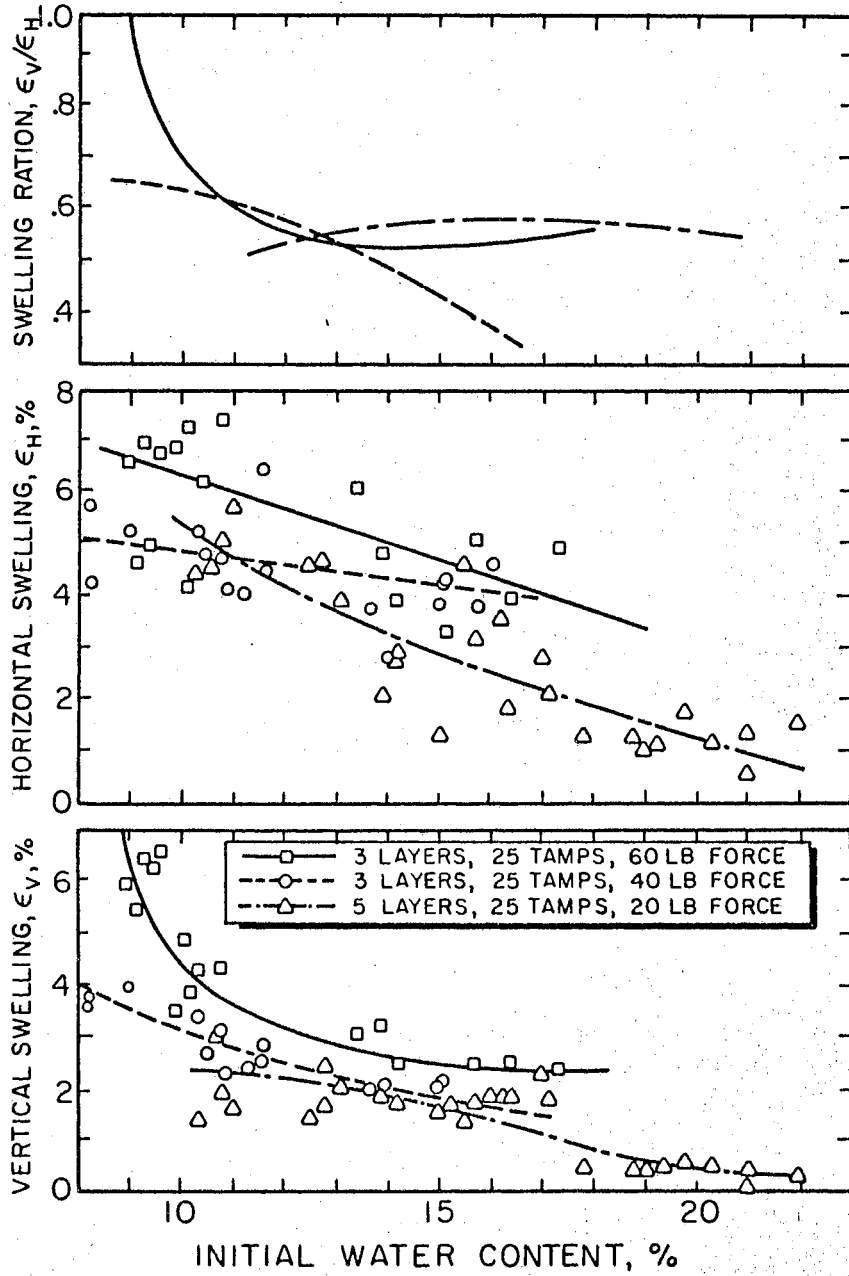


Figure 12. Effect of Compaction Energy on Swelling, Soil A (after Parcher and Liu, 1965).

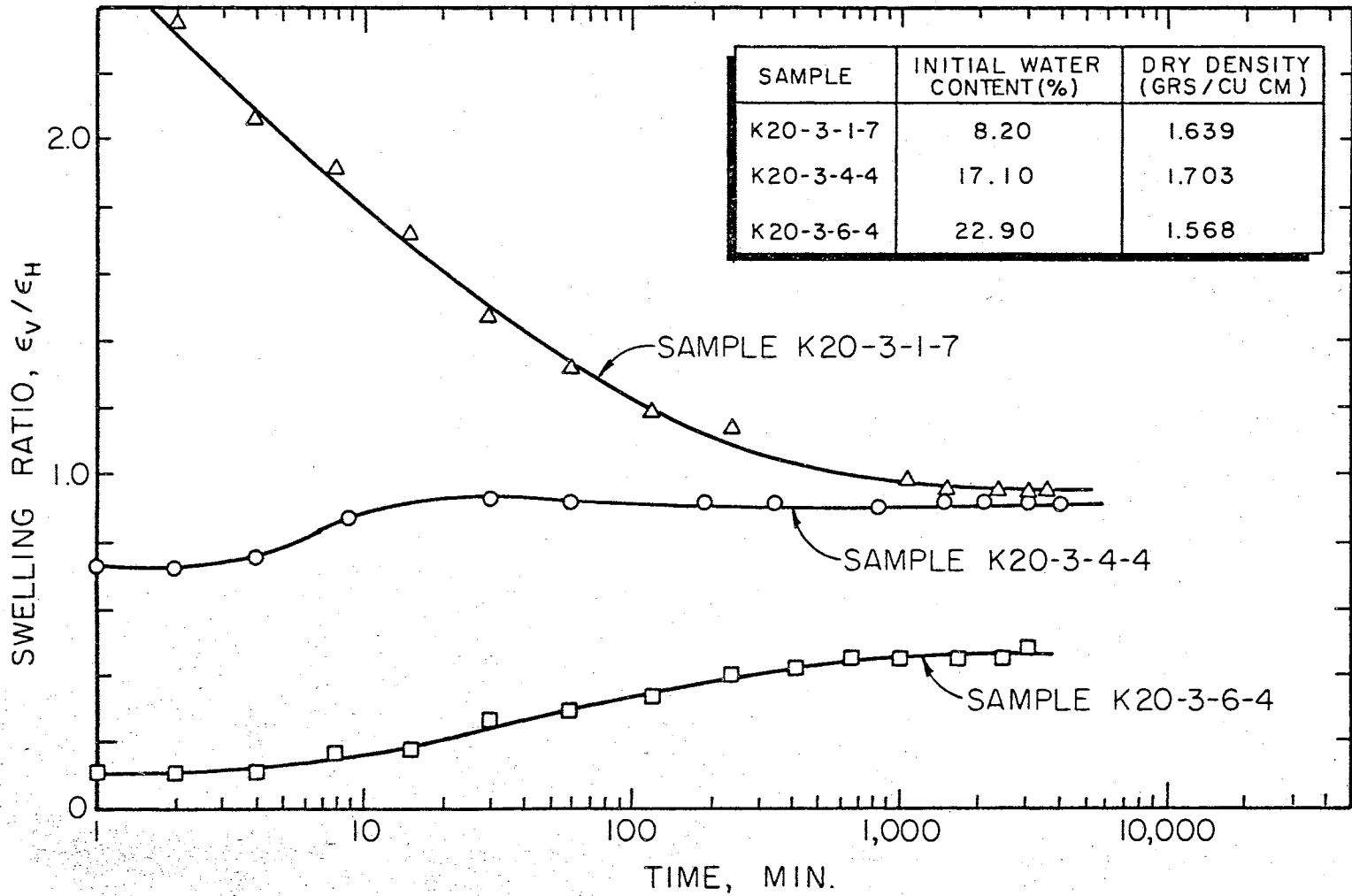


Figure 13. Swelling Ratio - Time Curves, Kneading Compaction, Soil B2 (after Parcher and Liu, 1965).

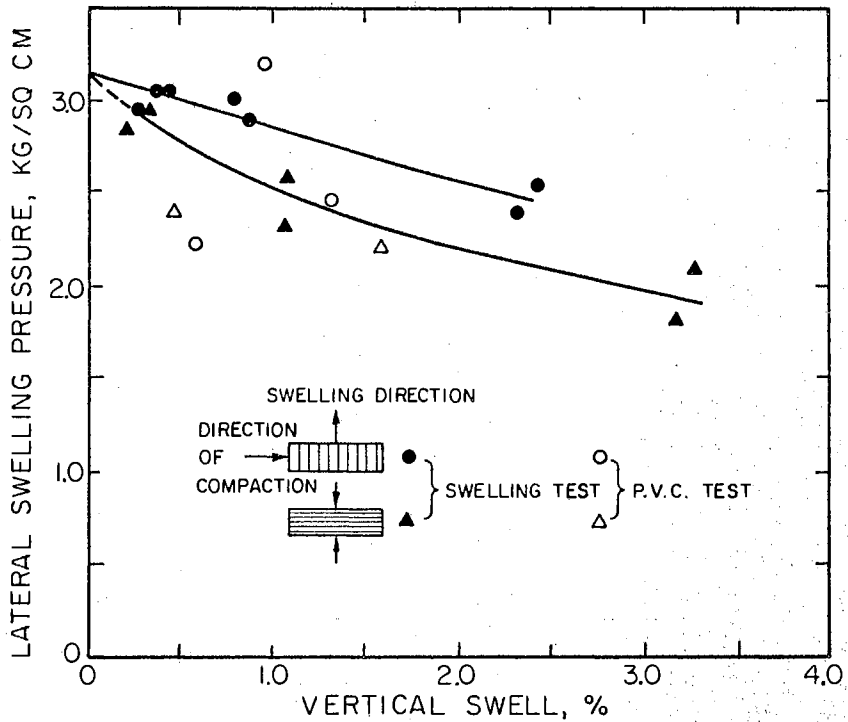
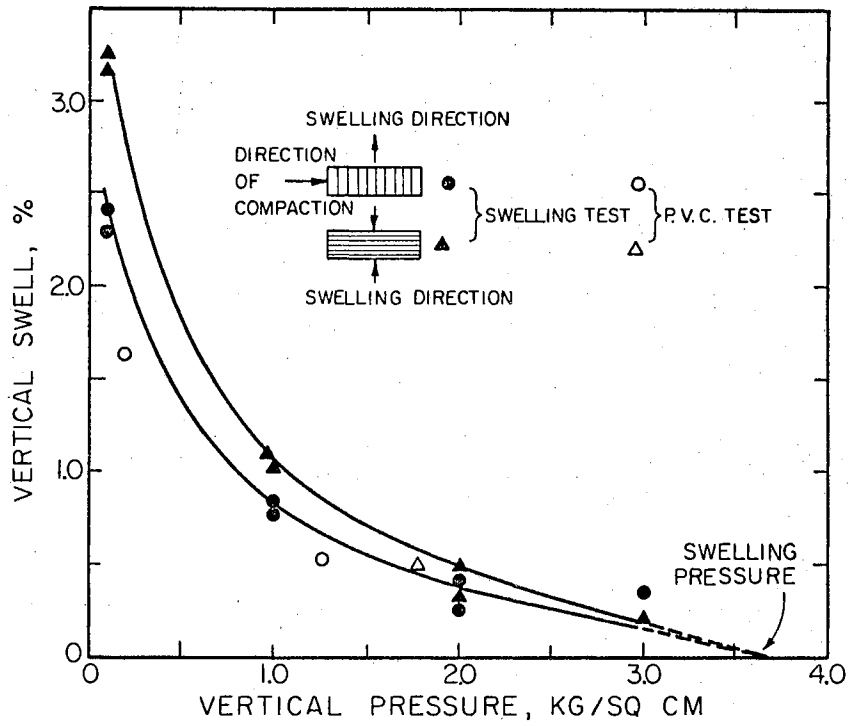


Figure 14. Effect of Anisotropy on the Swelling and Swell Pressure of Compacted Clay (after Komornik and Livneh, 1967).

#### 4. Availability and Properties of Water

The swelling of a soil results from an increase in its moisture content and therefore, availability of water is a requisite for swelling. The chemical properties of the pore fluid have an influence on the development of the diffuse double layers around the soil particles and consequently on the swelling characteristics of the soil. As discussed earlier, a lower concentration of the pore fluid and a lower valence of ions would result in an extended double layer and greater force of repulsion. Increasing either the concentration or the valence would reduce the double layer (Figure 4). The influence of the chemical properties of water on the swelling of compacted clays has been studied by Ladd (1959); A. W. Taylor (1959); Low (1959); Seed, Mitchell and Chan (1961); Ozkol (1965); S. N. Gupta, B. N. Gupta and K. P. Shukla (1967) and others.

Ladd (1959) reported that the swelling of a compacted soil can be effectively reduced by the replacement of low valency cations by higher valency cations, mixing salt with the compacted clay or by leaching the compacted soil with salt solutions. He also found that the initial rate of swelling is practically unaffected by the salt concentration and this was confirmed by Seed, Mitchell and Chan (1961). Although the swelling is actually suppressed as the electrolyte concentration increases, there is considerable evidence to indicate that swelling is not completely eliminated even at high electrolyte concentrations (Seed, Mitchell and Chan, 1961; S. N. Gupta, B. N. Gupta and K. P. Shukla, 1967 and others).

## 5. Confining Pressure

A soil on wetting will continue to swell until equilibrium is reached between the confining force and the net repulsive force. The confining force results from an external loading system while the net repulsive force is the sum of the double layer repulsive forces (osmotic pressures) and the London-van der Waals forces of attraction. An increase in the confining force reduces the magnitude of swelling, although (except for a saturated soil) this does not necessarily mean that no water will be imbibed. Consequently heavy buildings constructed upon expansive soils are generally subject to less heaving than light structures with shallow footings (Abelev, Sazhin and Burov, 1967 and Parcher and Means, 1968). Seed, Mitchell and Chan (1961) have studied the influence of confining pressure on the magnitude of swelling and found that the magnitude of this balancing pressure decreases as swelling progresses. Recently Ho (1967) and De Graft-Johnson, Bhatia and Gidigasu (1967) have investigated these aspects and their results indicate that the swell pressure decreases with increasing volume change.

## 6. Curing Period

Barber (1956) reported that the curing period (which is the time interval between compaction and swelling test) has an influence on the swelling pressure of compacted soils. A substantial reduction in the magnitude of swelling pressure was noted by Barber when the curing period was increased from 5 minutes to 24 hours. The effect of curing period on the magnitude of swelling is not known, although we might anticipate a similar influence. Also the curing period required to produce maximum reduction in swelling is not established.

## 7. Time Permitted for Swelling

When a compacted soil is allowed to absorb water, it will continue to swell until final equilibrium is reached between the internal and external forces. The amount of swelling at any instant depends on the quantity of water entering the soil. The time required for the water to enter into a swelling clay system is a function of the permeability of soil. It is obvious, therefore, that the rate of swelling is a function of the coefficient of permeability as well as the hydraulic gradient of the porewater. Lambe (1960) has studied the factors affecting the permeability and shown that the Kozeny-Carman equation can be used to characterize the tortuosity of flow which, in effect, is a measure of the soil structure. His results indicate that a soil compacted dry of optimum will have a much higher permeability than that compacted wet of optimum (Figures 15 and 16). From these data, it can be concluded that the rate of swelling of a soil compacted dry of optimum will be more than that for a soil compacted wet of optimum. The experimental results of Liu (1964) and Parcher and Liu (1965) substantiate this conclusion (Figure 9).

## 8. Temperature

Lambe (1960) studied the influence of temperature on the volume change of Boston blue clay and found that in a consolidation test at a constant load, the sample under consolidation swelled as the temperature was decreased and contracted with temperature increase, and he attributed this to the effect of temperature on the diffuse double layer. Recently Yong (1967) has studied the effect of elevated temperatures on

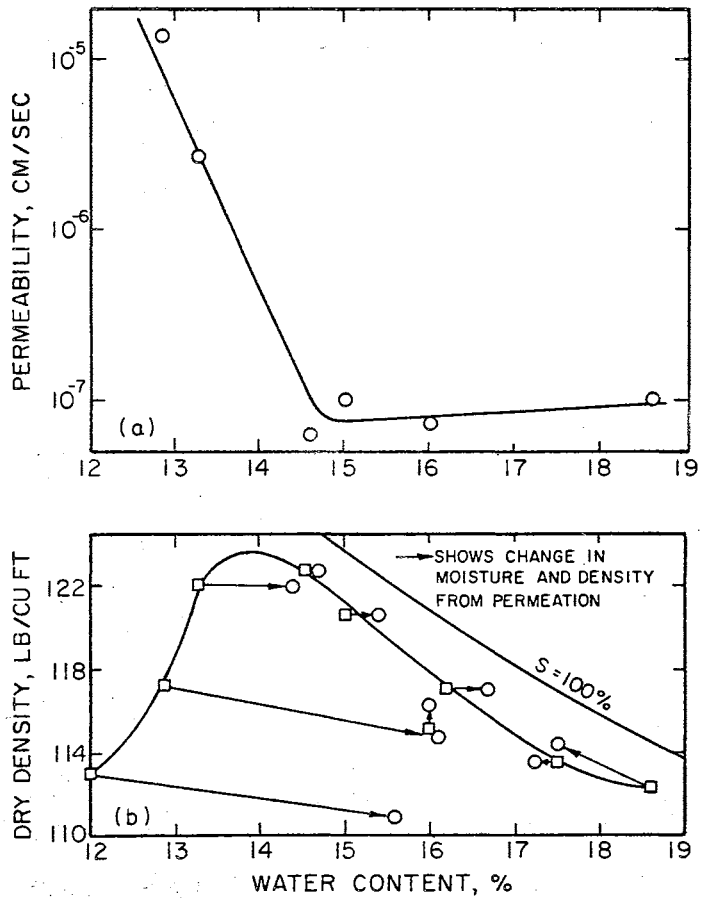


Figure 15. Compaction-Permeability Tests on Jamaica Sandy Clay (after Lambe, 1960).

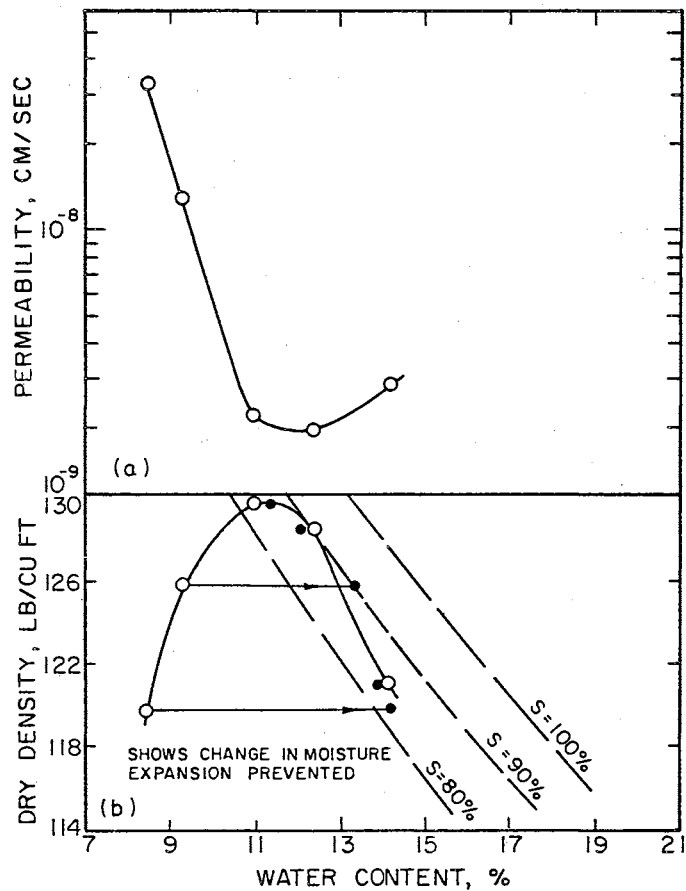


Figure 16. Compaction-Permeability Tests on Siburua Clay (after Lambe, 1960).

the swelling pressure of a pure sodium-montmorillonite clay and showed that a correction in terms of the effective dialysate concentration is required to predict the swelling behavior at elevated temperatures more correctly, based on the diffuse double layer theory.

### Swelling Characteristics of Undisturbed Clays

According to Holtz (1959), the swelling characteristics of natural expansive clays are, in general, dependent on the amount and type of clay minerals present, initial density, change in moisture, load conditions, soil structure and time. As the basic mechanism which contributes to the swelling is the same for both undisturbed and remolded clays, all the various factors which were discussed under remolded clays are applicable to undisturbed clays also. However the differences in the swelling behavior of undisturbed and remolded clays arise largely from the variations in their soil structure and diagenetic cementation of particles in the natural state.

In naturally sedimented soils, the particle arrangement will be influenced by the nature and size of the particles and also by the environmental conditions prevailing during their deposition. In fresh-water deposition, the development of repulsive forces between particles will be maximum due to the absence of dissolved salts and this would, in general, result in a semi-oriented structure. However, the presence of dissolved salts in a marine environment, effectively depresses the diffuse double layer between particles and this gives rise to a characteristic flocculated structure. Lambe (1953); Rosenqvist (1959); Trollope and Chan, (1960) and others have studied the structure of clay-water systems and proposed different models to explain their



natural structure. There is considerable evidence to show that the edges of clay particles can carry a charge opposite to that of the faces and the flocculated sediments are not entirely composed of parallel particles. Accordingly Lambe (1960) has shown that two types of flocculation can exist: salt type with an orientation approaching parallelism and a non-salt type with an orientation approaching a perpendicular array (Figure 17).

Holtz (1959) found that remolded soils exhibited greater swelling than undisturbed soils, although their initial water contents and densities were the same. The same effect has been reported by Liu (1964) and Parcher and Liu (1965) (Figure 18). This difference in swelling is due to the change in particle arrangement caused by remolding.

Casagrande (1932) has elaborately discussed the importance of soil structure in relation to engineering properties. The observed difference in the swelling characteristics of normally consolidated clays and the highly overconsolidated clays, is the direct consequence of the structural variations brought about by stress history. Similarly the swelling characteristics of a clay of fresh-water origin will be different from those of a clay deposited in a marine environment, because of the structural variations resulting from the different environmental conditions during their formation.

Another important factor that affects the structure of natural clays is the diagenetic cementation by which particles are cemented to each other by iron hydroxides, carbonates and various organic molecules. Whether the cementation of particles results in a structural restraint to swelling or in the alteration of the physico-chemical properties of the surface, is not clearly known. However, it is known that the

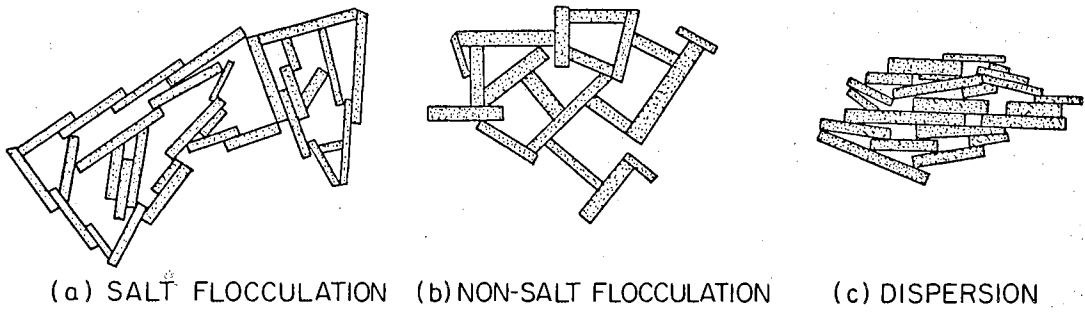


Figure 17. Sediment Structures (after Lambe, 1960).

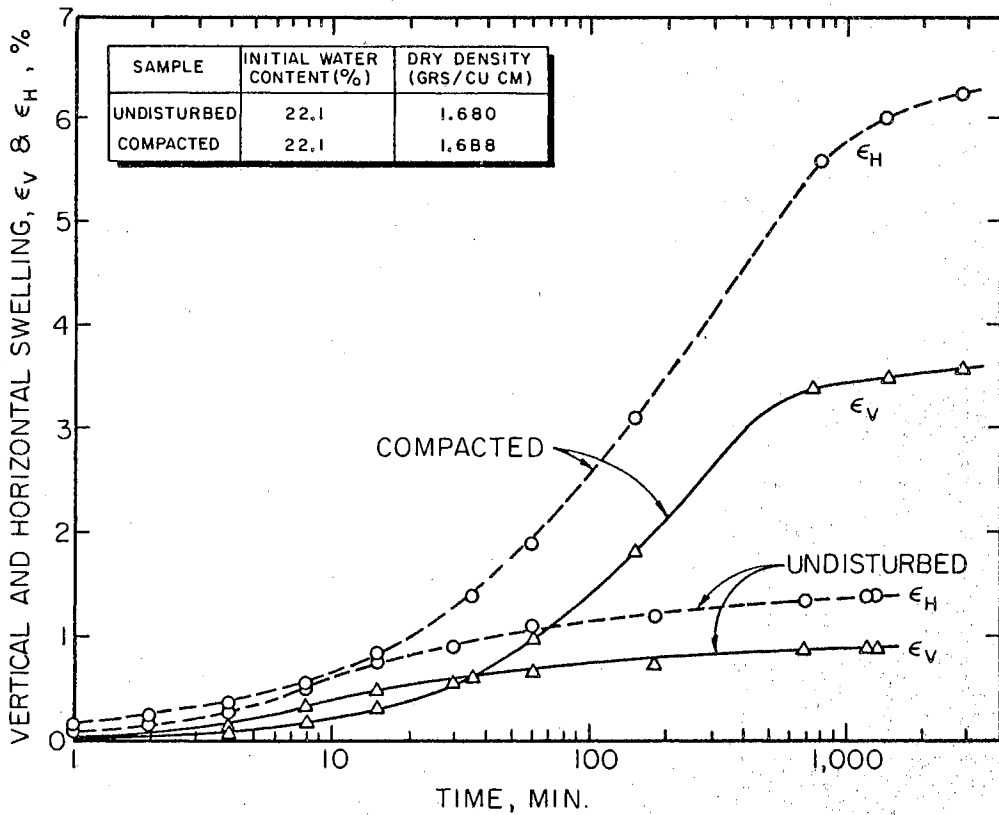


Figure 18. Swelling-Time Curves for Undisturbed and Compacted States, Soil B1 (after Parcher and Liu, 1965).

cementation between particles is an important factor limiting the volume increase of clays. The reduction of swelling caused by cementing materials is more for weathered clays subjected to cycles of wetting and drying. The results of Warkentin and Bozozuk (1961) indicate that the removal of iron oxides and carbonates resulted in only a small increase in swelling in the case of a high-swelling clay and reduced the volume regain in a low-swelling clay.

#### Structural Damages Caused by Swelling

Expansive soils occur in many parts of the world and considerable foundation difficulties are encountered in constructions involving these soils. Damage to structures resulting from the swelling of clay soils has been well documented over the years. Published literature indicate that, although the majority of the damages were attributed to the vertical component of swelling, there were instances where the damage was almost certainly caused by horizontal swelling, and in which there was little evidence of vertical swelling (Means, 1959).

In many areas, the surface clays are subjected to cycles of desiccation and saturation due to alternating dry and wet periods. Consequently these clays exhibit considerable seasonal volume change - shrinkage and cracking in summer and swelling in winter. The capillary forces in the drying clay result in overconsolidation of these clays to considerable depths. Structures erected on these overconsolidated desiccated clays have suffered extensive damage due to expansion of the clays upon increase in water content. In general, all clays are susceptible to volume changes due to seasonal moisture variation although those containing montmorillonite are affected to a greater degree.

Moisture variations in soil may arise from climatic conditions, ground water fluctuations and other environmental features. These aspects have been elaborately discussed by Means (1959) and Parcher and Means (1968). Numerous studies have been done in the past to identify and evaluate the factors contributing to the volume changes in clays (Ward, 1953; Jennings, 1953; Wooltorton, 1936, 1950; Baracos and Bozozuk, 1957; Morris, 1960 and others). In some cases, structural damages were attributed to the shrinkage of subsoil, resulting from moisture depletion caused by nearby vegetation and trees (Ward, 1953; Baracos and Bozozuk, 1957; Salas and Serratosa, 1957; Bozozuk and Burn, 1960).

Jennings (1953) studied the heaving of buildings on desiccated African clays and concluded that heaving of buildings may be anticipated in situations involving a clay profile, a low water table and a condition of desiccation in the soil. Based on the results of experimental and field observations, he has given practical solutions for building foundations on these expansive soils. Tschebotarioff (1953) reported structural damages sustained by residential buildings founded on the swelling clays of eastern Cuba, and he attributed the damages to the upward migration of moisture towards the center of the house and increased lateral pressure caused by the swelling of subsoil. Dawson (1953) studied the causes for the movement of small houses erected on an expansive clay soil in central Texas and has reported that these soils expand, lifting the structures considerably due to the intake of water. His results also indicate that these soils are subjected to considerable horizontal movement. Youssef, Sabry and Tewfik (1957) have reported damage to structures caused by the swelling Aswan clay and they attributed the damage to the vertical swelling of the subsoil.

Parcher and Means (1968), from their extensive consulting experience, have recorded a number of structural damages to buildings and other facilities within the Oklahoma State University campus and nearby areas, caused by the swelling of the highly overconsolidated Permian clays of Oklahoma. In all these cases, structural damages were manifested in the form of cracking and tilting of walls, heaving of floors, and differential uplift of lightly loaded columns and walls. They have attributed these damages to both the vertical and horizontal swelling of the subsoil and have suggested measures for preventing damage from expanding clays. Methods to prevent the detrimental effects of swelling soils have also been discussed by Dawson (1959) and McDowell (1959).

Case histories concerning the detrimental effects to structures caused by the swelling of clays are numerous and the brief review of a few cases given above serves only to illustrate the significance of both vertical and horizontal swelling. The influence of confining pressure on the swelling was discussed earlier. An increase in confining pressure generally results in a decrease in the magnitude of swelling. Consequently, only light buildings on shallow foundations suffer extensive damage due to the volume changes associated with clays while heavy multi-storied buildings, if structurally sound otherwise, stand indefinitely with little or no damage, except to lightly loaded members like floor slabs on the ground. As structural damage may arise from both the vertical and horizontal swelling of the subsoil, a clear understanding of the swelling characteristics of clays is essential for the proper design of foundations.

## CHAPTER III

### EXPERIMENTAL PROCEDURES

#### Physical Properties

The soil used in this study was the locally abundant Permian red clay. The bulk of the soil required for the various tests was obtained from the foundation excavations for the math-science building within the University campus. The natural soil is very stiff and overconsolidated and exhibits marked volume change characteristics when subjected to moisture variations.

As part of this investigation and to facilitate interpretation of the swelling test results, tests were conducted to determine the physical properties of the soil and the results are summarized in Table II. The various laboratory tests to determine the liquid limit, plastic limit, specific gravity, and the grain-size distribution of the soil were performed as per the standard ASTM procedures for testing soils. The grain-size distribution of the soil obtained from tests, is shown in Figure 19.

Tests were also conducted to establish the moisture-density relationships corresponding to the Standard and Modified AASHTO Compaction procedures. The compaction tests were performed as per the standard ASTM procedure. However, in compaction tests, material passing US sieve No. 40 was used, in order to evaluate the optimum moisture content

TABLE II

## PHYSICAL PROPERTIES OF PERMIAN CLAY

Liquid limit, percent	42
Plastic limit, percent	15
Plasticity index	27
Specific gravity	2.72
Passing US sieve No. 200, percent	89.50
Finer than 0.002 mm., percent	31.00
Activity number	1.15
<u>Compaction Data*</u>	
Standard AASHO:	
Optimum moisture content, percent	19.00
Maximum dry density, pcf.	102.00
Modified AASHO:	
Optimum moisture content, percent	14.50
Maximum dry density, pcf.	117.00

\*For soil passing US sieve No. 40





and maximum dry density of the soil fraction used in the triaxial swelling tests. The results of the compaction tests are shown in Figure 20. The test results indicate that the optimum moisture content and the maximum dry density of the soil (passing US sieve No. 40) are respectively 19% and 102 pcf for the Standard AASHO compaction and 14.5% and 117 pcf for the Modified AASHO compaction.

### Triaxial Swelling Tests

#### General

In order to compute the relative magnitudes of swelling parallel and perpendicular to the direction of compaction, the triaxial swelling apparatus developed in the School of Civil Engineering, Oklahoma State University, by Fost (1962) under the direction of Professor James V. Parcher, was used. This apparatus was extensively used to study the vertical and horizontal swelling characteristics of compacted and undisturbed soils and reported to be very satisfactory (Liu, 1964; Parcher and Liu, 1965). Six triaxial swelling apparatuses, manufactured by the Research and Development Laboratory of the Oklahoma State University were continuously used in this investigation. A brief description of the apparatus is given below.

#### Description of Apparatus

The special design of this apparatus permits both the magnitudes of vertical and horizontal (radial) swelling of the soil specimens to be measured simultaneously during the test. The apparatus is essentially made of Plexiglas and consists of a base plate, chamber and a top plate (Figures 21 and 22). The chamber rests on the circular recess in the base plate and the top plate is placed over the chamber and

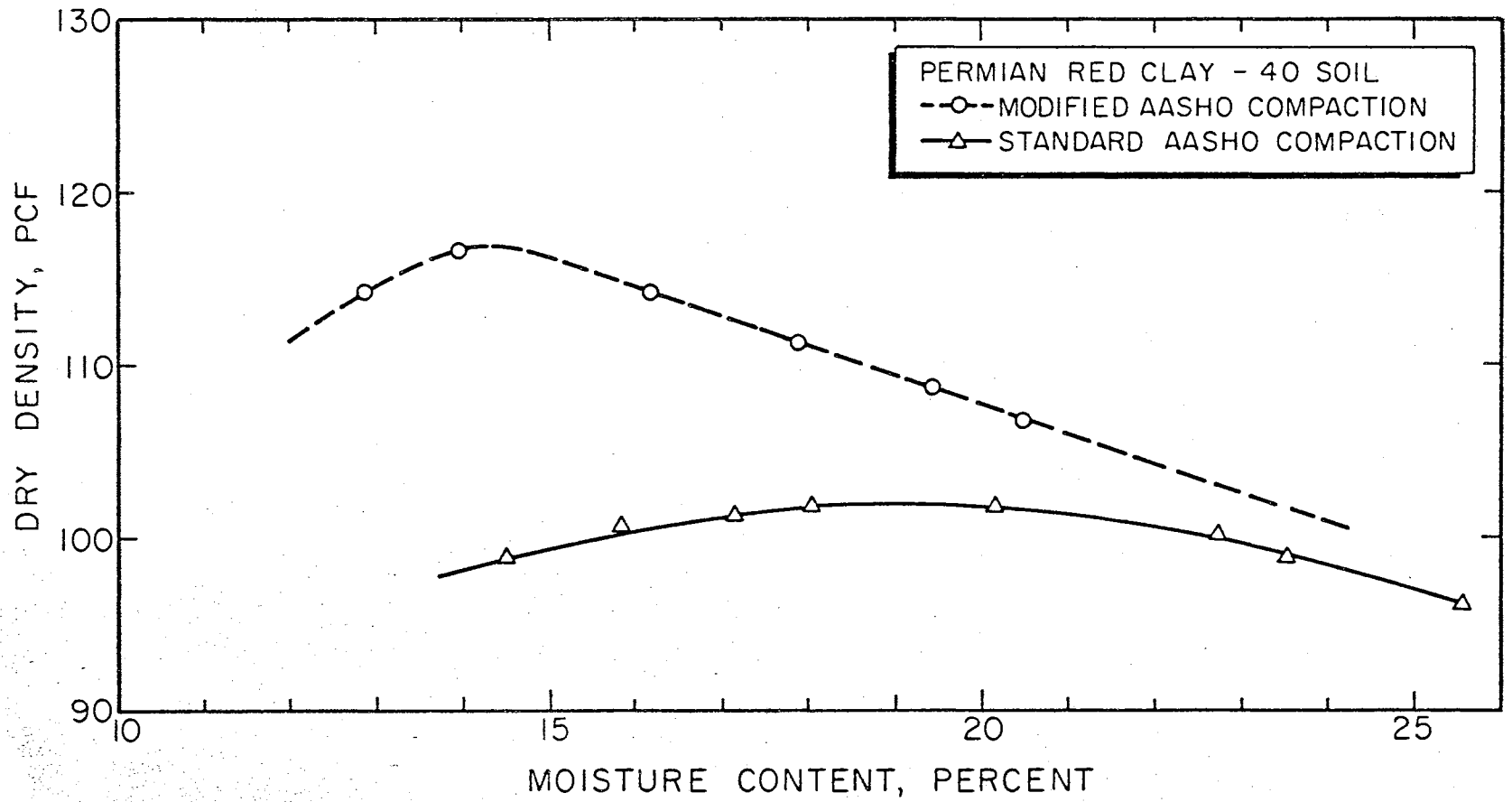
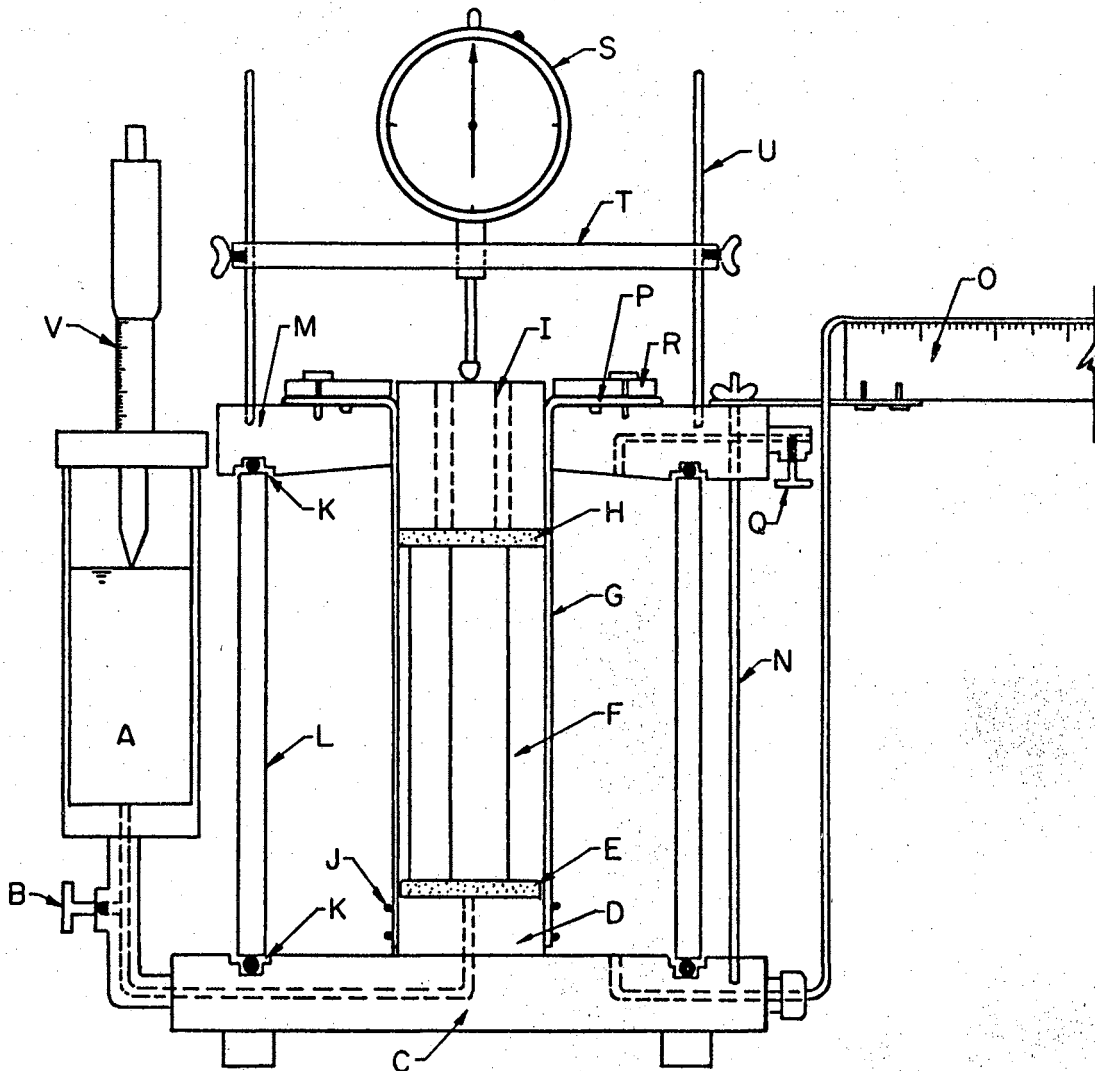


Figure 20. Moisture-Density Curves for Permian Clay



A - WATER RESERVOIR

B - LOWER VALVE

C - BASE PLATE

D - PEDESTAL

E - POROUS STONE 1

F - SPECIMEN

G - FLANGED MEMBRANE

H - POROUS STONE 2

I - CAP

J - LOWER O-RING MEMBRANE SEAL

K - O-RING CHAMBER SEAL

(TOP AND BOTTOM)

L - CHAMBER

M - TOP PLATE

N - VERTICAL TIE RODS

O - METER STICK

P - O-RING FLANGE SEAL

Q - UPPER VALVE

R - COVER PLATE

S - DIAL GAGE

T - GAGE HOLDER

U - GAGE HOLDER RODS

V - NEEDLE POINT MICROMETER

WATER LEVEL GAGE

Figure 21. Details of Triaxial Swelling Apparatus (after Parcher and Liu, 1965).

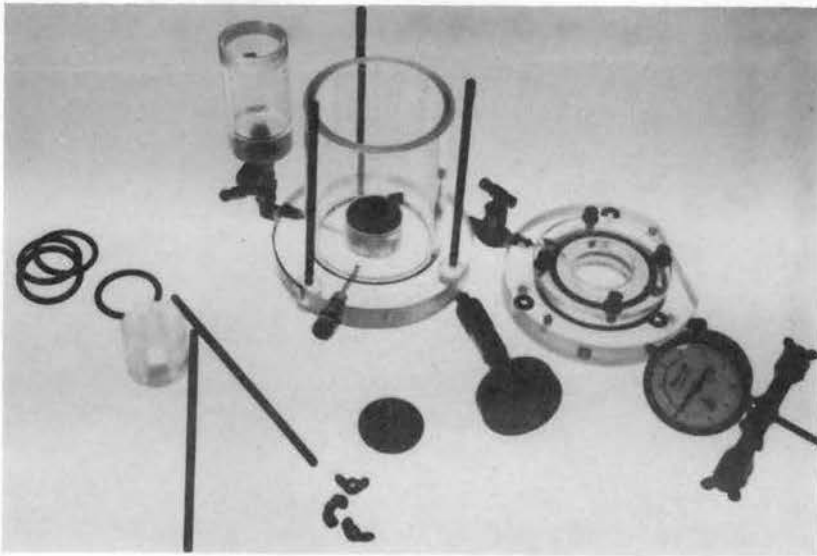


Figure 22. Parts of Triaxial Swelling Apparatus

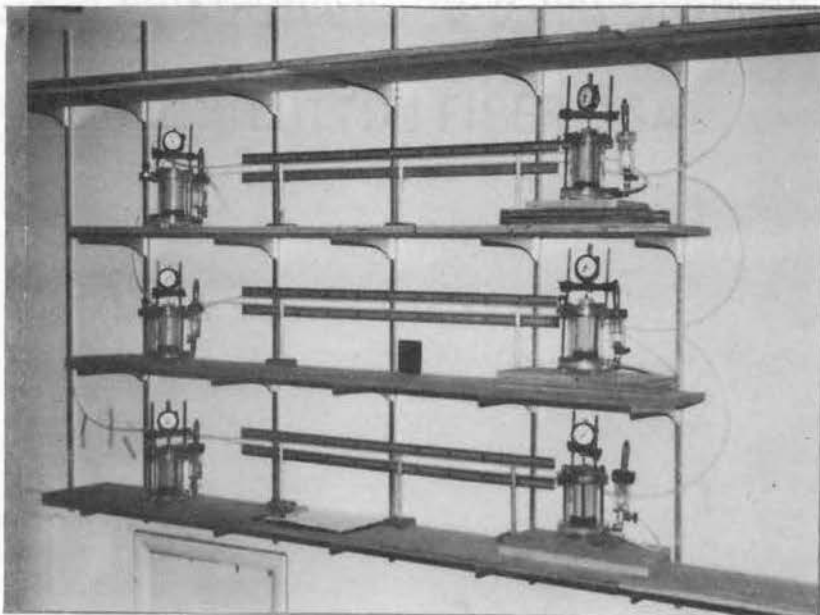


Figure 23. Test Assembly of Six Triaxial Swelling Apparatuses.

securely fixed to the base plate by means of tie rods and wingnut screws. The soil specimen to be tested is placed on the porous stone above the pedestal in the base plate. A hole drilled through the base plate permits the entry of water from the water reservoir into the soil. Another hole drilled through the base plate connects the chamber with the horizontal saran tube, in which the displacement of the air-water interface records the total radial swelling of the specimen. The soil specimen is fixed in place by means of a flanged rubber membrane whose flange is sandwiched between the top and cover plates. Water-leakage between the cover and top plates, top plate and chamber and chamber and base plate, is prevented by means of rubber O-rings. Gage-holders and gage-holder rods permit the attachment of a dial gage for the direct measurement of the vertical swelling. The top porous stone and the holes in the cap allow free escape of entrapped air during the swelling tests. The quantity of water absorbed by the soil during the swelling process is determined from observations of the drop in water reservoir level measured by a micrometer screw (least count 0.001 in.),

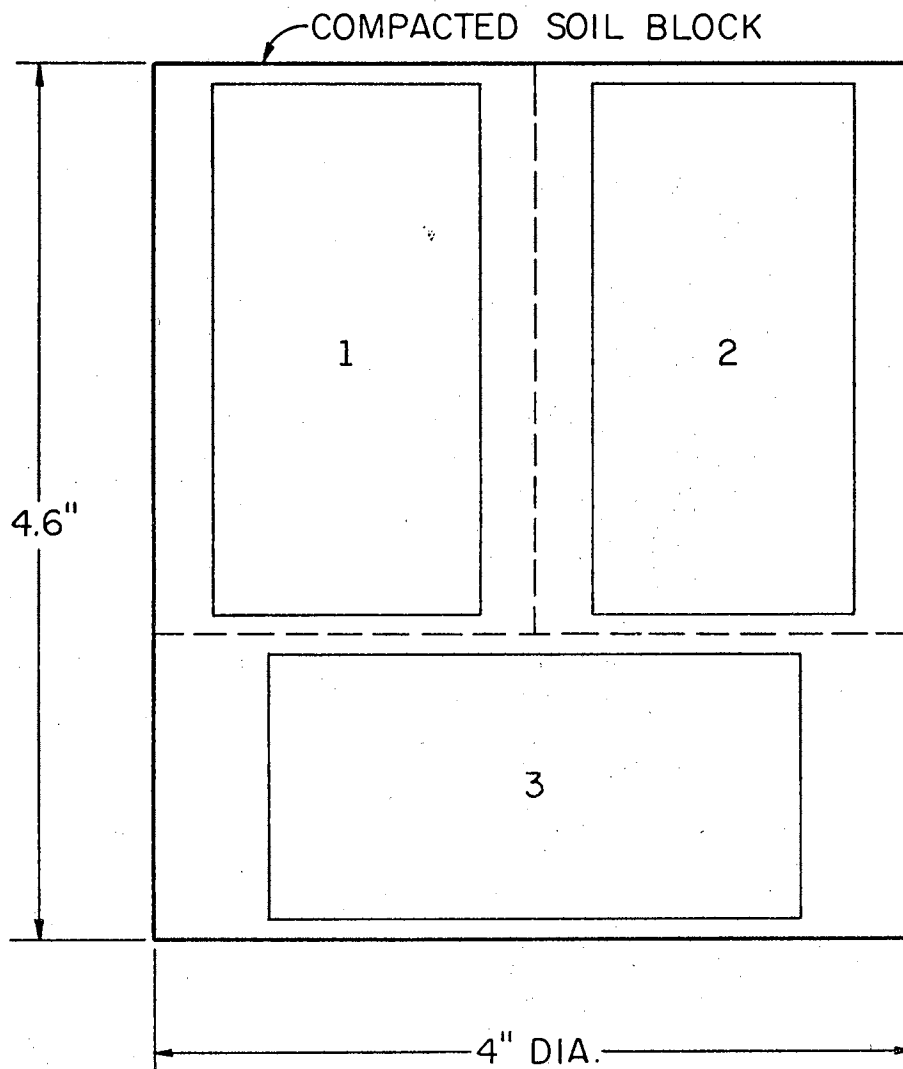
#### Preparation of Test Specimens

All the laboratory tests in this investigation utilized the locally abundant Permian clay, obtained from building excavations within the university campus. The raw soil was air-dried, pulverized and passed through US sieve No. 40 and the material passing No. 40 sieve was used in the preparation of the test specimens.

As outlined in Chapter I, the main aspect of this investigation is to study the swelling characteristics of compacted soil and to correlate the observed swelling behavior with the particle orientation.

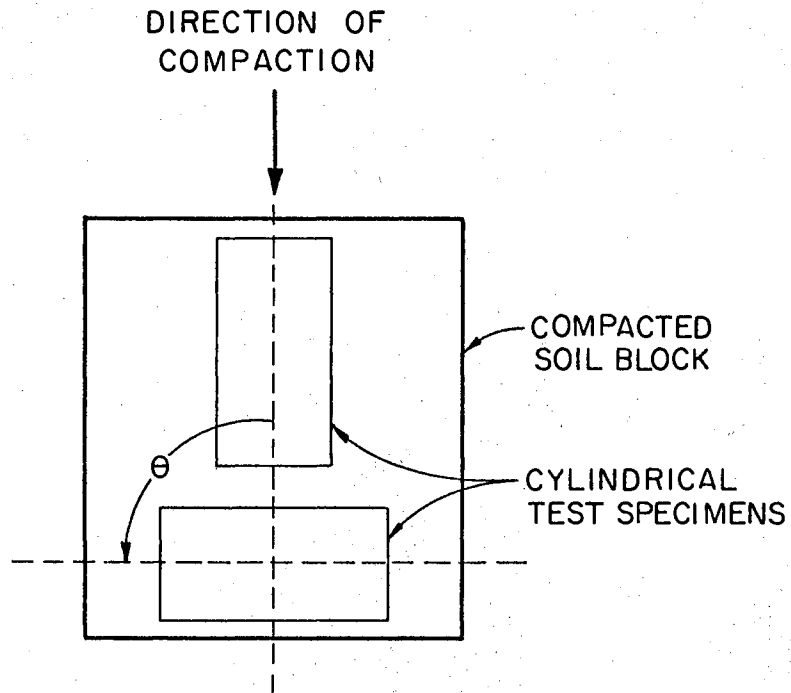
To achieve this objective, it is necessary to cut separate test specimens in two directions, namely one parallel to the direction of compaction and the other perpendicular to it. Therefore any method of compaction used should not only yield a remolded soil block of sufficient size to permit at least two test specimens to be cut out of it, but also be capable of producing variation in the soil fabric by controlling the compactive effort. These considerations led to the adoption of Standard and Modified AASHO compaction procedures for the preparation of the test specimens.

Soil blocks of 4 in. diameter and 4.6 in. height (standard Proctor mold size) were compacted using the Standard and Modified AASHO procedures. During compaction the molding water content was varied to include both the dry and wet sides of the optimum moisture content. Immediately after compaction, the soil block was ejected from the Proctor mold using a hydraulic compression machine. The required test specimens were trimmed out of this soil block as shown in Figure 24, using a special wire-saw and knives. Use of a split-Proctor mold with tightening screws, to hold the soil block during the trimming process was found to greatly assist the specimen preparation besides preventing breaking of the soil block. During this trimming process extreme precautions were taken to keep the disturbance of the soil fabric to a minimum. Also, special care was taken to mark off accurately the position of the test specimens at the desired orientation and to index them properly after trimming (Figure 25). Rectangular prisms of at least  $1\frac{5}{8}$  in. x 2 in x 3 in. size, in the required orientations were cut from the compacted soil blocks and these were properly indexed, waxed after wrapping in saran sheet and stored in a humid room until testing. In



1 AND 2: VERTICALLY ORIENTED SPECIMENS  
3: HORIZONTALLY ORIENTED SPECIMENS

Figure 24. Location of Test Specimen in Compacted Soil Block.



COMPACTION PROCEDURE	SPECIMEN DESIGNATION
STANDARD AASHO	$A_m - \theta - n$
MODIFIED AASHO	$B_m - \theta - n$

- $m$  - NUMBER OF COMPACTION SERIES  
 $\theta$  - ORIENTATION OF SPECIMEN, DEGREES  
 $n$  - NUMBER OF SPECIMEN

Figure 25. Designation of Test Specimens.



every compaction series an attempt was made to trim two test specimens— one parallel and the other perpendicular to the direction of compaction, although in many cases, particularly in blocks compacted dry of optimum, this could not be done as the block crumbled or cracked during trimming. However, only those soil prisms which could be trimmed without any perceptible damage or cracks were saved for the swelling tests. In some cases it was possible to extract two vertical specimens and one horizontal specimen and all of them were tested so as to have additional test data for checking the accuracy of the results. In order to distribute the influence of possible fabric variations within the compacted soil on the test data, the vertical and horizontal test specimens were cut alternately from the top and bottom portions of the soil block. The molding moisture content of the compacted specimens was determined using the shavings produced by the trimming process.

A minimum curing period of approximately a week between compaction and testing was allowed, so that there was sufficient time for uniform moisture distribution in the test specimen. In view of the limitations of test equipment and the longer duration of time required for the swelling tests, it was not possible to test the specimens in the same compaction series at the end of the same curing period. However, recognizing the fact that the magnitude of the swelling is dependent on the curing period, an accurate record was kept of the curing period allowed before each test.

All the swelling tests were performed using cylindrical specimens of about 1.4 in. diameter and 2.8 in. height, and the test specimen of the required size was prepared from the rectangular soil prisms stored. This final trimming to the correct size was made just before each test,

using special manually operated trimming equipment and with the help of a wire-saw and knives. As before, extreme care was taken to see that the test specimen was disturbed as little as possible, both during trimming and subsequent handling. Also, to prevent the loss of moisture by evaporation between the final trimming and the start of the test and consequent development of cracks, the specimen was wrapped in saran sheet and stored in a closed tare until the time of final placement in the test apparatus. In spite of these precautions, as there is a possibility of moisture loss during the final trimming, a second determination of moisture content, using the shavings of the final trimming, was made and this value was compared with the molding moisture content. It was found that the two moisture content determinations resulted in approximately the same values (average variation  $\pm 0.5\%$ ). To allow for the possible moisture redistribution during the curing period and the loss of moisture during the final trimming, the average of the two values was taken as representing the initial conditions of the test specimen.

#### Preparation of Flanged Membranes

The swelling tests require special flanged rubber membranes and these were made in the laboratory using liquid Latex, Type 1-V-10, supplied by General Latex and Chemical Corporation (of Ohio), Ashland, Ohio. Detailed procedures for the preparation of these flanged membranes in the laboratory and the other related information, may be obtained from the work of Post (1962). The technique followed in the preparation of the membranes for this investigation, was essentially the same as described by Post (1962) and consists of dipping a clean flanged glass

test tube of about 1.4 in. diameter in diluted liquid Latex and drying it - repeating this process several times until a membrane of the required thickness is obtained. The final thickness of the membrane is dependent on the dilution of the Latex solution as well as the number of dippings. Thicker membranes will be unsuitable for the swelling tests as they would offer greater restraint to the free swelling. A Latex-water mix in the ratio of 7:1 and about seven dipping and drying cycles were found to be satisfactory. The membranes used for the swelling tests, varied between 0.045 cm. and 0.050 cm. in thickness.

#### Apparatus Factors

#### Water Absorptivity of Plexiglas

The triaxial swelling apparatus is made essentially of Plexiglas. One of the important characteristics of Plexiglas is its water absorptivity, and Liu (1964) has reported that it can be as much as 0.6 percent by weight. This water absorptivity of Plexiglas, although small, will have an influence on the measured horizontal swelling.

To study the water absorption characteristics of Plexiglas, several tests were conducted, as part of this investigation, using Plexiglas units of different size, shape and surface roughness characteristics. These were kept immersed in water and the quantity of water absorbed was determined at different intervals of time, by directly weighing them, taking care to wipe the surface free of water. The results of these tests are shown in Figure 26. Plexiglas with smooth and rough surfaces in the ratio of about 10:1, was found to have a water absorptivity of approximately 0.3 percent on a weight basis. The results shown in Figure 26, indicate that the rate of water absorption of

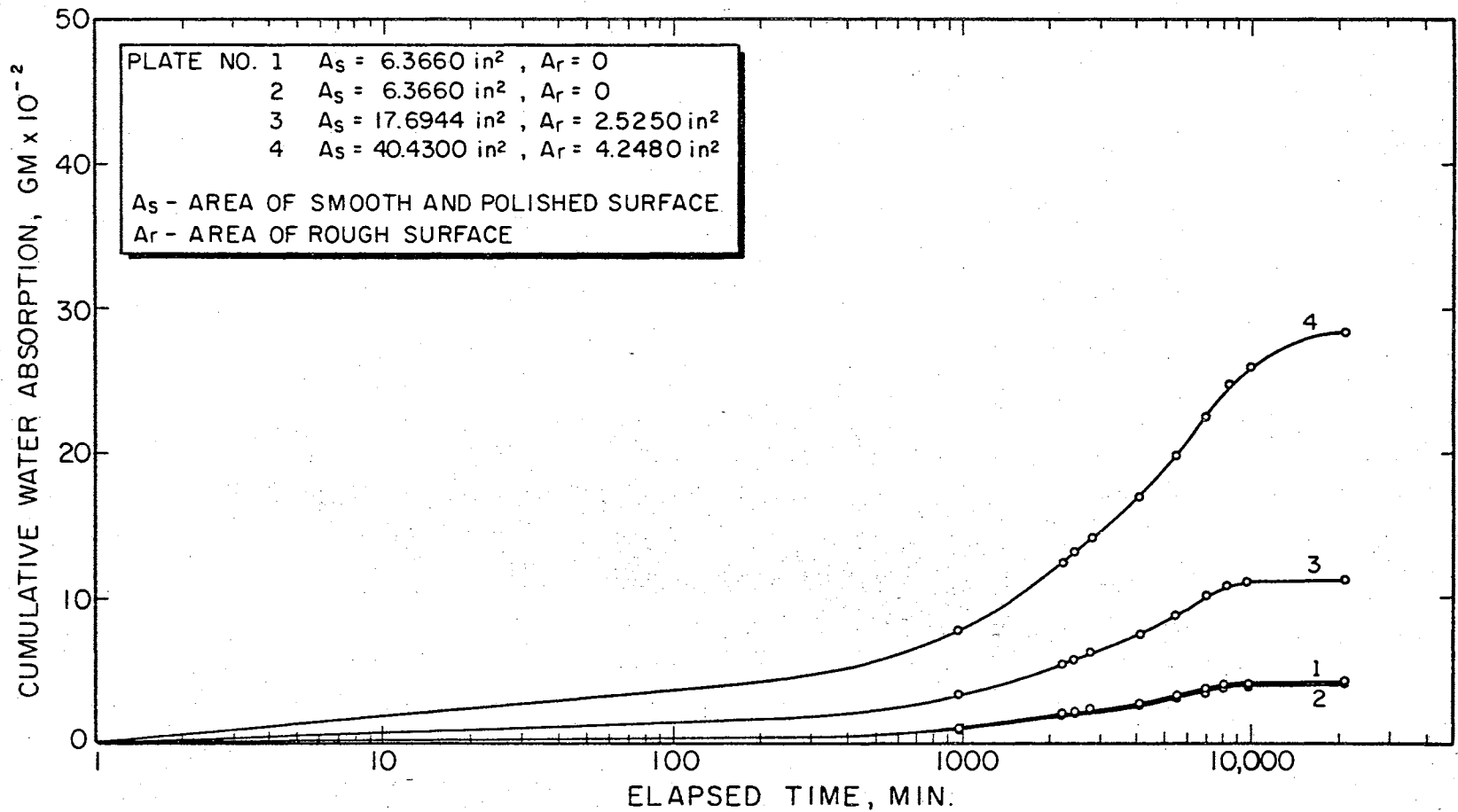


Figure 26. Water Absorptivity Curves for Plexiglas With Smooth and Rough Surfaces

Plexiglas varies with time - the rate of water absorption being maximum initially and tending to zero after considerable duration of time. Also, if the Plexiglas that has been subjected to wetting is allowed to dry, it loses water at a fast rate initially, the rate gradually decreasing with time (Figure 27). The triaxial swelling apparatus has about 48.57 sq.in. of smooth surface and 3.41 sq. in. of rough surface exposed to water and the resulting water absorption would have an influence on the saran tube readings.

To eliminate the effect of water absorptivity of Plexiglas on the test results, Liu (1964) conducted a series of calibration tests for the triaxial swelling apparatus and applied a correction factor to the measured saran tube readings, taking into account the time and duration of the tests. As the rate and quantity of water absorption is a function of time, it is essential to consider the duration of each test as well as the time lag between tests - that is the time during which the apparatus is kept idle as it represents the drying cycle. Also the correction factor based on the calibration curves has to be applied for all the saran tube readings of each test. This procedure is obviously time consuming and therefore was not adopted in the present study.

Instead, all the components of the apparatus were kept immersed in water for several days before the start of the tests, thus permitting complete saturation of the Plexiglas, and the swelling tests were started after this initial soaking. As the rate of water absorption virtually ceases after prolonged soaking, there will be practically no further water absorption during the test and consequently the measured swelling data will not require any correction. The same is true for all the subsequent tests also, as the absorbing surfaces are continuously in

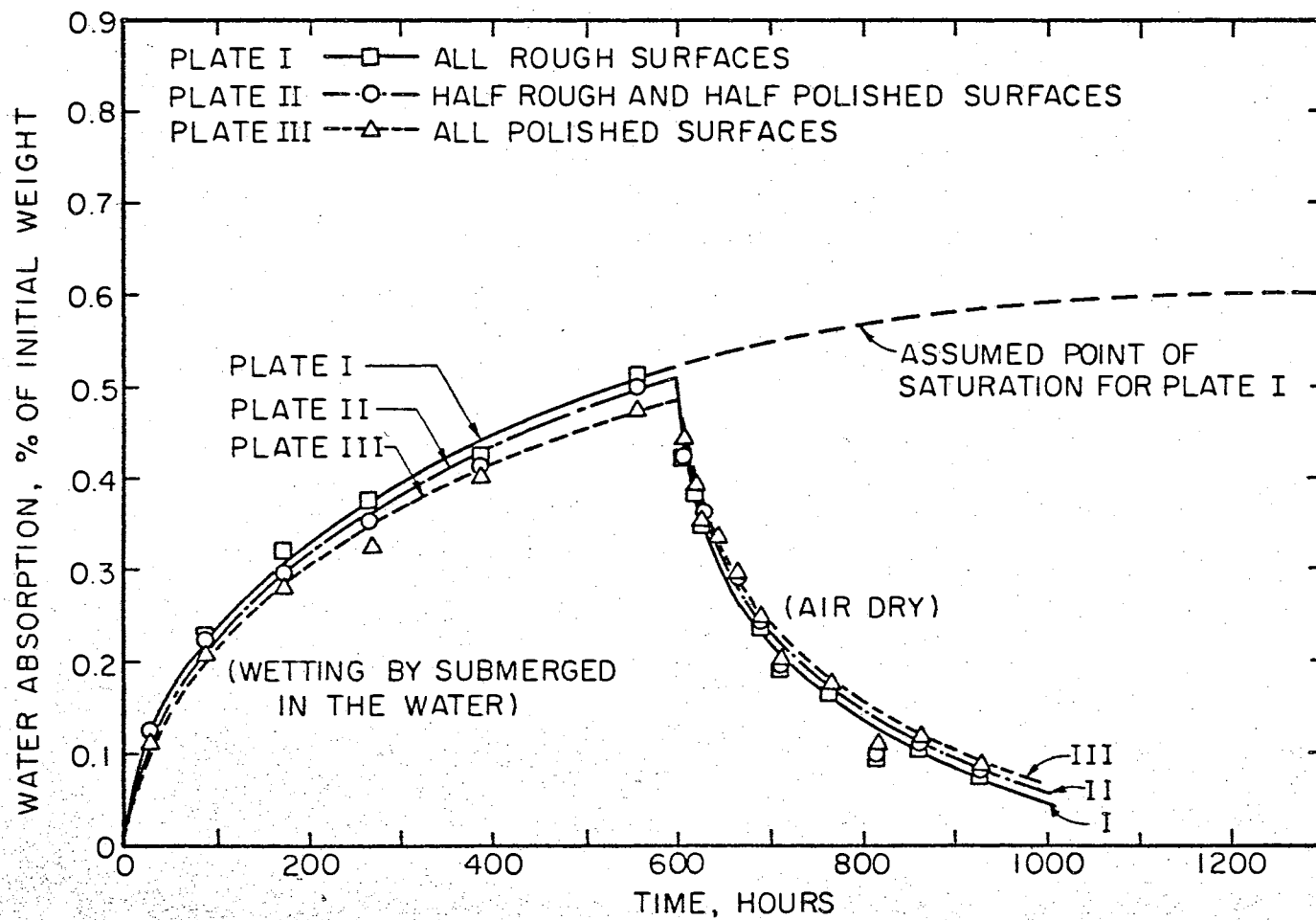


Figure 27. Water Absorptivity Curves for Plexiglas (after Liu, 1964)

contact with water. To avoid the possibility of water loss by drying during the idle period between successive tests, the components of the apparatus were kept immersed in water until the start of the next test. This test procedure, besides eliminating the possible influence of water absorptivity of Plexiglas on the test results, greatly facilitated the main test program and subsequent data analysis.

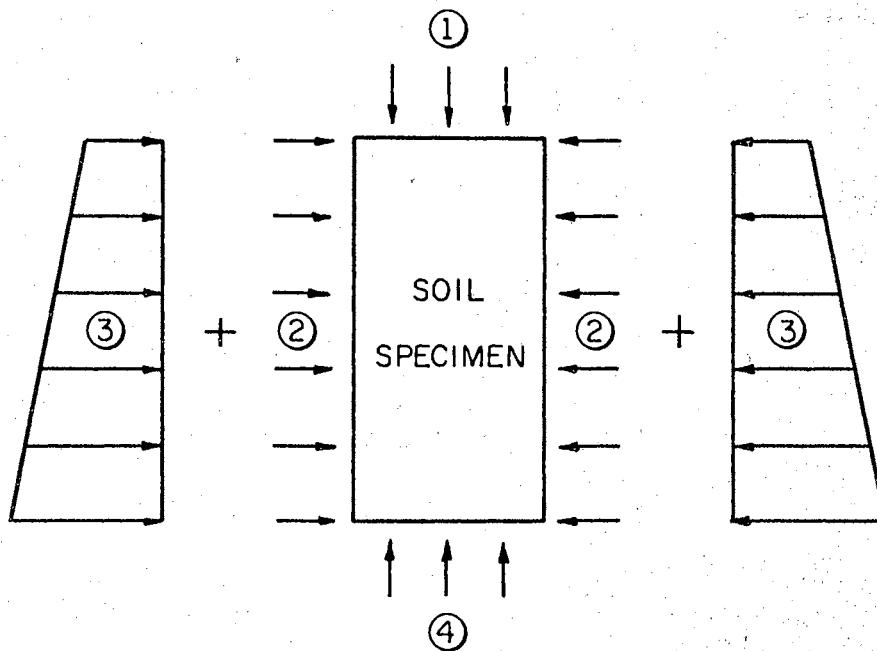
#### Water Loss Through Plexiglas by Diffusion

Although plastics, which are commonly used in the construction of laboratory equipment, can be considered as practically impervious to water movement, recent published experimental data indicate that the loss through them by diffusion may be significant, particularly in tests involving considerable duration of time (Willis, Nielsen and Biggar, 1965). They have reported an average diffusion coefficient of  $8 \times 10^{-6}$  cm<sup>2</sup>/sec for water through 0.053, 0.129 and 0.250 inch thick acrylic plastics. However in the present investigation, this aspect was not considered as the loss of water by diffusion, if any, would be insignificant for the test duration normally adopted.

#### Restraints to Free Swelling

The restraints to the free swelling of the specimen in the tri-axial swelling apparatus are shown in the Figure 28. These are:

- 1) A constant vertical downward force at the top of the specimen due to the dial gage and the weight of the top porous stone and cap.
- 2) A lateral restraint due to the rubber membrane which may vary along the length of the specimen owing to its fixity at the ends.



- ① DIAL GAGE RESISTANCE AND WEIGHT OF POROUS STONE AND CAP
- ② RESISTANCE OF RUBBER MEMBRANE
- ③ CHAMBER WATER PRESSURE
- ④ HYDROSTATIC PRESSURE OF ENTERING WATER

Figure 28. Restraints to Free Swelling of Soil Specimen in Triaxial Swelling Apparatus



- 3) A nonuniform lateral hydrostatic pressure varying linearly with the height of the specimen.
- 4) A nonuniform hydrostatic upward pressure at the bottom of the specimen due to the water column in the water reservoir, whose height decreases with the elapsed time from the start of the test.

Consequently the tests performed using this apparatus are not strictly free swelling tests, although they are in this study referred as such. The influence of these restraints on the swelling are not known. However Parcher and Liu (1965) have reported that the resistance due to the dial gage is approximately equal to that of the lateral hydrostatic pressure. In view of the fact that perfectly idealized conditions for the free swelling tests cannot be simulated in the laboratory, these restraints should be considered as inherent in the testing procedure involved. In any case, the restraints probably do not exceed a maximum value of about  $10 \text{ g/cm}^2$ .

#### Test Procedure

During the swelling tests, the magnitudes of both the vertical and horizontal swelling were simultaneously determined. The vertical swelling was measured directly by a dial gage while the horizontal swelling was computed from the horizontal volumetric displacement of the soil as reflected by the movement of air-water interface in the saran tube. As water is used in the chamber as a medium for recording the volumetric displacement, it is essential to de-air the apparatus before the test, as otherwise, the saran tube readings would be affected by the air entrapped in the connections. Complete instructions for de-airing the apparatus and other detailed procedures for this test, were

originally suggested by Professor Parcher and these were described by Fost (1962) and Liu (1964).

The procedure followed in all the swelling tests was essentially the same as given by Liu (1964). The saran tube, used to measure the water displacement was of regular laboratory polyvynyl tubing. Each piece of equipment was initially calibrated to evaluate the apparatus constants such as water reservoir radius and saran tube capacity. As discussed earlier, in order to eliminate the influence of water absorp-tivity of Plexiglas components of the apparatus on the test results, all the components of the apparatus were soaked in water before starting the test for the first time and in between successive tests. Also to reduce water absorption by the porous stones which will introduce an error in the estimated water intake, the porous stones were initially kept im-mersed in distilled-de-aired water and were wiped clean before use. Only distilled-de-aired water was used in the water reservoir so as to dissolve at least part of the air in the soil pores, as the soil absorbs water during swelling. De-airing of the water was done by applying vacuum to the container for at least 10 minutes, by means of a vacuum pump. As de-aired water would absorb air readily upon exposure and on prolonged storage, only the water needed for each test was de-aired at one time.

The test assembly used in this study is shown in Figure 23. In order to facilitate the de-airing of the equipment before the test and to prevent movement of the saran tube during the test, the saran tube and the attached scale were kept fixed on the wall with wire clips, in-stead of fixing one end to the apparatus and supporting the other end by independent supports. However, care was taken to see that the saran

tube was at about the same elevation as the top of the water chamber of the equipment as assembled, so that the test specimen will not be subjected to any additional lateral hydrostatic pressure due to the elevation of the saran tube.

The use of filter strips along the sides of a test specimen, to accelerate the rate of swelling, was suggested by Parcher and Liu (1965) and their experimental data indicate that the specimen with filter strips swelled at a much faster rate than the one without filter strips - the magnitude of the ultimate swelling remaining approximately the same for both (Figure 29). Most of the tests in this study were, therefore, done using filter strips to speed up the rate of swelling and to reduce the testing time. Strips of about 1 cm. wide cut out of large size circular filter papers or the commercially available chromatography paper strips were found to be satisfactory for this purpose. Some tests were, however, done without filter strips in connection with the study of moisture variation along the test specimen.

During the final trimming of the test specimens, it was not always possible to maintain a constant diameter for all the specimens. Therefore the diameter of the samples were accurately determined at three places (top, middle and bottom) with a vernier caliper (least count: 1/128 in.) and the mean value was taken. A similar procedure was used in finding the final diameter of the samples although accurate determination was not possible owing to the very moist condition of the specimen after swelling.

Final moisture content determinations were made by extracting samples from the top and bottom of the swollen samples. The two values did not differ much in tests with filter strips although an appreciable

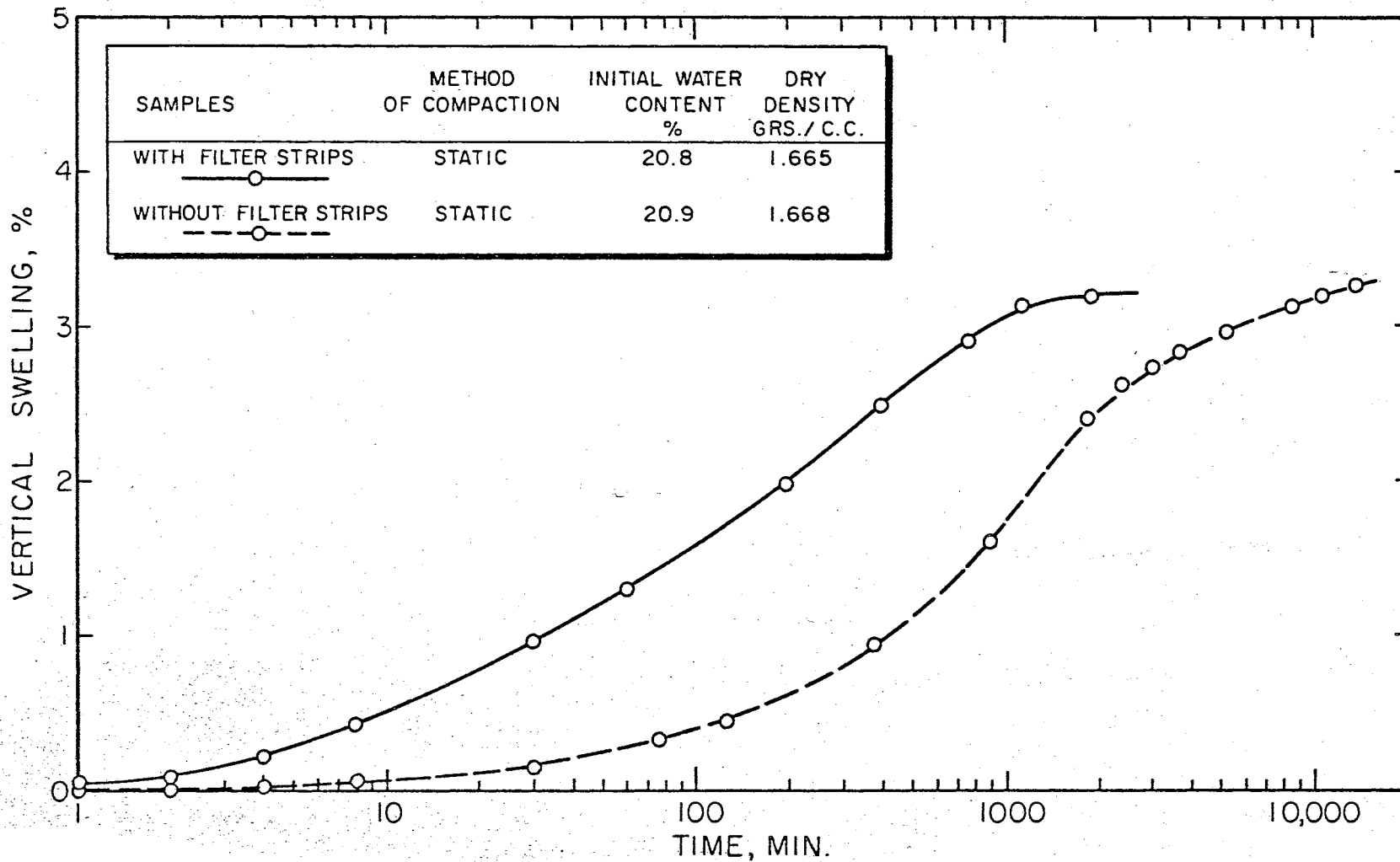


Figure 29. Time Period Required for Swelling for Specimens With and Without Filter Strips (after Liu, 1964).

difference was noticed in tests without filter strips. This is believed to be due to the enhanced drainage conditions obtained with the use of filter strips as compared to the other case. However, the average of the two values was taken for the final analysis of the swelling test data.

Determination of the weight of the rubber membrane used, before and after each test revealed that the water absorption by the membrane was negligible.

The various observational data recorded during the swelling tests included the following:

1. Details of test specimen

Method of compaction, specimen orientation with respect to the direction of compaction, curing period, molding, initial and final moisture contents and size and weight of specimen before and after test.

2. Details of apparatus

Saran tube capacity, diameter of water reservoir and initial and final weight of rubber membrane.

3. Test observations

Time, dial reading, movement of the air - water interface in the saran tube and the drop in water level in the water reservoir at different time intervals.

## Data and Discussion

From the experimental results, the various physical quantities characterizing the swelling behavior of compacted specimens were computed using the expressions summarized in Table III. The derivations for

TABLE III

## DEFINITIONS RELATING TO TRIAXIAL SWELLING TEST

PHYSICAL QUANTITY	SYMBOL	DEFINITION
UNIT VERTICAL SWELLING	$\epsilon_v$	$\frac{\Delta H}{H}$
UNIT HORIZONTAL SWELLING	$\epsilon_h$	<p><u>ACCURATE:</u></p> $\sqrt{1 + \frac{C \cdot \Delta R}{\pi r^2 H (1 + \epsilon_v)}} - 1$ <p><u>APPROXIMATE:</u> (LIU, 1964; PARCHER AND LIU, 1965)</p> $\frac{C \cdot \Delta R}{2\pi r^2 H (1 + \epsilon_v)}$
VOLUME INCREASE	$\Delta V$	$\pi r^2 H [\epsilon_v + \epsilon_h (1 + \epsilon_v) (2 + \epsilon_h)]$
VOLUMETRIC SWELLING	$\eta$	$\epsilon_v + \epsilon_h (1 + \epsilon_v) (2 + \epsilon_h)$
SWELL-INTAKE RATIO		$\frac{r^2 H}{R_c^2 \Delta \alpha} [\epsilon_v + \epsilon_h (1 + \epsilon_v) (2 + \epsilon_h)]$
SWELLING RATIO		<p><u>FOR VERTICAL SPECIMENS:</u> (LIU, 1964; PARCHER AND LIU, 1965)</p> $\frac{\epsilon_v}{\epsilon_h}$ <p><u>FOR COMPACTED SOIL:</u></p> $\frac{\epsilon_o}{\epsilon_{90}}$ <p>(COMPUTATION BASED ON TEST DATA OF ORIENTED SPECIMENS HAS LIMITATIONS)</p>

these expressions are presented in Appendix A. The entire data analysis was done with the aid of IBM-360 computer available in the Oklahoma State University Computer Center.

As described earlier, cylindrical test specimens of approximately 1.4 in. diameter and 2.8 in. height were used in the swelling tests. The average initial moisture content and dry density of the test specimens as well as their final moisture contents are given in Tables IV and V. For each test specimen, the magnitudes of the unit vertical swelling,  $\epsilon_v$ , and the unit horizontal swelling,  $\epsilon_h$ , were computed at different time intervals. Typical swelling - time curves developed for the oriented test specimens are presented in Figures 30 through 35. In Figure 30 are shown the swelling - time curves for two specimens compacted by Standard AASHO procedure - one cut parallel to the direction of compaction and the other perpendicular to it. Similar curves for specimens compacted by Modified AASHO procedure are given in Figure 31. These figures illustrate the variations of the unit vertical and horizontal swelling with time. The swelling process is time - dependent and the time period required for swelling is a function of the physico-chemical interactions within the system as well as the permeability. The results in Figures 30 and 31 indicate that the rate of swelling is high during the initial stages of tests and that it decreases rapidly with time. After considerable lapse of time the rate of swelling decreases and becomes practically zero.

The structure of compacted soil is dependent on the method of compaction, the compactive energy and the molding water content. Previous studies have demonstrated the effect of particle arrangement on the swelling characteristics of compacted soils (e.g., Seed and Chan,

TABLE IV

## DETAILS OF TEST SPECIMENS-STANDARD AASHO COMPACTION

Specimen Number	Orientation Degrees	Initial Conditions		Final Moisture Content %
		Average Moisture Content %	Dry Density g/cc	
A1-0-1	0	10.74	1.683	35.41
A3-90-2	90	13.57	1.679	30.80
A4-0-1	0	14.79	1.661	29.59
A4-0-2	0	14.60	1.638	30.34
A4-90-1	90	14.83	1.668	28.10
A11-0-1	0	17.63	1.684	29.57
A11-0-2	0	17.70	1.697	29.80
A11-90-1	90	17.55	1.759	30.11
A14-0-1	0	20.30	1.697	30.08
A14-90-1	90	19.90	1.704	31.09
A15-0-1	0	23.69	1.605	29.88
A15-90-1	90	23.50	1.595	30.84
A16-0-1	0	25.56	1.539	30.88
A16-90-1	90	25.44	1.577	31.11
A17-0-1	0	18.30	1.652	33.78
A17-90-1	90	18.39	1.708	31.24
A20-0-1	0	15.71	1.729	33.26



TABLE IV (continued)

A20-0-2	0	15.82	1.697	34.32
A20-90-1	90	15.51	1.556	41.49
A21-0-1	0	18.07	1.720	32.02
A21-0-2	0	18.25	1.718	31.25
A21-90-1	90	18.01	1.600	33.98
A22-0-1	0	18.04	1.676	32.22
A22-0-2	0	17.96	1.654	29.50
A22-90-1	90	17.96	1.645	34.55
A23-0-1	0	20.95	1.658	30.66
A23-0-2	0	20.86	1.645	31.52
A23-90-1	90	20.71	1.655	30.89
A24-0-1	0	18.64	1.673	32.21
A24-0-2	0	18.73	1.628	33.02
A24-90-1	90	18.63	1.538	34.67

---

TABLE V

## DETAILS OF TEST SPECIMENS-MODIFIED AASHO COMPACTION

Specimen Number	Orientation Degrees	Initial Conditions		Final Moisture Content %
		Average Moisture Content %	Dry Density g/cc	
B1-0-2	0	17.20	1.680	25.70
B1-90-1	90	16.53	1.707	25.50
B2-0-1	0	14.14	1.858	24.76
B2-0-2	0	14.32	1.906	23.71
B2-90-1	90	14.48	1.838	23.19
B3-0-1	0	11.75	1.815	22.23
B3-0-2	0	11.73	1.817	24.49
B4-0-1	0	14.39	1.846	22.83
B6-0-1	0	14.16	1.877	22.06
B6-90-1	90	13.41	1.948	23.44
B8-0-1	0	15.10	1.727	24.61
B8-0-2	0	15.59	1.803	22.89
B8-90-1	90	15.48	1.801	24.46
B9-0-1	0	15.04	1.724	22.87
B9-0-2	0	15.22	1.827	24.66
B9-90-1	90	14.57	1.964	24.63
B10-0-1	0	13.79	1.912	30.62

TABLE V (continued)

B10-90-1	90	13.94	1.899	28.77
B11-0-1	0	16.73	1.818	27.30
B11-90-1	90	16.37	1.782	26.97
B12-0-1	0	18.45	1.796	24.96
B12-90-1	90	18.46	1.723	26.34
B13-0-1	0	17.66	1.757	25.46
B13-90-1	90	17.41	1.815	25.32
B14-0-1	0	15.26	1.891	28.77
B14-90-1	90	15.21	1.871	28.81
B15-0-1	0	16.74	1.853	26.62
B15-90-1	90	16.60	1.849	26.46
B16-0-1	0	19.25	1.743	27.88
B16-90-1	90	19.07	1.745	27.84
B17-0-1	0	19.89	1.723	26.71
B17-90-1	90	20.63	1.702	28.50
B25-0-1	0	15.84	1.843	28.73
B25-0-2	0	16.16	1.848	29.66
B25-90-1	90	15.86	1.872	28.50
B26-0-1	0	17.99	1.777	28.13
B26-0-2	0	17.67	1.780	29.44
B26-90-1	90	17.52	1.792	27.63
B27-0-1	0	19.51	1.726	30.52
B27-0-2	0	19.52	1.721	28.42
B27-90-1	90	19.21	1.740	29.80

---

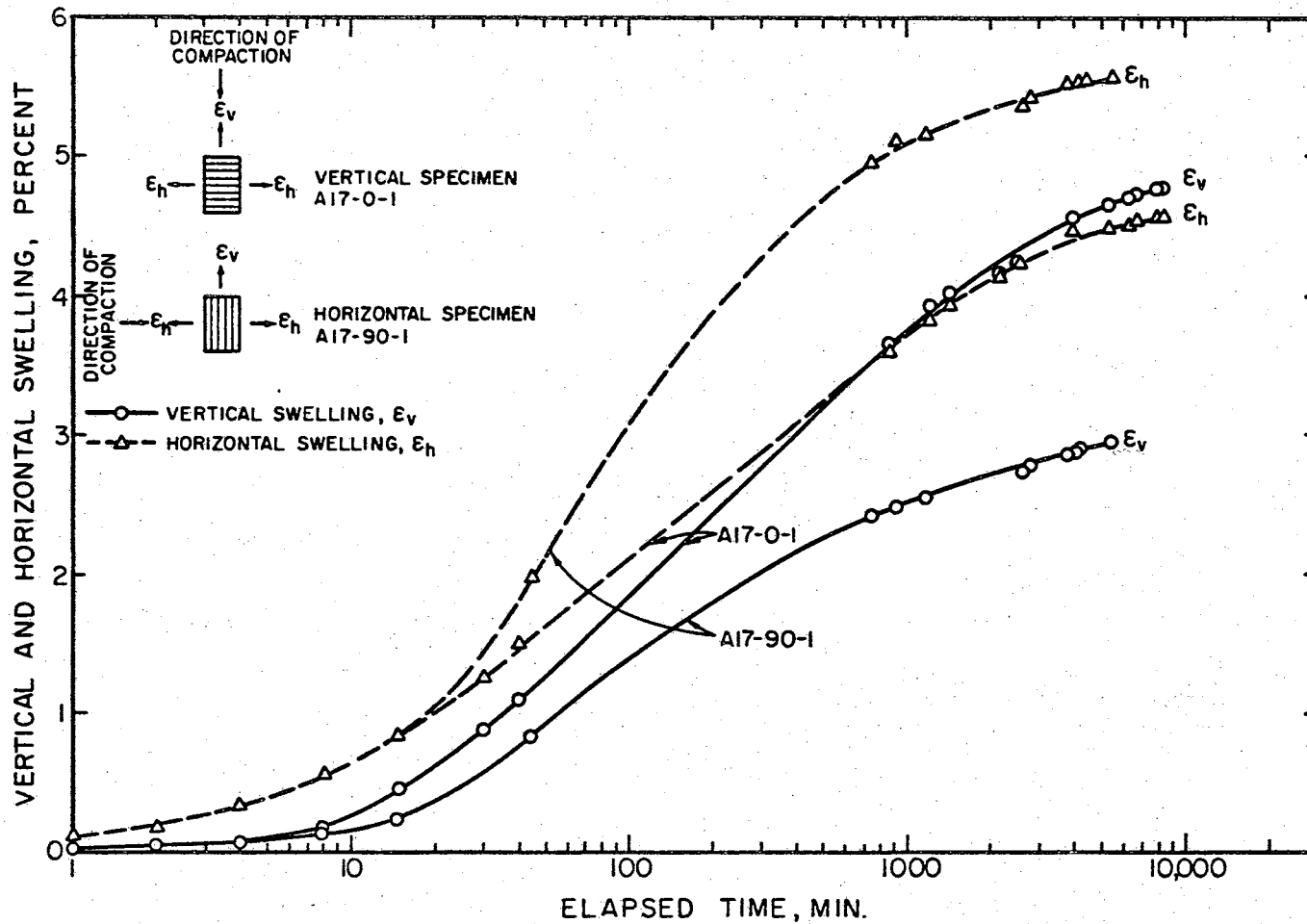


Figure 30. Swelling-Time Curves for Oriented Specimens - Standard AAHSO Compaction

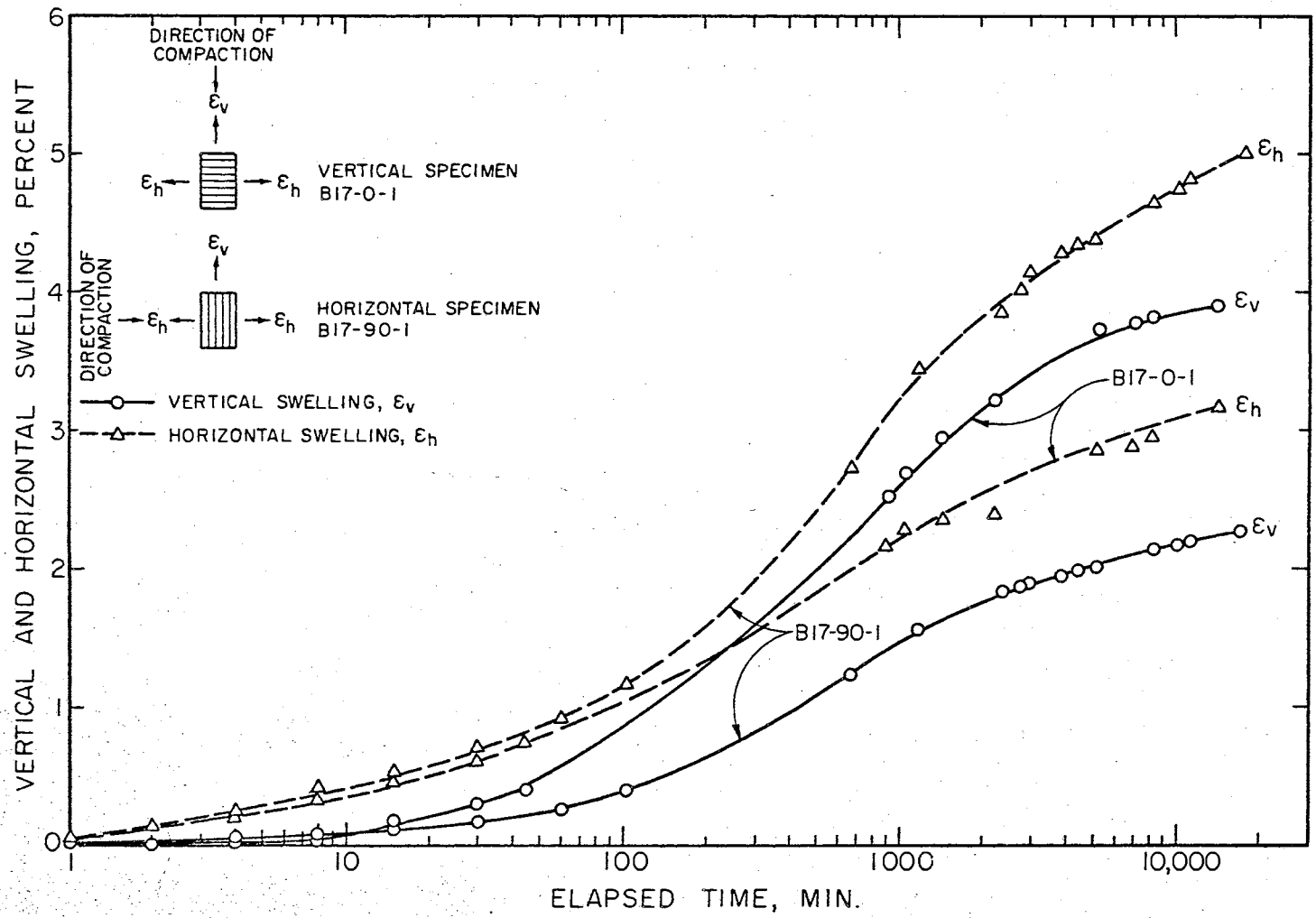


Figure 31. Swelling-Time Curves for Oriented Specimens - Modified AASHO Compaction

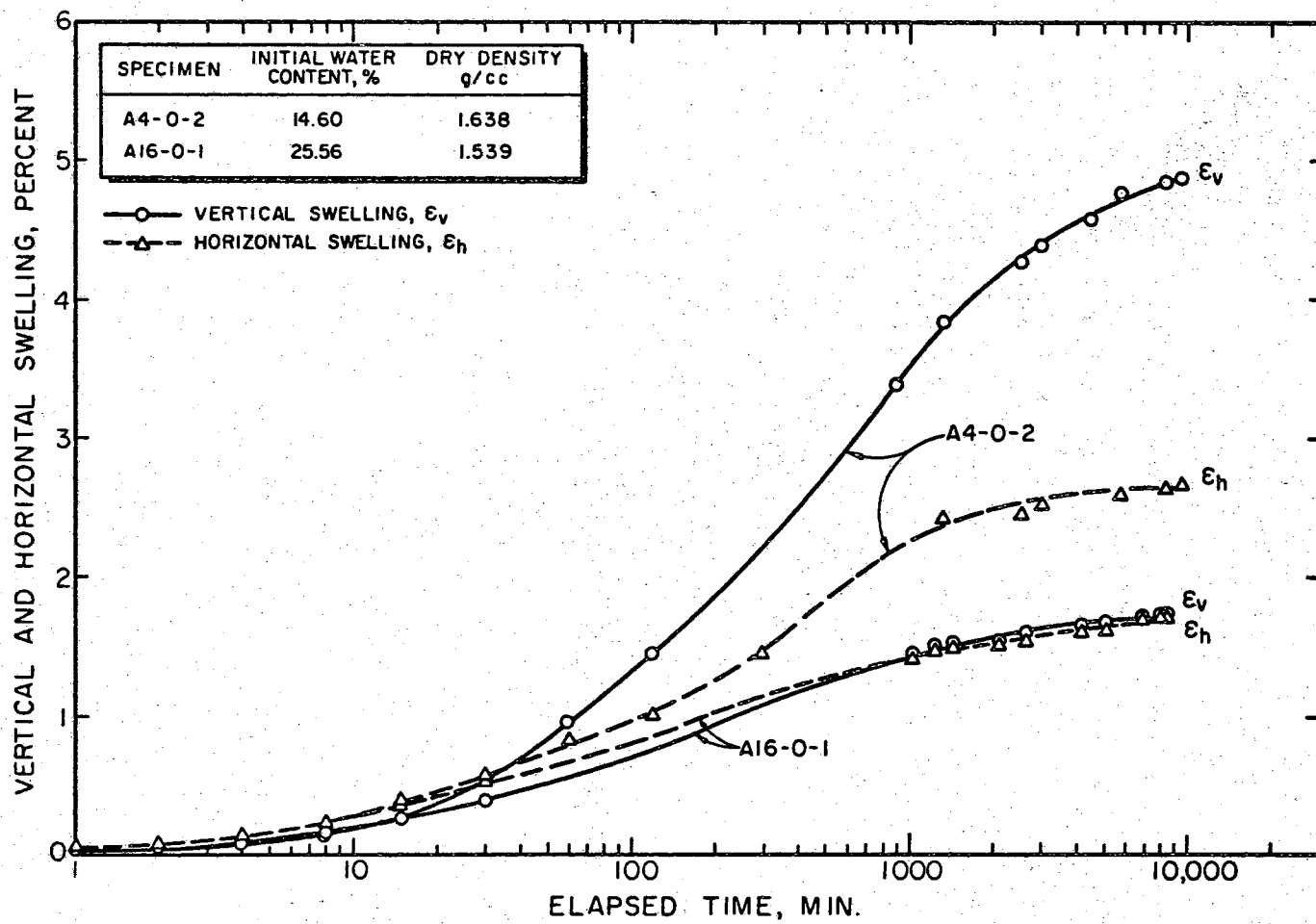


Figure 32. Swelling-Time Curves for Vertical Specimens at Different Initial Moisture Contents - Standard AASHO Compaction.

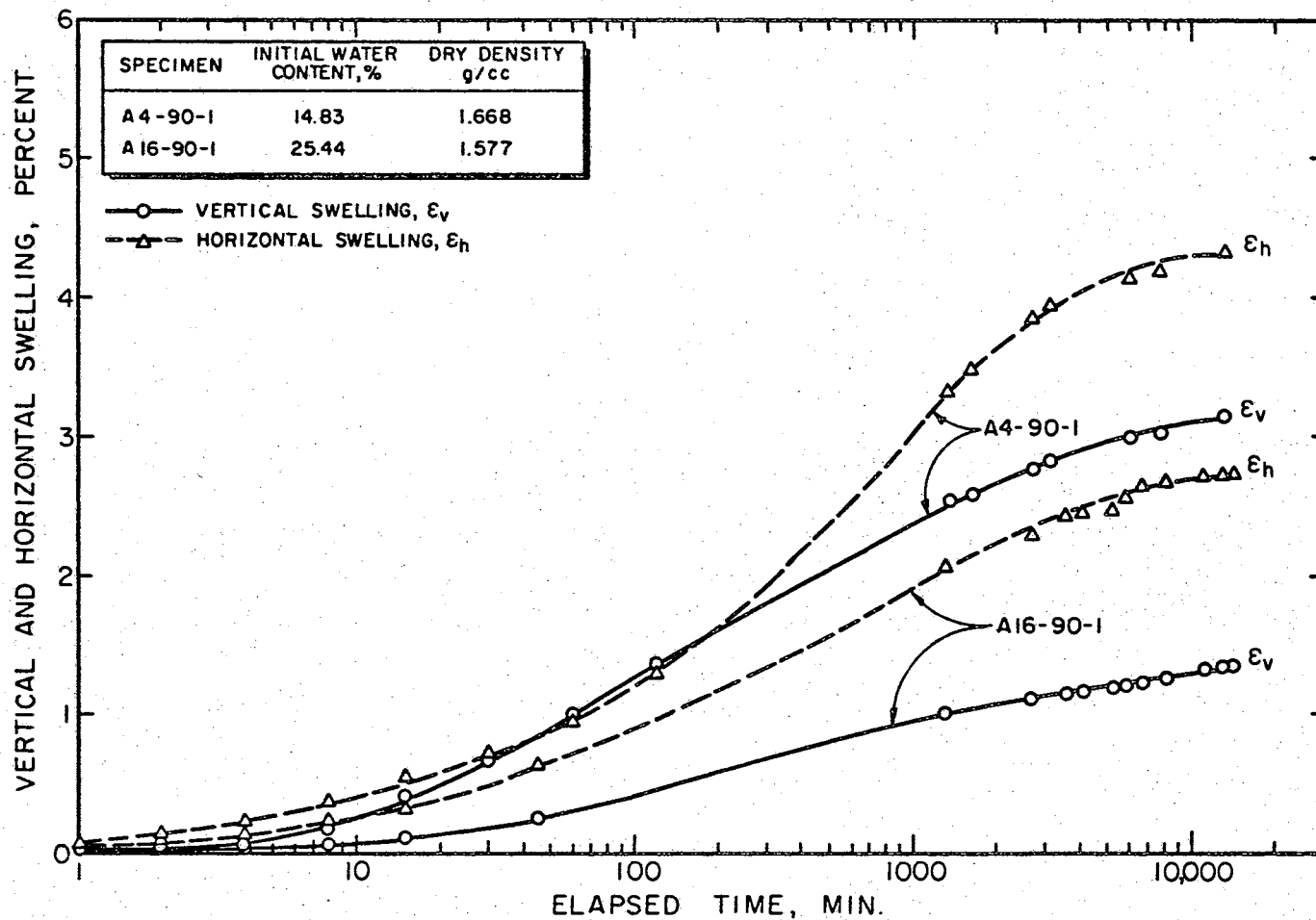


Figure 33. Swelling-Time Curves for Horizontal Specimens at Different Initial Moisture Contents - Standard AASHO Compaction.

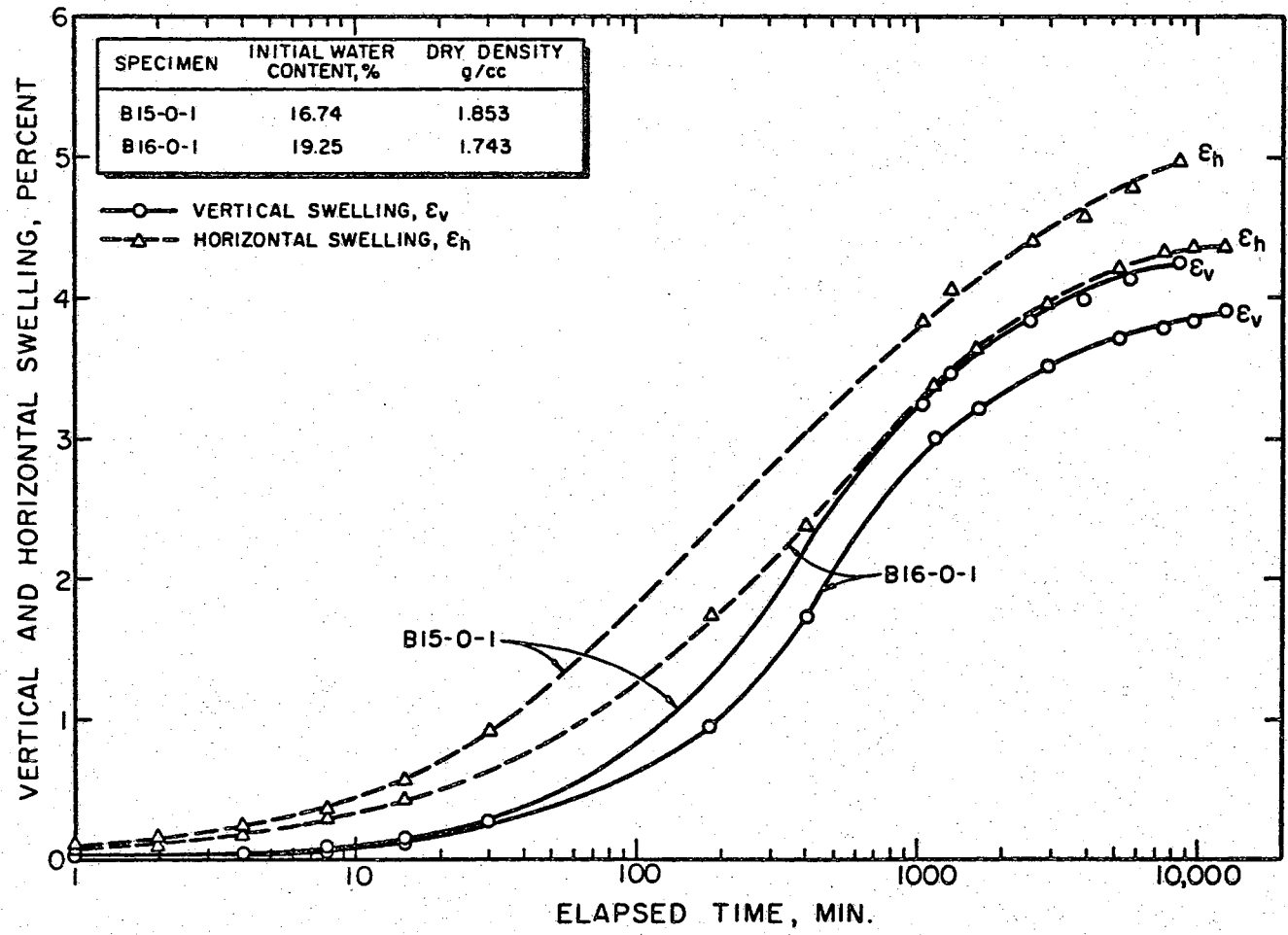


Figure 34. Swelling-Time Curves for Vertical Specimens at Different Initial Moisture Contents - Modified AASHO Compaction.



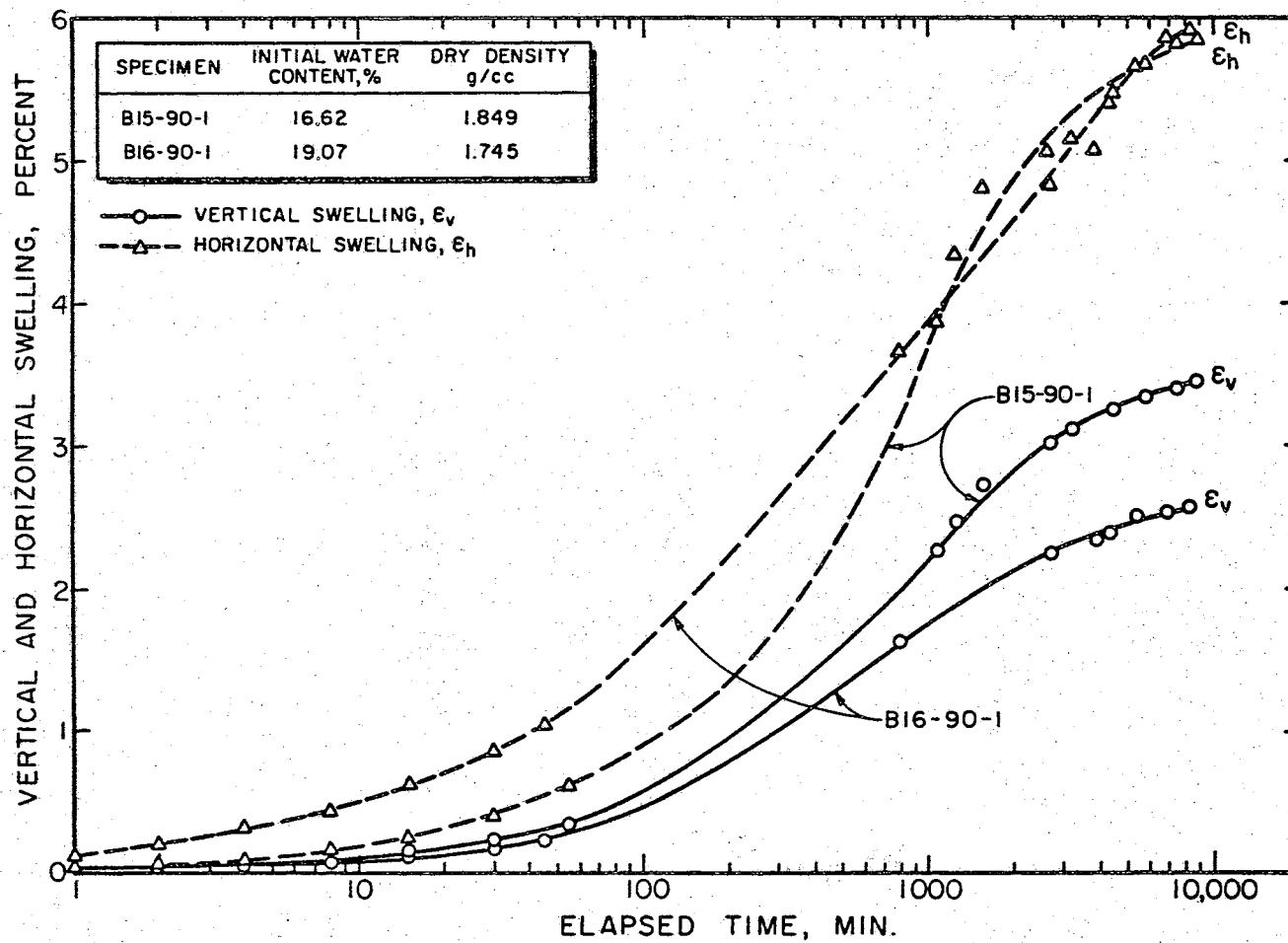


Figure 35. Swelling-Time Curves for Horizontal Specimens at Different Initial Moisture Contents - Modified AASHO Compaction.

1961; and Parcher and Liu, 1965). Figures 30 through 35 illustrate the influence of structural anisotropy on the swelling characteristics of compacted soils. It can be observed that the magnitudes of the unit vertical and horizontal swelling vary considerably for specimens cut at different orientations with respect to the direction of compaction.

The unit vertical swelling of a vertically oriented specimen,  $(\epsilon_v)_0$ , corresponds to swelling parallel to the direction of compaction,  $\epsilon_0$ , while the horizontal or radial swelling,  $(\epsilon_h)_0$ , represents the swelling perpendicular to the direction of compaction,  $\epsilon_{90}$  (Figure 42). However, if we consider a horizontally oriented specimen, the values of the unit horizontal and vertical swelling,  $(\epsilon_h)_{90}$  and  $(\epsilon_v)_{90}$ , would correspond respectively to the swelling parallel and perpendicular to the direction of compaction ( $\epsilon_0$  and  $\epsilon_{90}$ ). Consequently one might anticipate that the unit vertical and horizontal swelling of the vertically cut specimen would be equal respectively to the unit horizontal and vertical swelling of the horizontally cut specimen. However the test results shown in Figure 30 through 35 indicate that this is not generally true. It is seen that there is an appreciable difference between the  $(\epsilon_v)_0$  and  $(\epsilon_h)_{90}$  values as also between  $(\epsilon_h)_0$  and  $(\epsilon_v)_{90}$ . Similar anomaly was noticed in all the swelling tests in this investigation (Tables VI and VII). The reason for the observed difference in the swelling values of the oriented specimens may be due to variations in the soil structure and/or experimental errors. These aspects are discussed in detail elsewhere.

The effect of the initial moisture content on the rate and amount of swelling of compacted soil specimens, is illustrated in

TABLE VI

## SUMMARY OF SWELLING TEST DATA-STANDARD AASHO COMPACTION

Specimen Number	Orientation Degrees	Unit Vertical Swelling, $\epsilon_v$ %	Unit Horizontal Swelling, $\epsilon_h$ %
A1-0-1	0	4.863	4.373
A3-90-2	90	2.968	4.266
A4-0-1	0	4.666	2.994
A4-0-2	0	4.888	2.689
A4-90-1	90	3.146	4.306
A11-0-1	0	3.679	5.128
A11-0-2	0	3.697	5.394
A11-90-1	90	3.297	7.550
A14-0-1	0	3.161	4.929
A14-90-1	90	2.724	6.018
A15-0-1	0	1.802	2.987
A15-90-1	90	1.748	3.458
A16-0-1	0	1.713	1.713
A16-90-1	90	1.362	2.743
A17-0-1	0	4.780	4.566
A17-90-1	90	2.953	5.552
A20-0-1	0	5.871	6.265
A20-0-2	0	5.009	7.899

TABLE VI (continued)

A20-90-1	90	4.262	7.469
A21-0-1	0	4.902	7.868
A21-0-2	0	3.887	6.394
A21-90-1	90	3.179	5.324
A22-0-1	0	4.226	6.954
A22-0-2	0	3.922	4.627
A22-90-1	90	3.608	6.988
A23-0-1	0	2.900	3.578
A23-0-2	0	3.221	3.858
A23-90-1	90	2.367	4.770
A24-0-1	0	4.122	7.067
A24-0-2	0	3.028	4.740
A24-90-1	90	2.378	5.650

---

TABLE VII

## SUMMARY OF SWELLING TEST DATA-MODIFIED AASHO COMPACTION

Specimen Number	Orientation Degrees	Unit Vertical Swelling, $\epsilon_v$ %	Unit Horizontal Swelling, $\epsilon_h$ %
B1-0-2	0	2.031	2.248
B1-90-1	90	1.076	3.479
B2-0-1	0	2.578	1.951
B2-0-2	0	2.785	1.815
B2-90-1	90	2.174	3.336
B3-0-1	0	3.951	2.097
B3-0-2	0	3.643	2.020
B4-0-1	0	2.796	2.098
B6-0-1	0	2.149	4.162
B6-90-1	90	3.586	7.556
B8-0-1	0	3.643	4.553
B8-0-2	0	3.672	3.553
B8-90-1	90	2.771	5.239
B9-0-1	0	3.568	2.425
B9-0-2	0	2.674	2.779
B9-90-1	90	2.256	2.891
B10-0-1	0	7.054	8.964
B10-90-1	90	5.024	9.059

TABLE VII (continued)

B11-0-1	0	4.291	6.110
B11-90-1	90	3.193	3.135
B12-0-1	0	2.800	2.589
B12-90-1	90	2.442	4.501
B13-0-1	0	3.668	3.115
B13-90-1	90	2.560	3.148
B14-0-1	0	2.231	7.659
B14-90-1	90	4.473	8.366
B15-0-1	0	4.273	4.976
B15-90-1	90	3.454	5.858
B16-0-1	0	3.908	4.379
B16-90-1	90	2.567	5.918
B17-0-1	0	3.901	3.179
B17-90-1	90	2.281	5.083
B25-0-1	0	6.679	7.947
B25-0-2	0	6.450	7.629
B25-90-1	90	4.405	9.277
B26-0-1	0	4.723	5.455
B26-0-2	0	4.891	6.395
B26-90-1	90	2.864	6.394
B27-0-1	0	4.484	4.652
B27-0-2	0	3.600	4.451
B27-90-1	90	2.510	7.022

---

Figures 32 through 35. In Figure 32 are shown typical swelling - time curves for two vertically oriented specimens, compacted by the Standard AASHO procedure at different moisture contents. Similar curves for the horizontally oriented specimens are given in Figure 33. Swelling-time curves for the oriented specimens compacted by the Modified AASHO procedure at different moisture contents, are presented in Figures 34 and 35. These results indicate that specimens whose molding moisture contents were less swelled more and at a faster rate than those compacted at higher water contents, and this was true for samples compacted by both Standard and Modified AASHO compaction procedures. Barring the anomaly in the unit swelling values of the oriented specimens, the influence of the initial moisture content on the magnitude of swelling, is clearly seen in the results shown in Figures 32 through 35.

The water intake of specimens during swelling was determined from observations of the drop in the level of water in the reservoir. The total volume increase and the volumetric swelling of test specimens were computed from the measured values of  $\epsilon_v$  and  $\epsilon_h$ . The relationship between the total volume increase and the water intake of test specimens is shown in Figure 36. The water intake determined from the drop in the water reservoir level was found to be slightly greater than the value computed from the initial and final weights of test specimens. The observed difference is believed to be due to the slight accumulation of free water on the top of specimen - between the top porous stone and cap, possibly due to the enhanced drainage conditions through the filter strips. Consequently the curves shown in Figure 36 would tend to be shifted slightly towards the 1:1 slope line. Nevertheless, the results indicate that the total volume increase is always less than the water

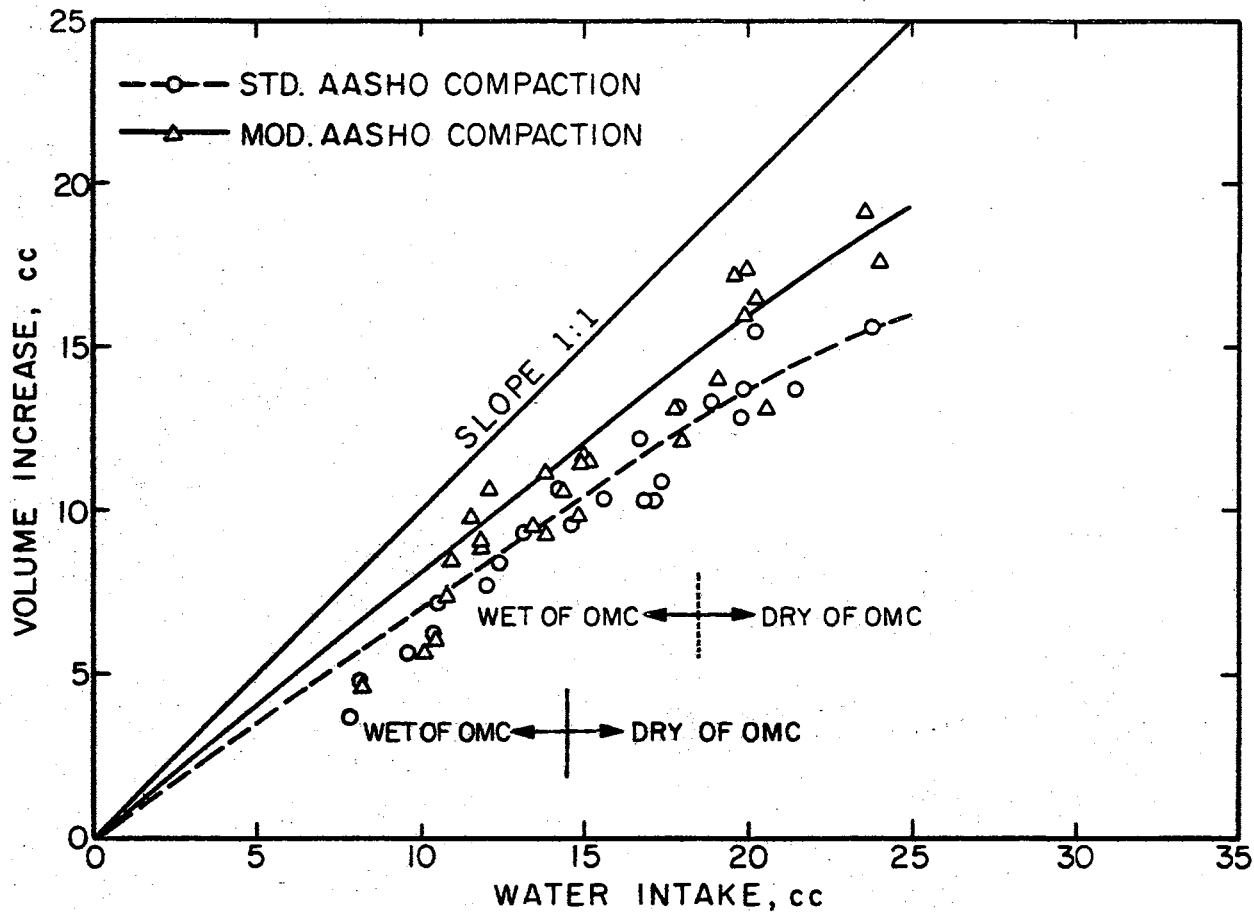


Figure 36. Relationship Between Volume Increase and Water Intake



intake for specimens compacted by both the Standard and Modified AASHO procedures. For a constant water intake, specimens compacted by Modified AASHO procedure swelled more and registered a greater total volume increase than those compacted by Standard AASHO procedure. This increased swelling tendency of Modified AASHO specimens is obviously due to the greater compactive effort which results in a closer packing of particles and consequent greater double layer repulsion. Further, the higher the initial water content of a specimen, the smaller is the difference between the total volume increase and the water intake. The difference between the total volume increase and the water intake is dependent on the initial and final degrees of saturation. The relationship between the initial and final degree of saturation as a function of the initial moisture content, is shown in Figures 37 and 38. It can be observed that although the initial degree of saturation varies with the molding water content, the final degree of saturation attained after swelling is not very much dependent on the initial water content. In other words, specimens with less initial degree of saturation swell more than those with high initial degree of saturation, although the final degree of saturation attained is approximately the same for both. Generally the final degree of saturation is found to be less than 100 percent. The initial degree of saturation for specimens compacted by Modified AASHO procedure is greater than that of Standard AASHO compaction specimens. However the final degree of saturation attained by both follows the general trend indicated above.

In Figure 39 is shown the effect of compactive energy on the final moisture content after swelling. The results indicate that for a constant initial moisture content, Standard AASHO compaction specimens

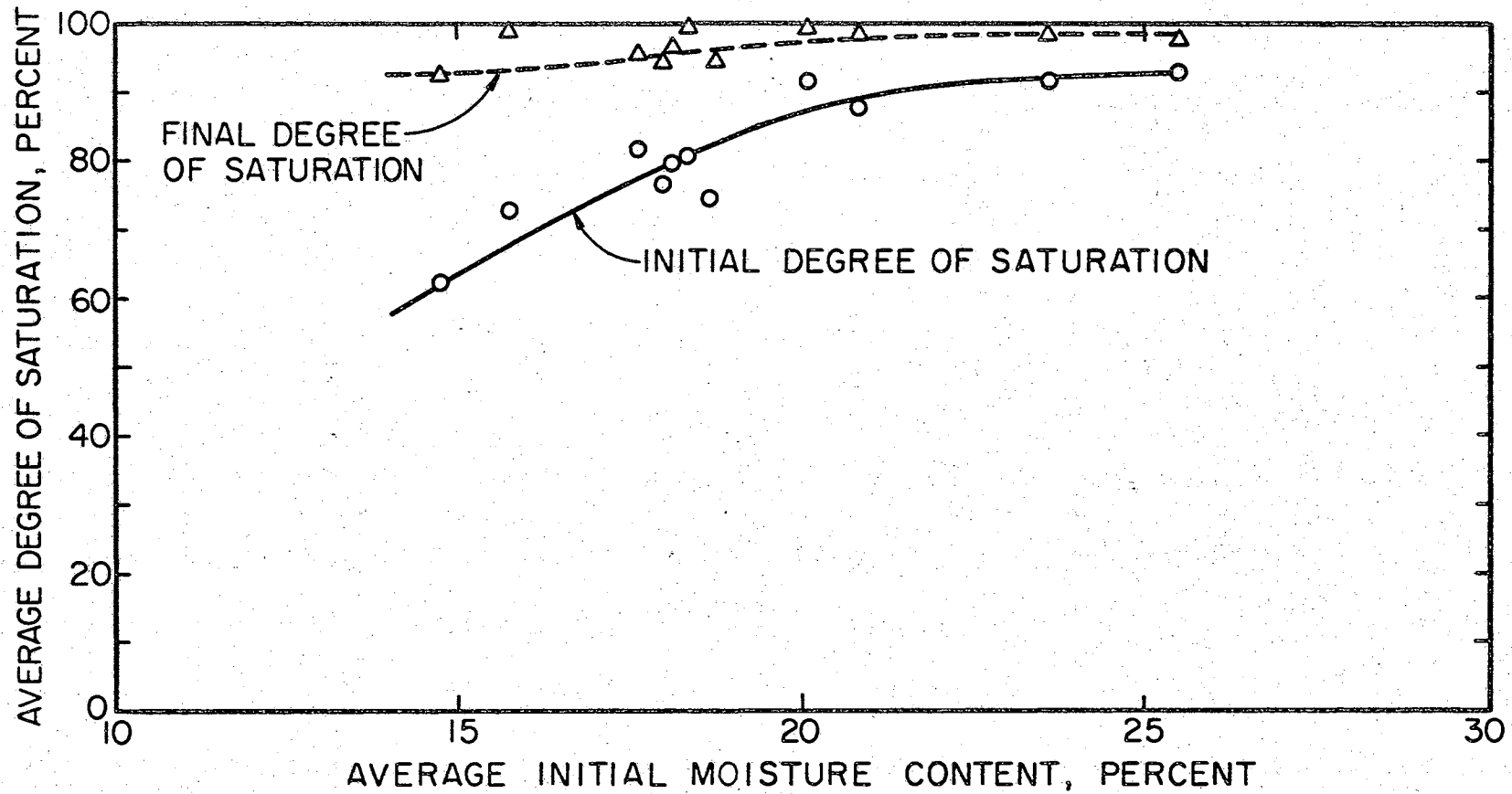


Figure 37. Initial and Final Degrees of Saturation for Standard AASHO Specimens

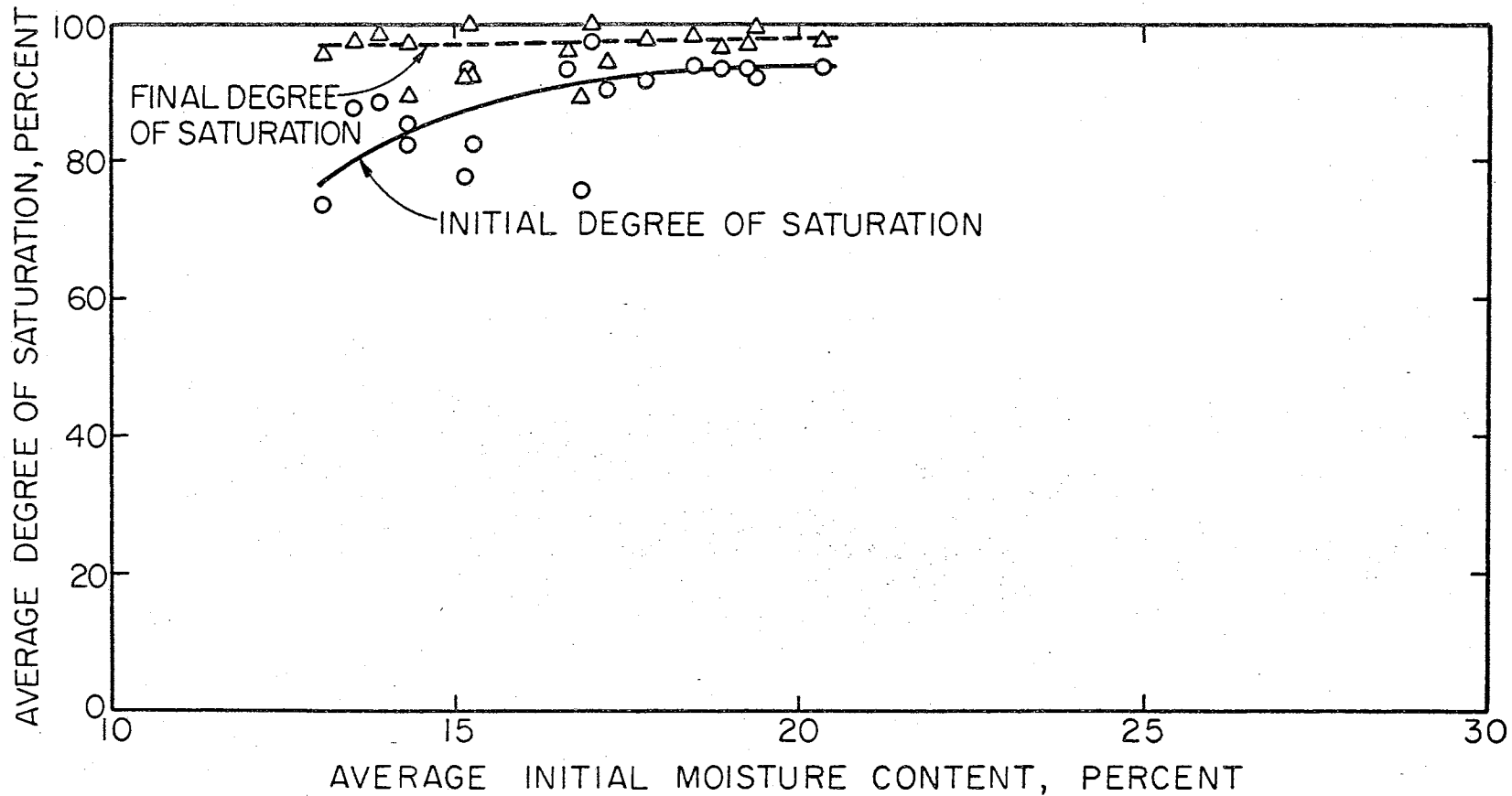


Figure 38. Initial and Final Degrees of Saturation for Modified AASHO Specimens

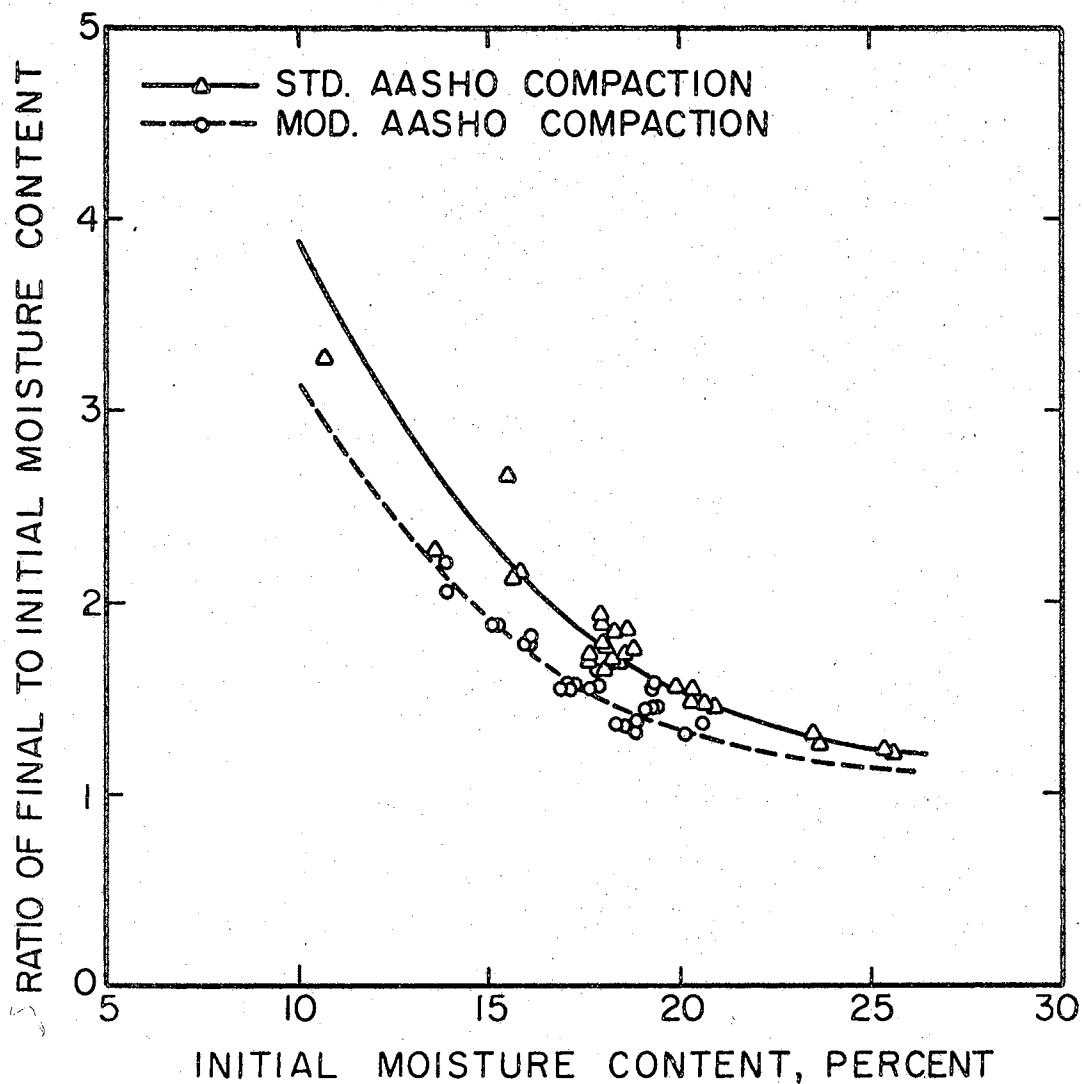


Figure 39. Effect of Compactive Energy on the Final Moisture Content after Swelling.

reached a higher final moisture content after swelling than those compacted by Modified AASHO procedure and this is evidently due to the lower initial degree of saturation and higher initial void ratio of Standard AASHO compaction specimens. For both Standard and Modified AASHO compaction, the difference between the initial and final moisture contents is greater for specimens with initial moisture contents less than optimum and this difference practically becomes zero for specimens compacted very much on the wet side of optimum. Also for both the Standard and Modified AASHO compaction specimens, the final moisture contents are approximately the same for molding moisture contents very much wet of optimum.

The volumetric swelling is a function of the unit vertical and horizontal swelling. Using the  $(\epsilon_v)_0$  and  $(\epsilon_v)_{90}$  values, the volumetric swelling was computed and the results, as a function of the initial moisture content, are shown in Figure 40. It is seen that the volumetric swelling generally shows an increasing tendency with decreasing initial moisture content, both for Standard and Modified AASHO compaction. However, for Modified AASHO compaction there is wide scatter of points near the optimum moisture content (14.5%), probably due to wide variations in the soil structure.

The majority of the swelling tests in this research were performed with filter strips, to accelerate the rate of swelling. Some tests were, however, done without filter strips in connection with the study of moisture variation along the length of the test specimen. Accurate determination of the moisture contents at ten points along the length of swollen specimens with and without filter strips was made and the results are shown in Figure 41. It is seen that there is an

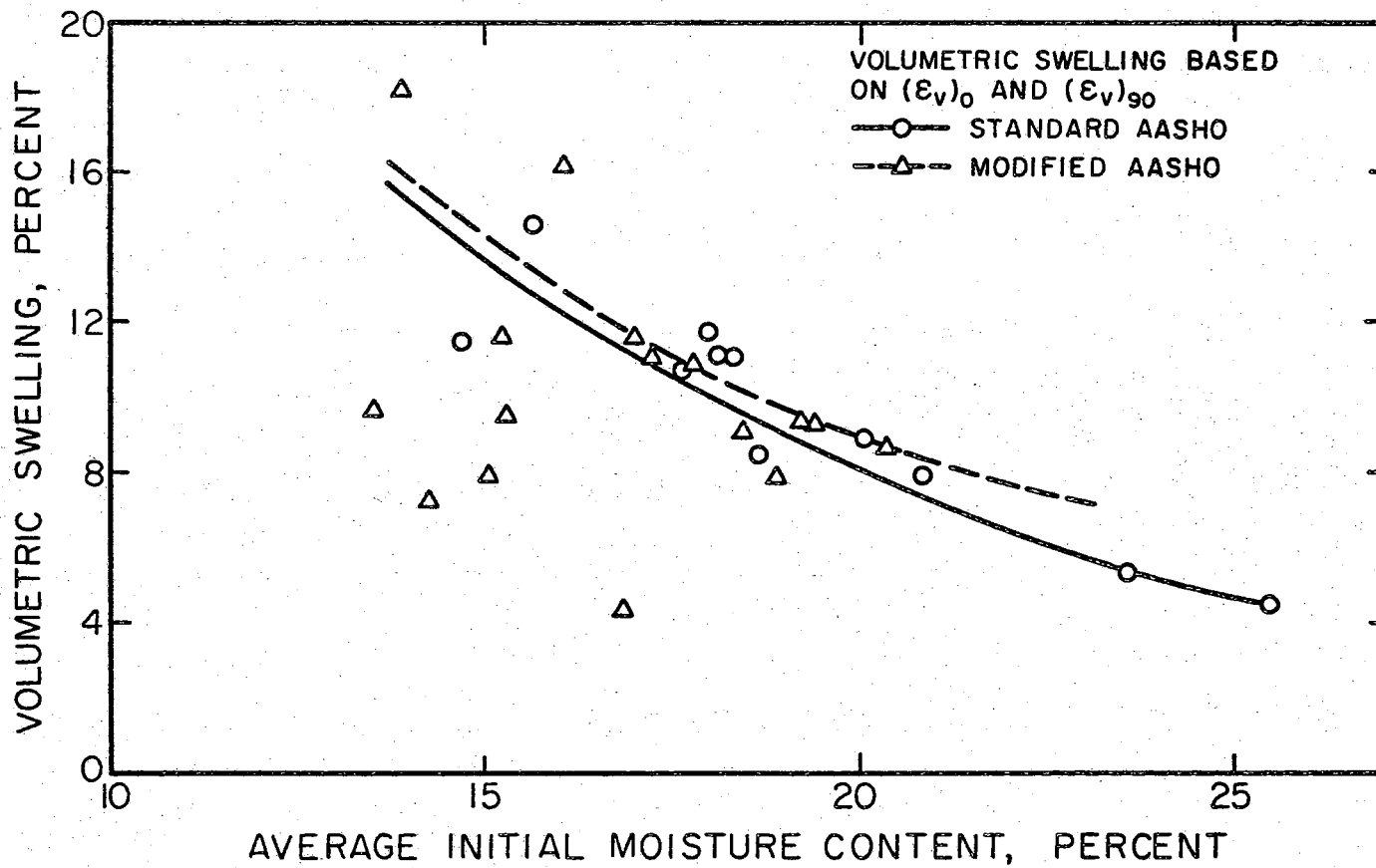


Figure 40. Relationship Between Volumetric Swelling and Initial Moisture Content-Standard and Modified AASHO Compaction.

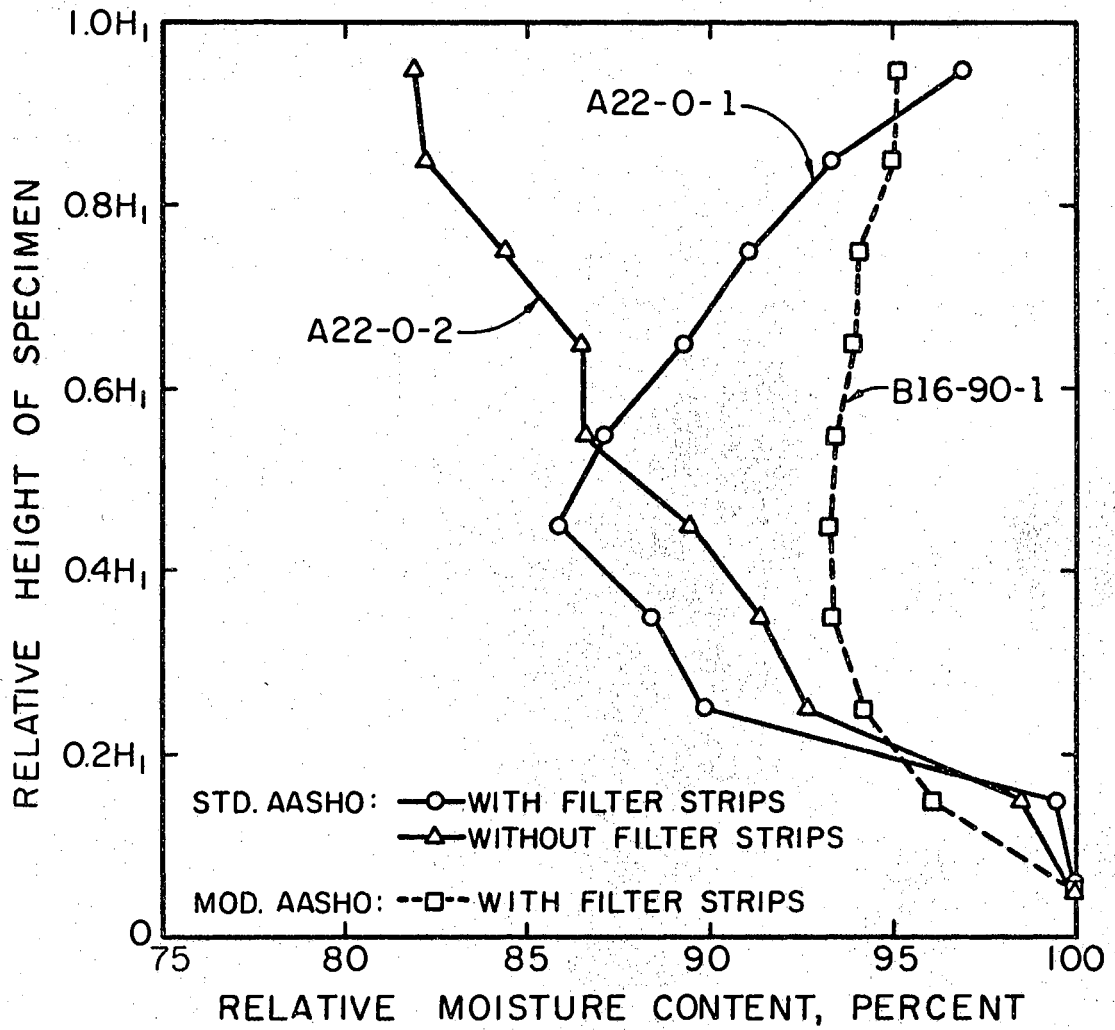


Figure 41. Moisture Content Variation in Test Specimens After Swelling.

appreciable difference between the moisture contents at the top and bottom of the sample in tests without filter strips while this difference tends to be small in tests with filter strips. For example, the moisture content at the top of the sample (A22-0-2) compacted by Standard AASHO procedure and tested without filter strips, was about 82% of that at the bottom while in the specimen (A22-0-1) tested with filter strips it was 97% of that at the bottom. Thus the use of filter strips along the sides of specimen tends to equalize the moisture content along the specimen. However, even with the use of filter strips, the water content at the middle of the sample differed significantly from that at either the bottom or top. A similar effect was observed with Modified AASHO compaction samples also. The relatively greater uniform distribution of moisture in the samples with filter strips is believed to be due to the enhanced drainage conditions obtained as compared to tests without filter strips.

The orientations of test specimens relative to the direction of compaction, as well as the computed  $\epsilon_v$  and  $\epsilon_h$  values, are summarized in Tables VI and VII. As illustrated in Figure 42, if we denote the unit swelling of the compacted soil parallel to the direction of compaction by  $\epsilon_o$ , and that perpendicular to it by  $\epsilon_{90}$ , then it is obvious that  $\epsilon_o$ ,  $(\epsilon_v)_o$  and  $(\epsilon_h)_{90}$  correspond to the vertical direction while  $\epsilon_{90}$ ,  $(\epsilon_h)_o$  and  $(\epsilon_v)_{90}$  correspond to the horizontal direction. However, the experimental results presented in Figures 30 through 35 and in Tables VI and VII indicate that there is an appreciable difference between the unit swelling values of the oriented specimens even corresponding to the same direction. The reason for this anomaly may be due to fabric variations in the test specimens and/or experimental errors in the measure-



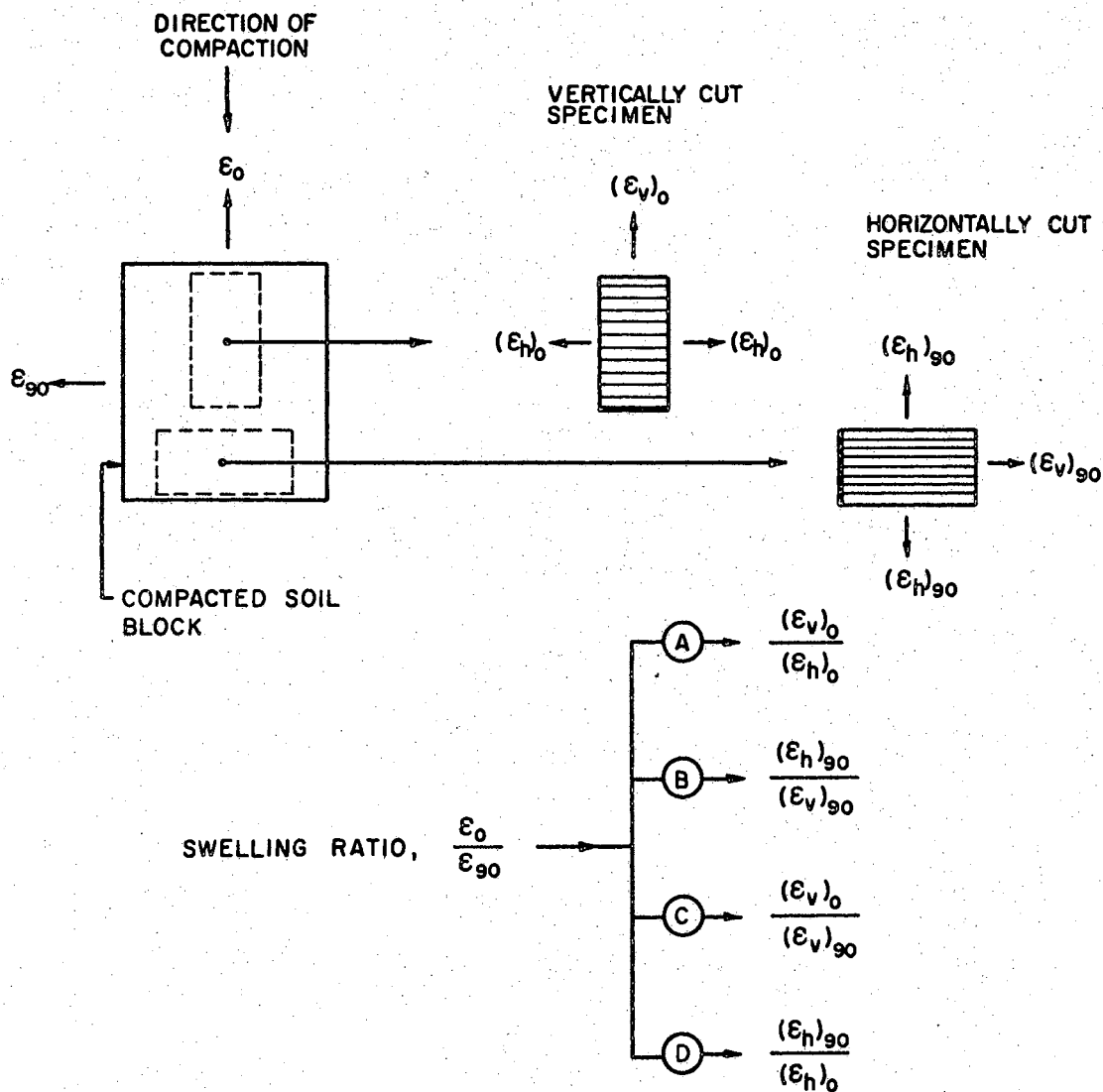


Figure 42. Definition Diagram for Swelling Ratio of Compacted Soil.

ment of  $\epsilon_v$  and  $\epsilon_h$  values.

In an ideal disperse system such as the one illustrated in Figure 43, the particles would tend to have a parallel arrangement normal to the direction of compaction. In such a model,  $(\epsilon_v)_o$  would represent the swelling due to face-to-face repulsion of particles while  $(\epsilon_h)_o$  and  $(\epsilon_v)_{g0}$  would correspond to the swelling resulting from edge-to-edge repulsion. However,  $(\epsilon_h)_{g0}$  would represent the swelling resulting from a combination of face-to-face and edge-to-edge repulsion. Although such an idealized model would not represent the actual case, a similar effect might be anticipated in compacted soils.

As explained earlier the vertical swelling of specimens was measured directly by a sensitive dial gage and therefore it can reasonably be assumed that the measured  $\epsilon_v$  values are free from any experimental errors. The unit horizontal swelling,  $\epsilon_h$ , on the other hand, was computed from the apparent volumetric displacement of the chamber water as reflected by the movement of the air-water interface in the saran tube. It is in the measurement of the saran tube readings that some difficulties were experienced by the author. In spite of adequate precautions to prevent water loss by leakage through the connections, absorption by the Plexiglas components and temperature variations, and to completely de-air the equipment prior to testing, in some tests there was accumulation of air as swelling progressed and the water meniscus in the saran tube showed erratic movements for some inexplicable reasons. It is believed that the saran tube readings are susceptible to errors resulting from the air entrapped in the apparatus, vibrations and other causes. In view of these considerations, the  $\epsilon_h$  values obtained from the swelling tests may not be as reliable as the  $\epsilon_v$  values obtained

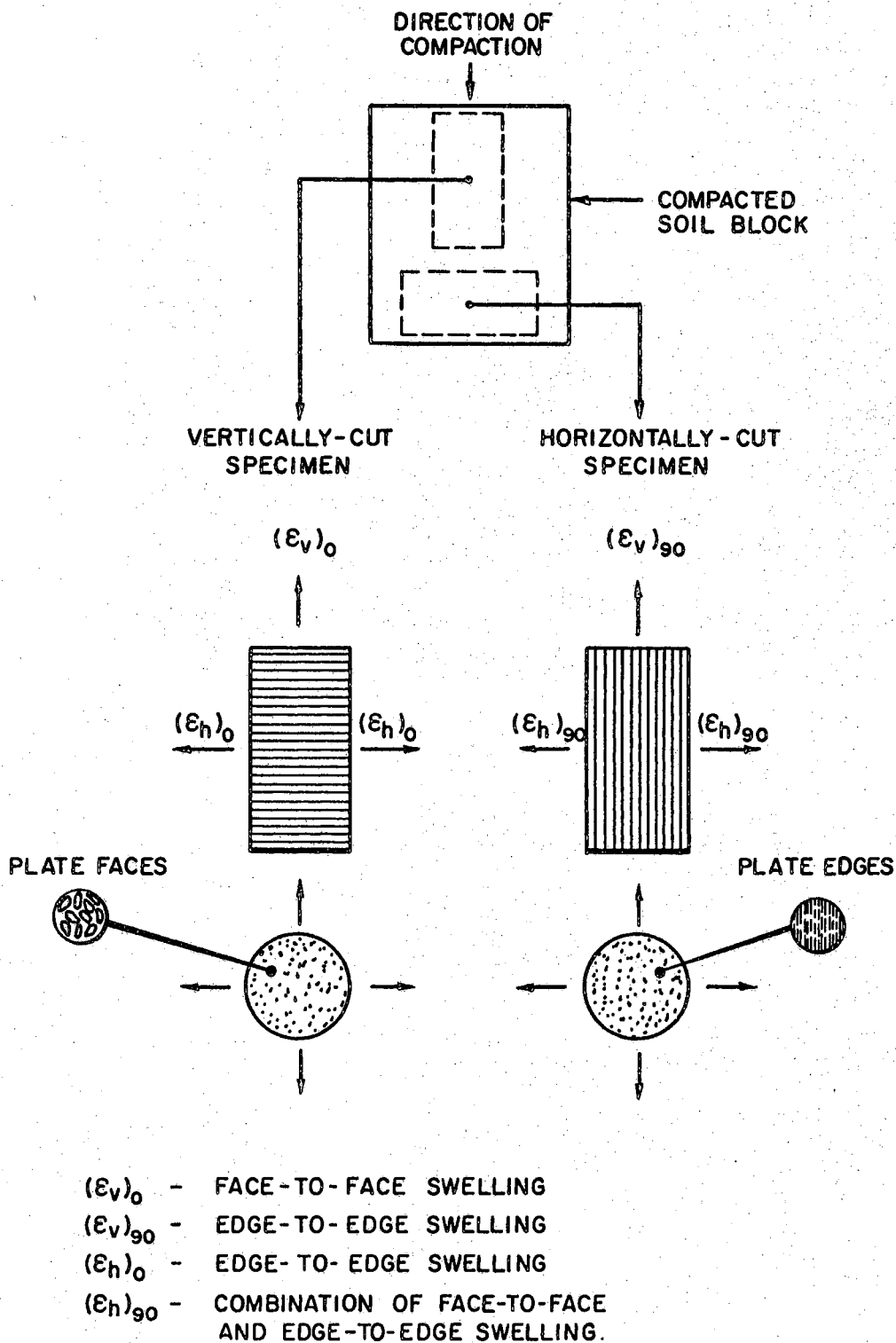


Figure 43. Particle Arrangement in Oriented Specimens in an Ideal Disperse System.

from dial gage readings.

To study the influence of structural anisotropy on the swelling characteristics of compacted soils, it would be expedient, therefore, to tacitly consider only the  $(\epsilon_v)_o$  and  $(\epsilon_v)_{90}$  values obtained directly from dial gage readings. The relationships between the average initial moisture content and the unit swelling parallel and perpendicular to the direction of compaction for Standard AASHO samples are shown in Figure 44. Similar relationships for Modified AASHO samples are given in Figure 45. The results indicate that the unit swelling  $(\epsilon_o)$  parallel to the direction of compaction is generally greater than the unit swelling  $(\epsilon_{90})$  perpendicular to it. For samples compacted dry of optimum, the difference between the  $\epsilon_o$  and  $\epsilon_{90}$  values tend to be greater than for those compacted wet of optimum. For Modified AASHO compaction the wide scatter of points at or near optimum is probably due to the non-uniform nature of the soil structure associated with different trials, all of which produce a flocculent structure in which the particle arrangement is unique for each trial.

The swelling ratio as defined in this study is the ratio of the unit swelling parallel to the direction of compaction to the unit swelling perpendicular to it. Expressed symbolically:

$$\text{Swelling Ratio} = \frac{\epsilon_o}{\epsilon_{90}}$$

As illustrated in Figure 42, it would be possible to arrive at four different values for the swelling ratio, based on the measured unit swelling values of the oriented specimens. These computed values are summarized in Tables VIII and IX. From the previous discussions it is obvious that, of the four possible values for the swelling ratio,

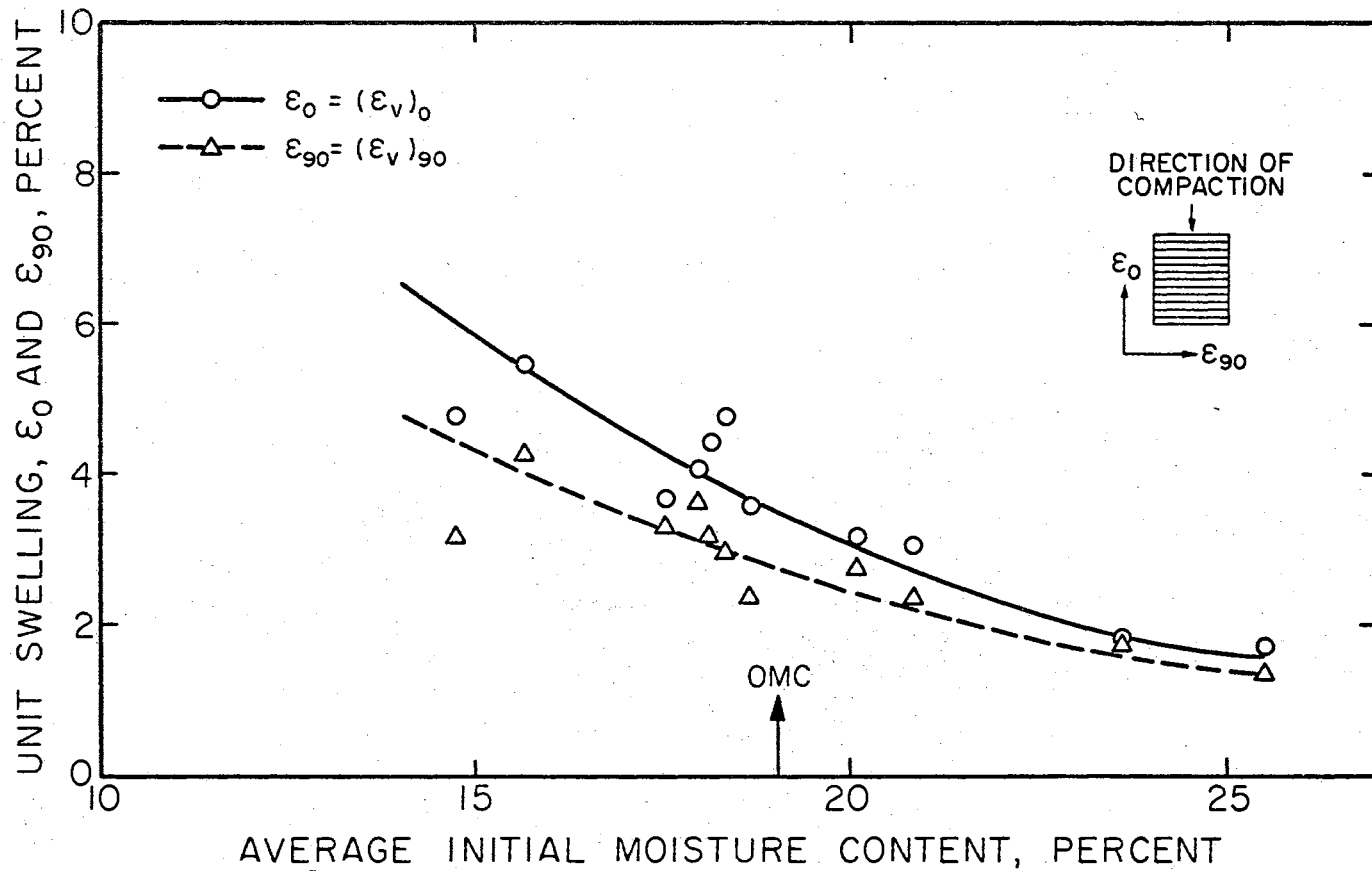


Figure 44. Effect of Initial Moisture Content on Unit Swelling-Standard AASHTO Compaction.

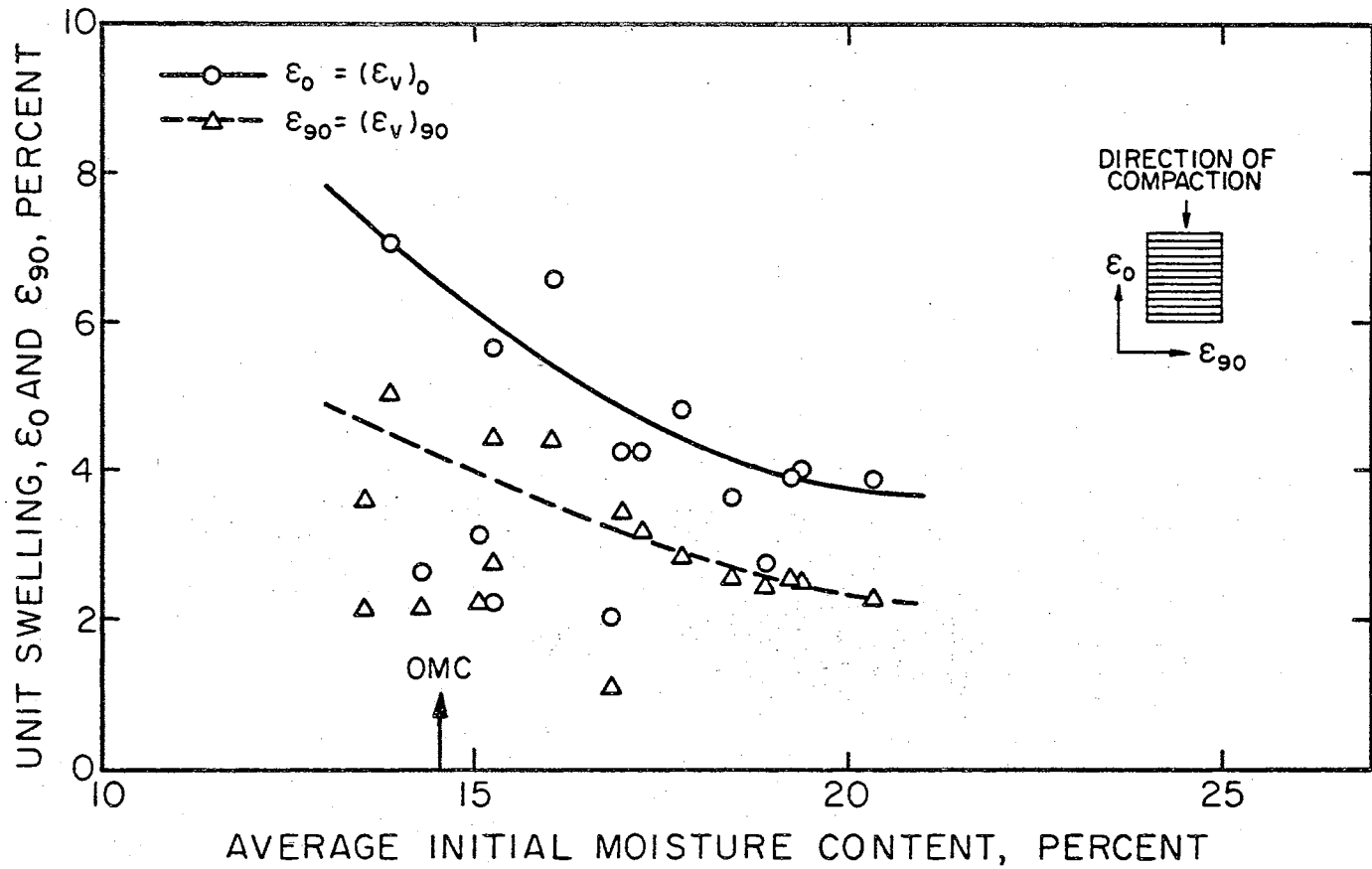


Figure 45. Effect of Initial Moisture Content on Unit Swelling-Modified AASHO Compaction.

TABLE VIII

SWELLING RATIOS FOR COMPACTED SOIL -  
STANDARD AASHO COMPACTION

Compaction Series	Swelling Ratio*			
	$\frac{(\epsilon_v)_o}{(\epsilon_h)_o}$	$\frac{(\epsilon_h)_{90}}{(\epsilon_v)_{90}}$	$\frac{(\epsilon_v)_o}{(\epsilon_v)_{90}}$	$\frac{(\epsilon_h)_{90}}{(\epsilon_h)_o}$
A1	1.112	...	...	...
A3	...	1.438	...	...
A4	1.559 1.818 <u>1.688</u>	1.369	1.483 1.553 <u>1.518</u>	1.438 1.601 <u>1.520</u>
A11	0.717 0.685 <u>0.701</u>	2.290	1.116 1.121 <u>1.119</u>	1.472 1.400 <u>1.436</u>
A14	0.641	2.209	1.160	1.221
A15	0.603	1.978	1.031	1.158
A16	1.000	2.013	1.257	1.601
A17	1.047	1.880	1.619	1.216
A20	0.937 0.634 <u>0.786</u>	1.753	1.378 1.175 <u>1.276</u>	1.192 0.946 <u>1.069</u>
A21	0.623 0.608 <u>0.615</u>	1.675	1.542 1.223 <u>1.382</u>	0.677 0.833 <u>0.755</u>
A22	0.608 0.848 <u>0.728</u>	1.937	1.171 1.087 <u>1.129</u>	1.005 1.510 <u>1.258</u>

TABLE VIII (continued)

A23	0.810	2.015	1.225	1.333
	0.835		1.361	1.236
	<u>0.823</u>		<u>1.293</u>	<u>1.285</u>
<hr/>				
A24	0.583	2.376	1.734	0.799
	0.639		1.274	1.192
	<u>0.611</u>		<u>1.504</u>	<u>0.996</u>
<hr/>				

\* Underlined data represent mean values.



TABLE IX

SWELLING RATIOS FOR COMPACTED SOIL -  
MODIFIED AASHO COMPACTION

Compaction Series	Swelling Ratio*			
	$\frac{(\epsilon_v)_o}{(\epsilon_h)_o}$	$\frac{(\epsilon_h)_{90}}{(\epsilon_v)_{90}}$	$\frac{(\epsilon_v)_o}{(\epsilon_v)_{90}}$	$\frac{(\epsilon_h)_{90}}{(\epsilon_h)_o}$
B1	0.903	3.233	1.887	1.548
B2	1.321 1.534 <u>1.428</u>	1.534	1.186 1.281 <u>1.234</u>	1.710 1.838 <u>1.774</u>
B3	1.884 1.804 <u>1.844</u>	...	...	...
B4	1.333	...	...	...
B6	0.516	2.107	0.599	1.815
B8	0.800 1.034 <u>0.917</u>	1.891	1.315 1.325 <u>1.320</u>	1.151 1.475 <u>1.313</u>
B9	1.472 0.962 <u>1.217</u>	1.281	1.582 1.185 <u>1.384</u>	1.192 1.040 <u>1.116</u>
B10	0.787	1.803	1.404	1.011
B11	0.702	0.982	1.344	0.513
B12	1.081	1.843	1.146	1.738
B13	1.178	1.230	1.433	1.011
B14	0.291	1.870	0.499	1.092
B15	0.859	1.696	1.237	1.177

TABLE IX (continued)

B16	0.892	2.305	1.522	1.351
B17	1.227	2.228	1.710	1.599
B25	0.840 0.845 <u>0.843</u>		1.516 1.464 <u>1.490</u>	1.167 1.216 <u>1.192</u>
B26	0.866 0.765 <u>0.815</u>	2.233	1.649 1.708 <u>1.679</u>	1.172 1.000 <u>1.086</u>
B27	0.964 0.809 <u>0.886</u>	2.798	1.786 1.434 <u>1.610</u>	1.509 1.577 <u>1.543</u>

\* Underlined data represent mean values.

the ratio,  $(\epsilon_v)_o / (\epsilon_v)_{90}$ , should be considered as most reliably representing the true swelling ratio  $(\epsilon_o / \epsilon_{90})$  of the compacted soil block. This ratio is therefore used to study the anisotropic swelling characteristics of compacted soil. The relationship between the swelling ratio,  $\epsilon_o / \epsilon_{90}$  and the average initial moisture content for the Standard and Modified AASHO compaction samples are presented in Figures 46 and 47. The appreciable scatter of points in these plots appears to be due to the variations in the structure of the oriented samples. As these plots are based on the test results of independent oriented specimens, it would be more realistic to study the relationship from statistical considerations. Linear regression analysis of the test data has shown that the relation between the swelling ratio and the initial moisture content of the compacted soil can be characterized by the following equations:

Standard AASHO compaction:  $(14.74\% \leq X \leq 25.50\%)$

$$Y = - 0.02437 X + 1.76675$$

Modified AASHO compaction:  $(13.54\% \leq X \leq 20.38\%)$

$$Y = + 0.09266 X - 0.21268$$

where

X = Initial moisture content, percent, and

Y = Swelling ratio,  $\epsilon_o / \epsilon_{90}$ .

The results shown in Figure 46 indicate that the swelling ratio of soil compacted by Standard AASHO procedure is greater than unity and that it tends to decrease slightly with increasing moisture content.

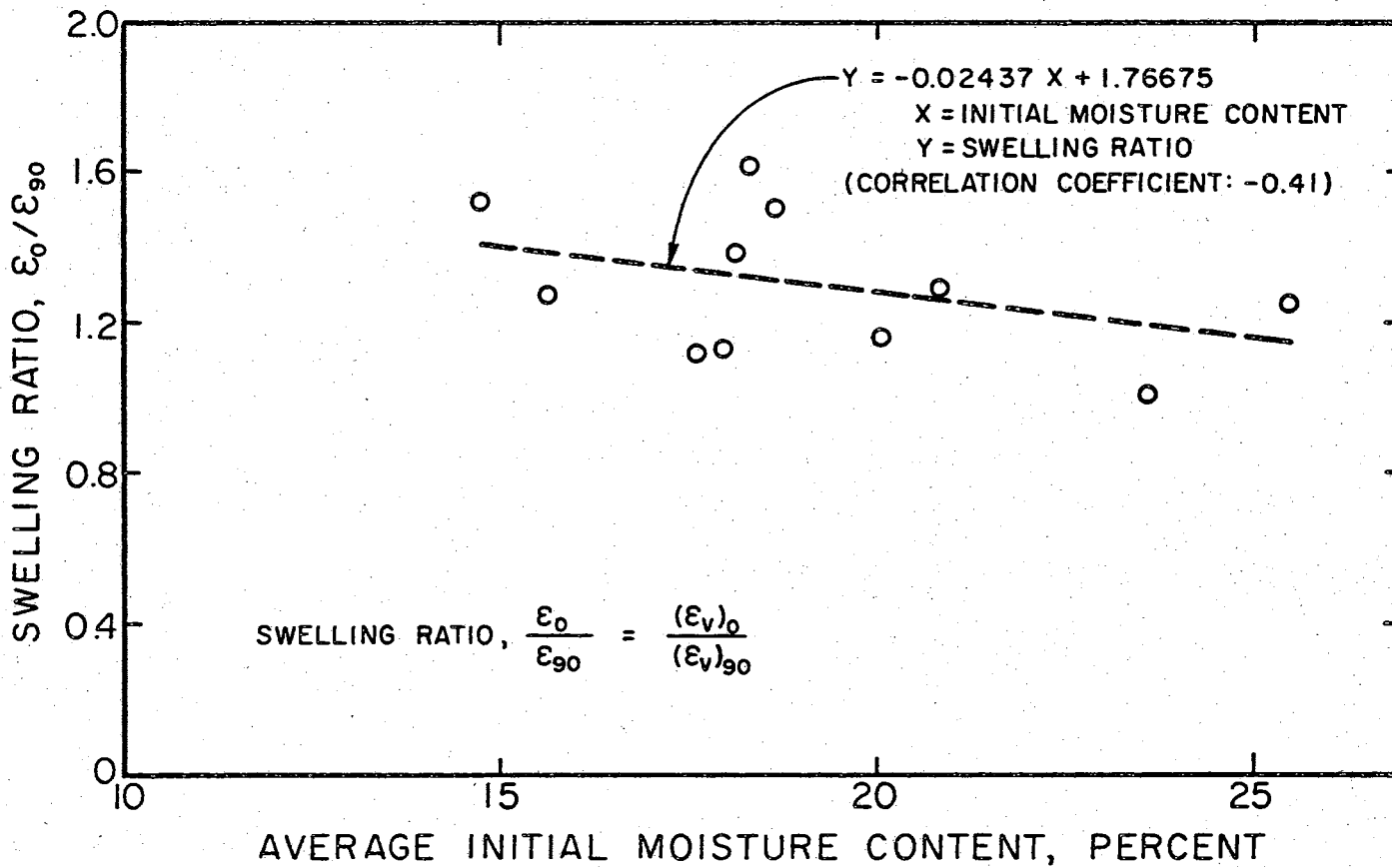


Figure 46. Effect of Initial Moisture Content on Swelling Ratio-Standard AASHO Compaction.

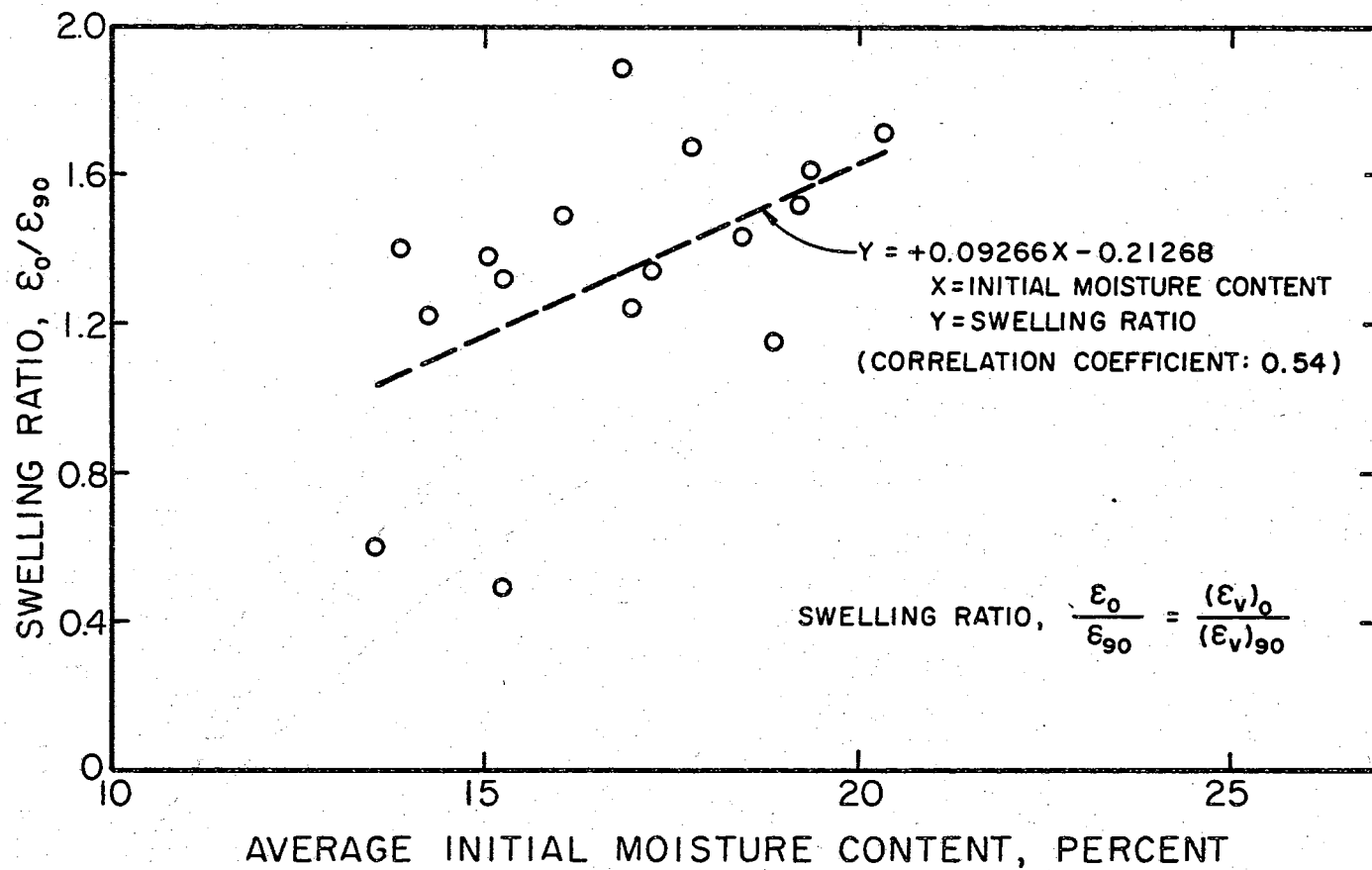


Figure 47. Effect of Initial Moisture Content on Swelling Ratio-Modified AASHO Compaction.

This tendency is probably due to soil disturbance caused by repeated penetrations of the hammer during compaction at higher moisture contents. The data for Modified AASHO compaction shown in Figure 47 indicate that the swelling ratio has a definite increasing tendency with increasing initial moisture contents. Although disturbance by hammer penetration during compaction at higher moisture contents is possible in this case also, the increased compactive effort seems to have a more pronounced effect in increasing the swelling ratio at higher water contents.

The experimental results presented herein have indicated that structural anisotropy has an influence on the swelling characteristics of compacted soil. In the preceding analysis two-dimensional swelling isotropy is assumed on planes normal to the direction of compaction. Even in an ideal disperse system with parallel particle arrangement, swelling anisotropy on planes parallel to the particle faces might exist in limited regions owing to edge effects resulting from the configuration of particles, although from statistical considerations, it would seem that swelling parallel to particle faces would be isotropic. If this is indeed the case, then this might explain some of the observed discrepancies in the magnitudes of the measured swelling of oriented specimens. In an attempt to investigate this aspect, expressions for three-dimensional anisotropic swelling were derived which are applicable to tests using the triaxial swelling apparatus and these are given in Appendix B. In this approach, the unit swelling values in any two coordinate directions are expressed in terms of the measured unit swelling in the other coordinate direction and the saran tube readings corresponding to three oriented specimens parallel to the three

coordinate axes. In this study an attempt was made to compute the unit swelling values parallel and perpendicular to the direction of compaction using these expressions. However, only in a few cases did the values obtained from these expressions agree with the experimental observations. Discrepancies probably arise from errors associated with the saran tube readings and the orientational inconsistency of the test specimens extracted from the cylindrical Proctor mold. Nevertheless, it is believed that this approach, with proper instrumentation for the accurate measurement of the apparent radial volumetric swelling of test specimens in the triaxial swelling apparatus, would be able to detect three-dimensional swelling anisotropy in soils.

### Soil Fabric Analysis

#### General

In soils, the individual components consisting of skeleton grains, soil matrix, and pores (intrapedal voids) are arranged in a continuous system which is commonly referred to as structural or fabric pattern. There are two aspects of fabric analysis: (1) Spatial distribution which refers to the distribution and orientation of skeleton grains, treating them as individuals or with reference to other individual features or patterns, and (2) Spatial orientation which is concerned with an assessment of the kind and degree of preferred orientation of the individual components either basically referred, or related to other features. In many instances these features can be observed microscopically.

Numerous fabric studies have been made based on microscopic observations of thin sections and these essentially involve the direct measurement of the apparent long axes of grains, grain selection by

point count techniques and observations in randomly chosen fields (Dapples and Rominger, 1945; Potter and Mast, 1963 and others). These methods are generally best suited to megascopic individuals which can be directly and accurately measured. However, the matrix in soil materials which consist of very fine clay and colloid fractions, occur in compound units or domains and so are recognizable only at high magnifications. Many indirect methods for studying the soil fabric have been employed. Methods involving the detection of dielectric, sonic and thermal anisotropies and inductive conductivity anomalies in the materials to infer fabric orientation have also been reported. In the simplest microscopic technique, the extinction phenomenon in thin section under crossed nichols is interpreted, based on the optical properties of the mineral species involved. The majority of the minerals in the matrix, exhibiting preferred orientation, have a layer lattice structure and an elongated or platy form. Most clay crystals are birefringent and if they are arranged with a preferred orientation, the aggregate will also exhibit birefringence. Increasing parallelism of platy crystals will correspond with increasing aggregate birefringence. Based on these principles, the microstructure of clays has been studied by many investigators (Kerr, 1937; Williamson 1947 and others). Mitchell (1956) studied the illumination and extinction stages of oriented thin sections using a petrographic microscope and determined qualitatively the degree of preferred orientation and correlated the particle arrangement with the engineering properties. Following a similar technique, Pacey (1956) studied the structure of compacted soils and found that compaction dry of optimum produces a flocculent structure while compaction wet of optimum results in a parallel particle arrangement.



Morgenstern and Tchalenko (1967) proposed a model distribution function for the spatial orientation of the particles to predict the birefringent behavior of the aggregate and studied the microstructure of consolidated kaolin using a petrographic microscope. They used a very stable light source and measured the refracted intensities with a photometer. The measured intensities were used to obtain an orientation ratio for characterizing quantitatively the soil fabric.

X-ray diffraction techniques have been successfully used in recent years, in the identification and quantitative determination of mineral constituents in clays. In addition, this method has proved very useful in the determination of the lattice structures of many complex materials and in the study of mixed-layer minerals. Most of the clay minerals occur in flake-shaped units and consequently any aggregate orientation of the flakes results in enhanced basal reflections in the diffraction pattern. Brindley (1953) introduced an X-ray diffraction technique for quantitatively expressing the orientation of micaceous minerals in shales and clays and this method formed the basis for many subsequent studies concerning the orientation of undisturbed clays (Silverman and Bates, 1960; O'Brien, 1964 and others). Using Mitchell's (1956) method of sample preparation and a modified version of Brindley's (1953) X-ray technique, Martin (1962, 1965) studied the fabric of consolidated kaolinite and proposed the peak ratio technique for quantizing clay fabric. This peak ratio technique was successively applied in soil fabric studies by many investigators (Quigley and Thompson, 1966 and Campagna, 1967). Tice (1967) studied the fabric of compacted kaolinite by comparing the peak intensities of oriented thin sections and showed that the degree of domain orientation perpendicular to the compacting

direction increases with increase in molding water content.

The development of the electron microscope has permitted the precise determination of the shape of the particles of the various clay minerals. With this equipment, magnifications as high as 250,000 X can be obtained. With the most modern equipment, combining electron microscopy, electron diffraction and electron probe microanalysis, chemical, structural and morphological data can be obtained from individual grains as small as 0.5  $\mu$ . Sloan and Kell (1965) used the electron microscope to study the fabric of kaolinite compacted by kneading, static and impact compaction. Their results generally confirmed Pacey's (1956) data and showed that all compaction methods produce random fabric dry of optimum, while on the wet of optimum they produce a more oriented fabric.

Another recent development is the scanning electron microscope which differs from the conventional transmission electron microscope both in regard to its principles and applications. This instrument has found extensive applications in diverse fields. The high magnification and depth of field obtainable with a scanning electron microscope make it especially suited in studies concerning soil fabric and other related aspects.

The two methods used in this research for studying the fabric of compacted soil are the X-ray diffraction method and scanning electron microscopy. In the X-ray diffraction method, diffraction patterns for the oriented thin sections were prepared and the peak intensity counts corresponding to predominant X-ray reflections were made. In the scanning electron microscope study, faces at the required orientations in the impregnated specimens were shadowed and micrographs of the faces

were prepared, for studying the degree of preferred particle orientation relative to the direction of compaction.

## X-ray Diffraction Study

### Introduction

It was in 1923 that the X-ray diffraction technique was first applied to the study of clay minerals and since then advances in X-ray instrumentation, sample preparation methods and identification procedures have greatly contributed to mineralogical characterization and lattice structure determination of many complex and mixed-layer minerals.

Crystalline structures are characterized by a systematic and periodic arrangement of atoms or ions in a three-dimensional array and consequently they contain atomic planes separated by a constant distance. X-rays are electromagnetic radiations of short wavelength (of the order of 0.01 to 100 Å). The phenomenon of diffraction involves the scattering of X-rays by the atoms of a crystal and the reinforcement of scattered rays in definite directions away from the crystal. The condition for in-phase scattering by a set of regularly spaced parallel planes in a crystal is given by Bragg's equation:

$$n \lambda = 2d \sin \theta$$

where

$\lambda$  = wavelength of reflected X-radiation,

$d$  = spacing of reflecting planes, and

$\theta$  = angle of reflection.

If  $n = 1$ , there is first order diffraction. Other positive integral values for  $n$  give rise to successively higher orders of diffraction.

Since no two minerals have exactly the same interatomic distances in three-dimensions, the angles at which diffraction occurs will be distinctive for a particular mineral. The interatomic distances within a crystal result in a unique diffraction pattern which serves to identify the mineral. For a detailed discussion of the principles of X-ray diffraction and X-ray crystallography, the reader should refer to standard texts on the subject (for example Cullity, 1956; Nuffield, 1966; and Azaroff, 1968).

The crystalline nature of clay minerals was discussed earlier. When a beam of X-rays is made to impinge on a clay sample—either a powder sample or thin section, the resulting diffraction pattern will depict intensity peaks characteristic of its mineral constituents as well as their atomic structures. In general, the intensity of an X-ray beam diffracted by a system of anisotropic crystals is dependent, inter alia, on their size, orientation and concentration in the bulk mass. Owing to the effect of extinction, the average intensity is found to be smaller for the larger crystal sizes. For constant particle concentration, greater particle orientation with flat surfaces parallel to the surface results in strong reflections from planes parallel to the flat surfaces of crystals. Conversely planes approximately at right angles to the surface will produce very weak reflections (Klug and Alexander, 1954). The other factors which have an influence on the diffraction intensity are chemical composition, crystal imperfections, presence of amorphous substances, variations in relative humidity and temperature, fluctuations in the power to measuring and recording instruments and errors in machine alignment.

X-ray diffraction techniques have been successively applied in studies concerning the quantitative determination of the fabric of clays (Brindley, 1953; Martin, 1962, 1965; O'Brien, 1964; and others). The peak ratio (defined as the ratio of the measured diffraction intensities corresponding to chosen planes in a crystal) obtained from the X-ray diffraction patterns, is reported to be a reliable measure to quantize the clay fabric (Martin, 1962). Tice (1967) computed the peak ratio corresponding to (002) and (020) reflections, in oriented thin sections and studied the fabric of compacted kaolinite. His results indicate that the degree of domain orientation normal to the direction of compaction increases with increase in molding moisture content.

In this research, oriented thin sections parallel, perpendicular and at 45 and 135 degrees to the direction of compaction were prepared from soil blocks compacted by Standard and Modified AASHTO procedures, and these were analysed in the X-ray diffractometer. Based on the intensity counts corresponding to predominant reflections, an attempt was made to study the degree of particle orientation on planes inclined at different angles with the direction of compaction.

#### Preparation of Thin Sections

The thin sections required for X-ray diffraction study were prepared from the soil blocks compacted by Standard and Modified AASHTO procedures. As discussed earlier, oriented test specimens required for the triaxial swelling tests were cut out of the compacted soil blocks. During this phase, additional small soil blocks, about 1"x1"x1.5" size, were carefully trimmed from the compacted soil block and these were immediately waxed and stored in a humid room, until the time of thin

section preparation. In order to facilitate the preparation of thin sections at the proper orientations relative to the direction of compaction, an accurate record was kept of the orientation of the small soil blocks. Generally the soil blocks were cut vertically, that is, with their longitudinal axes parallel to the direction of compaction. Two thin sections were prepared out of each soil block - one parallel and the other perpendicular to the longitudinal axis, and this, in effect, resulted in thin sections parallel and perpendicular to the direction of compaction. For the purpose of studying the soil structure in the compacted soil along planes other than the vertical and horizontal planes, two soil blocks (one using Standard AASHO compaction and the other using Modified AASHO compaction) with their longitudinal axes inclined at 45 degrees to the direction of compaction, were also cut and, as before, two thin sections were prepared from each. This resulted in thin sections inclined at 45 and 135 degrees to the direction of compaction.

All the thin sections required for this study, were prepared using standard impregnation procedures. Epoxy plastic was used for impregnating the samples prior to thin sectioning. Thin sections required for this study were prepared by the Gary Section Service, Tulsa, Oklahoma.

#### Test Procedure

The XRD - 6 diffractometer (manufactured by the General Electric Company), available in the Agronomy Department at Oklahoma State University, was used in this study. Diffraction patterns for the oriented thin sections were obtained for a  $2\theta$  range of 3 to 30 degrees. To

determine the diffraction intensity, the goniometer was set at the  $2\theta$  value corresponding to the predominant reflections and intensity counts were made for a constant time interval of 10 seconds. Using a similar procedure, the background intensity was measured by setting the goniometer on either side of the peak and the mean background intensity was subtracted from the total intensity to obtain the net intensity of reflection. The net peak intensity counts were used to study the degree of particle orientation on different planes within the compacted soil mass.

#### Data and Discussion

The purpose of this phase of investigation was to study the degree of particle orientation in thin sections cut at different angles with respect to the direction of compaction. To achieve this objective, 18 oriented thin sections were analysed in the X-ray diffractometer. Typical diffraction patterns for two Standard AASHO thin sections - one parallel and the other perpendicular to the direction of compaction, are shown in Figures 48 and 49. Similar diffraction patterns for two Modified AASHO thin sections are given in Figures 50 and 51. These figures indicate only two predominant reflections - one at  $2\theta = 20.80^\circ$  ( $d = 4.27 \text{ \AA}$ ) and the other at  $2\theta = 26.60^\circ$  ( $d = 3.35 \text{ \AA}$ ).

It is reported that the Permian clays contain approximately 40% montmorillonite, 30-35% illite and 25-30% unidentified material, believed to be quartz, kaolinite and iron oxide (Greco, 1964). No attempt was made in this investigation to determine quantitatively the relative proportions of the various minerals present in the soil. However, to identify the important minerals present in the soil, several powder

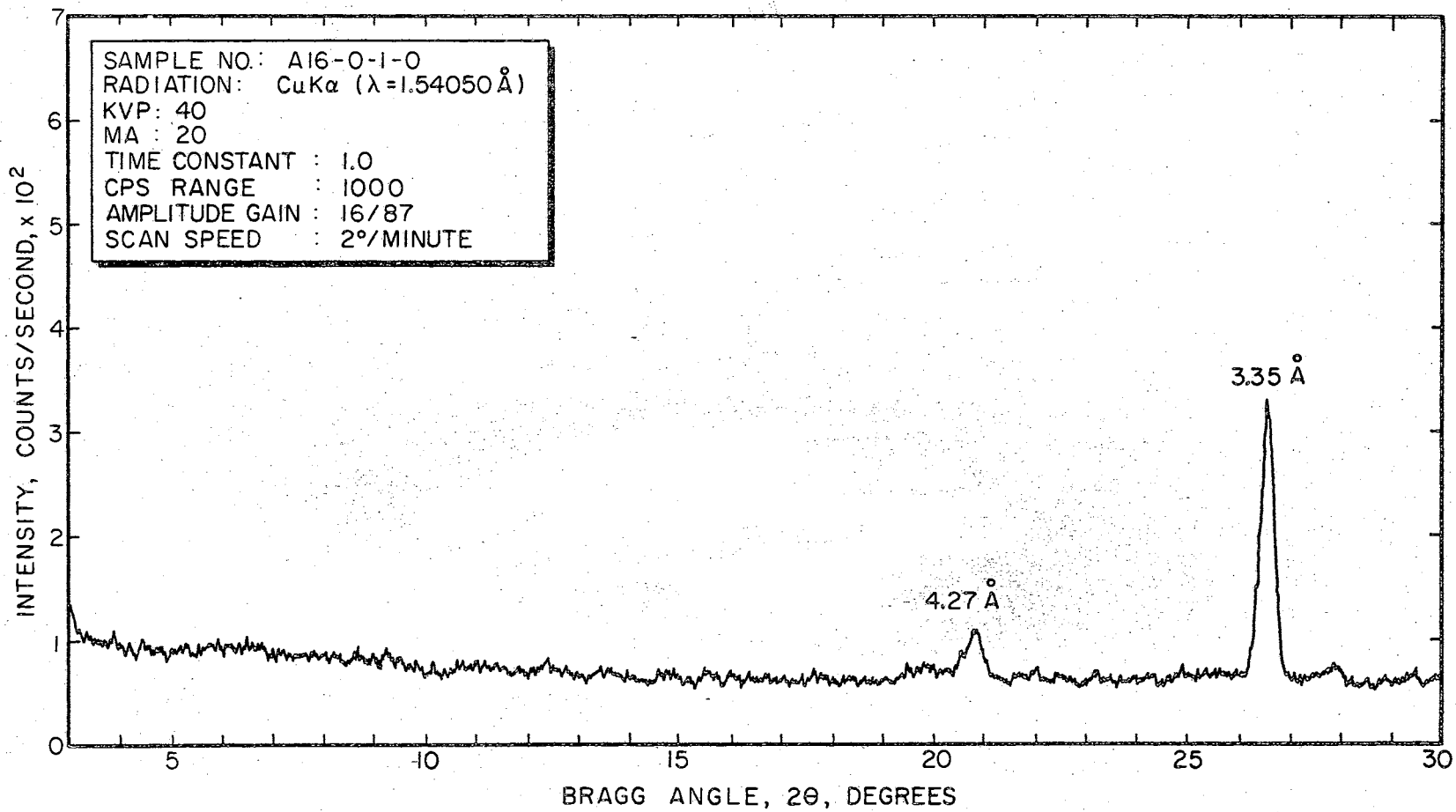


Figure 48. X-ray Diffraction Pattern for Thin Section Parallel to Compaction Direction - Standard AASHO Compaction.



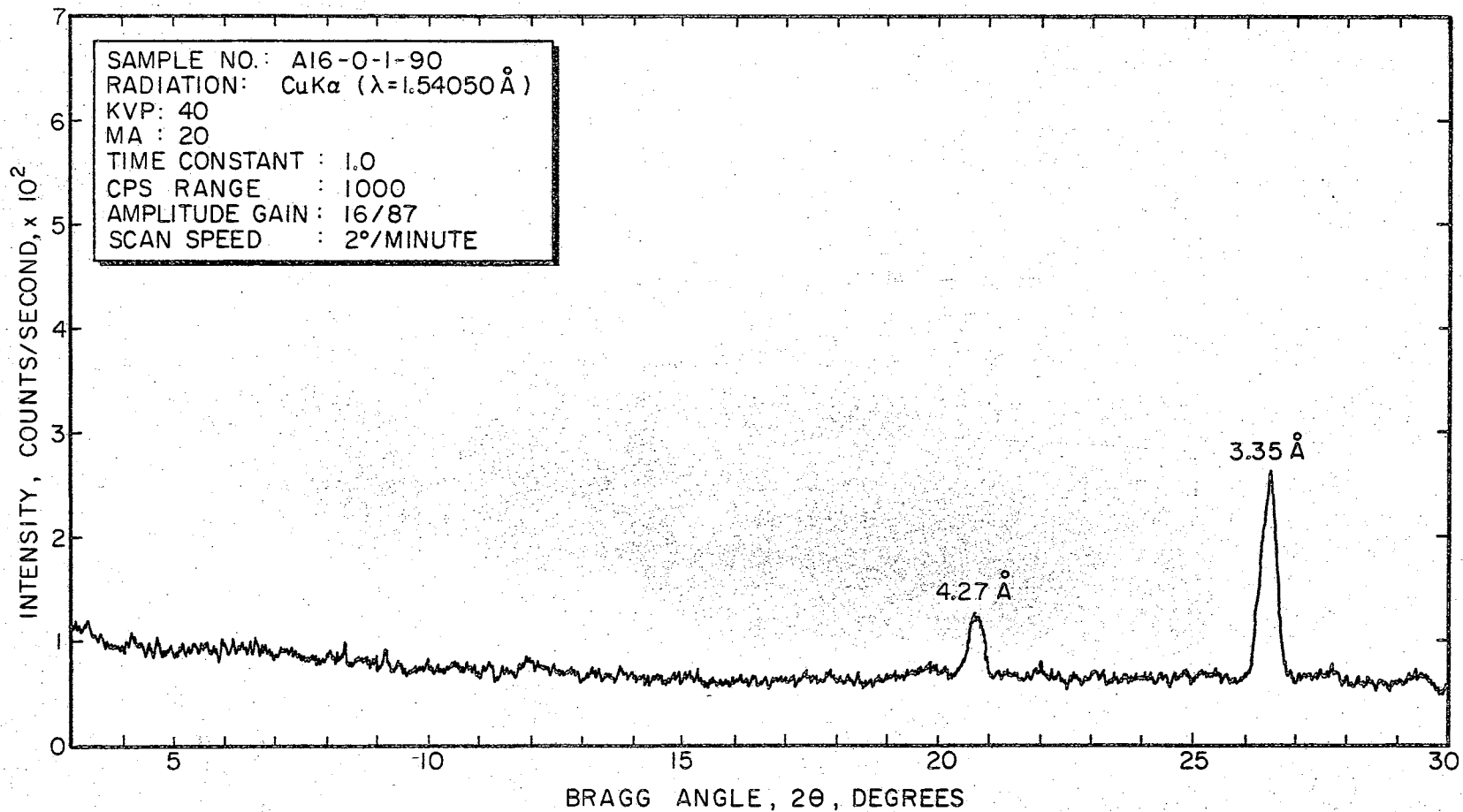


Figure 49. X-ray Diffraction Pattern for Thin Section Perpendicular to Compaction Direction - Standard AASHO Compaction.

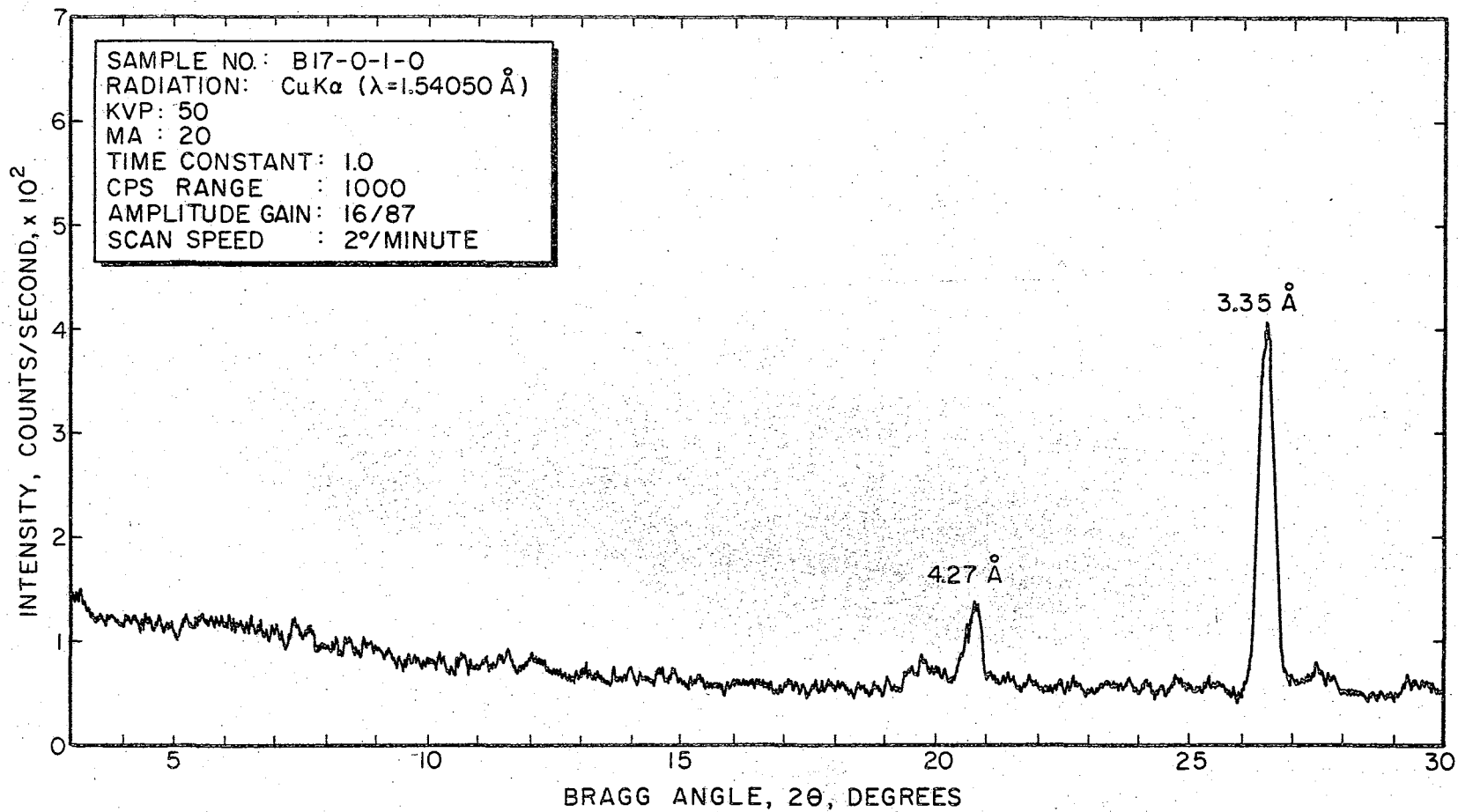


Figure 50. X-ray Diffraction Pattern for Thin Section Parallel to Compaction Direction - Modified AASHO Compaction.

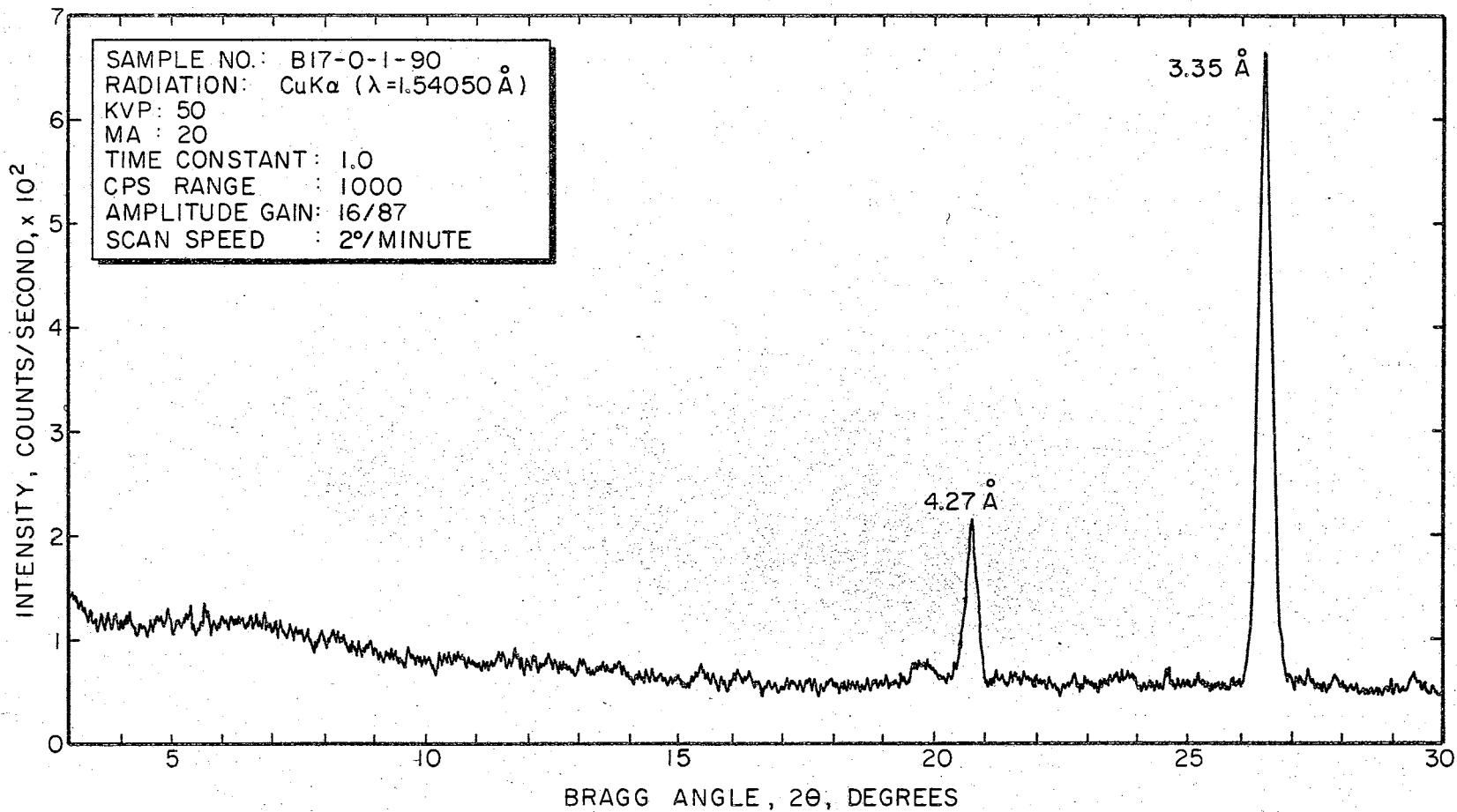


Figure 51. X-ray Diffraction Pattern for Thin Section Perpendicular to Compaction Direction - Modified AASHO Compaction.

samples and samples prepared by air drying a thin soil slurry on glass slides were studied in the diffractometer. Diffraction patterns for a typical minus 40 powder sample and a sample prepared by the slurry method are given in Figures 52 and 53. The desirable fraction to use in powder samples is that passing 300 mesh and retained on 500 mesh. However, since the degree of preferred particle orientation in oriented thin sections is under study, diffraction pattern of a typical minus 40 powder sample is given in Figure 52 for the purpose of comparison with the diffraction data of oriented thin sections. Sample preparation by the slurry technique is not generally desirable as it is highly conducive to preferred orientation and surface imperfections besides the possibility of reduced diffraction intensity. Nevertheless its diffraction pattern would approximately indicate the reflections characteristic of the minerals present in the soil. The diffraction data shown in Figure 53 indicate the presence of interstratified layer silicates, disordered kaolinite or partially dehydrated halloysite, mica, montmorillonite or chlorite, quartz and gypsum.

As mentioned earlier, the oriented thin sections for this study were made from compacted soil (passing US sieve No. 40) and consequently they included coarser fractions like silt and sand. The presence of coarse fractions in the thin sections is believed to be responsible for the suppression of the predominant basal reflections of clay minerals which were noticed in Figure 53. The reflection at about 20.8 degrees ( $d = 4.27 \text{ \AA}$ ) may be due either to quartz (100), or muscovite (111) or gypsum ( $12\bar{1}$ ). The reflection at about 26.60 degrees ( $d = 3.35 \text{ \AA}$ ) appears to be due either to quartz (101) or kaolinite although the strong nature of the peak suggests that quartz is more probable. In view of

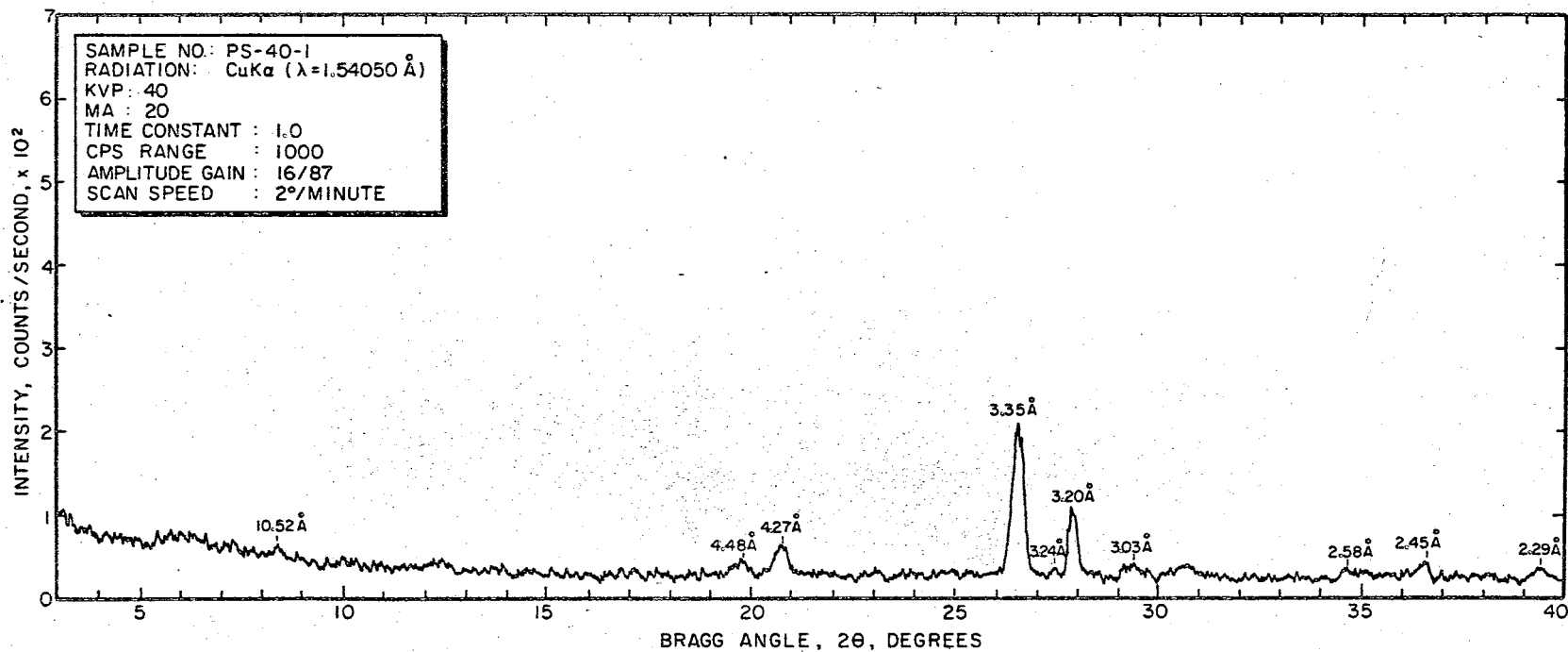


Figure 52. X-ray Diffraction Pattern for a Typical Powder Sample (Minus 40 Fraction)

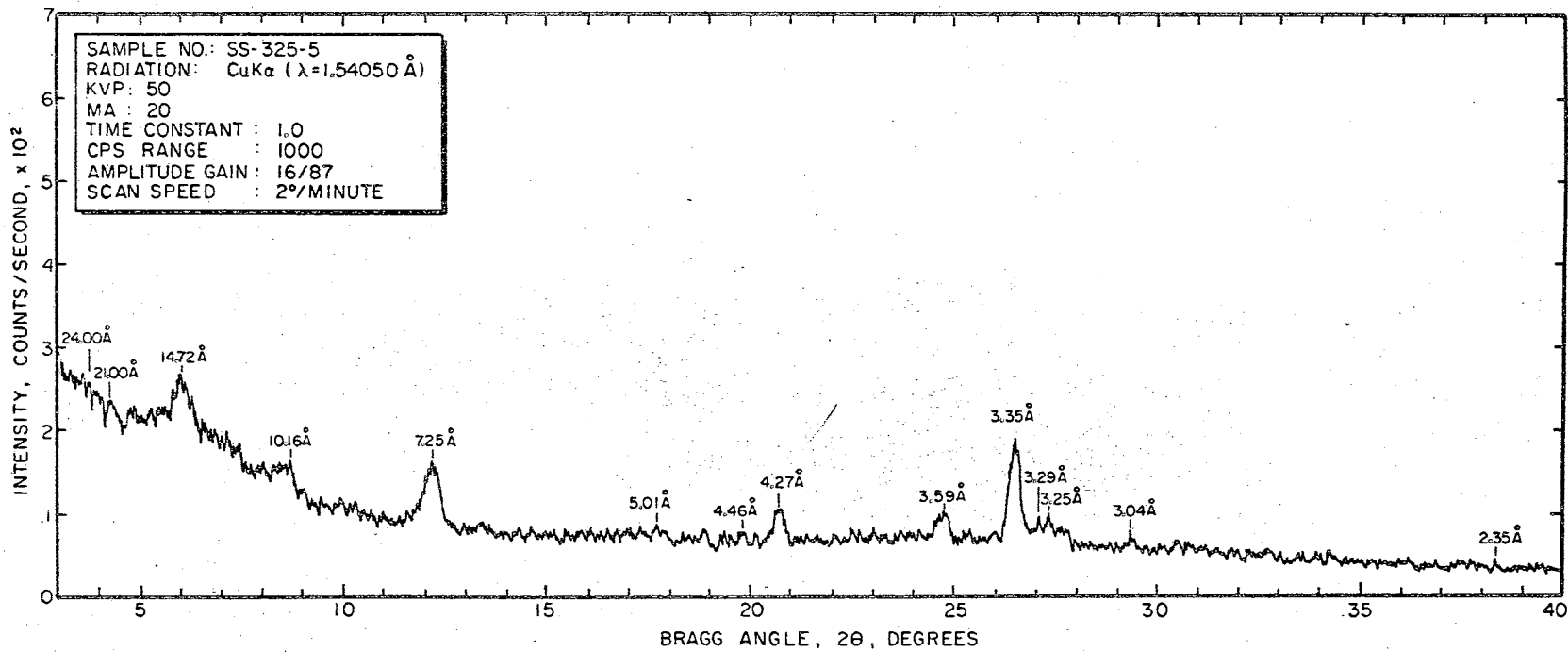


Figure 53. X-ray Diffraction Pattern for a Typical Slurry Sample (Minus 325 Fraction)

their platy nature, the clay particles would tend to be oriented more during compaction and consequently diffraction intensities corresponding to the basal reflections of the clay particles would be more realistic in the characterization of the particle orientation and its correlation to the swelling characteristics. Such a procedure could not be used in the present study in view of the reasons given earlier. However, it is believed that the observed variations in the diffraction intensities are indicative of the degree of particle orientation.

It was indicated earlier that, all other factors remaining the same, the observed diffraction intensity is a function of the particle orientation. The net intensity corresponding to the 20.80 and 25.60 degree reflections in the powder sample were respectively 415 and 2268 counts per 10 seconds. The diffraction intensities of oriented thin sections shown in Figures 48 through 51 are appreciably greater than those of a powder sample, in which the particle orientation may be assumed to be random (Figure 52). This indicates that there is a certain degree of particle orientation in the oriented thin section as compared to the powder sample. The results presented in Figures 48 through 51 indicate that the observed diffraction intensity for the thin sections A 16-0-1-90 and B 17-0-1-90 (which are oriented perpendicular to the direction of compaction) are greater than those of A 16-0-1-0 and B 17-0-1-0 (which are oriented parallel to the direction of compaction). The increased diffraction intensity for the thin sections normal to the direction of compaction is believed to be due to the increased degree of particle orientation on planes normal to the direction of compaction.

The observed net intensity counts for the 20.8 and 26.60 degree reflections, for all the thin sections analysed, and also the

orientation of the thin sections relative to the direction of compaction are summarized in Tables X and XI. The relationship between the initial moisture content of the soil blocks from which the thin sections were prepared and the ratio of the observed net diffraction intensities of corresponding oriented thin sections, for both Standard and Modified AASHO compaction are shown in Figure 54. The peak intensity ratio is defined in this study as follows:

$$\text{Peak Intensity Ratio} = \frac{I_{\alpha}}{I_{(\alpha-90^{\circ})}}$$

where

$I_{\alpha}$  = net intensity for a particular  $2\theta$  reflection in an oriented thin section whose plane is inclined at an angle  $\alpha$  with the direction of compaction, and

$I_{(\alpha-90^{\circ})}$  = net intensity for the same  $2\theta$  reflection in an oriented thin section inclined at an angle  $(\alpha-90^{\circ})$  with the direction of compaction.

In Figure 54 is shown the relationship between  $I_{90}/I_0$  and the initial moisture content for the thin sections analysed. It can be observed that for the 20.8 degree reflection the ratio,  $I_{90}/I_0$ , increases with increasing moisture content, for both Standard and Modified AASHO compaction procedures. For the 26.60 degree reflection, the peak intensity ratio increases with moisture content for Modified AASHO compaction but it shows a decreasing tendency for Standard AASHO compaction. Although the meager test data do not permit any generalization concerning the exact relationship between the peak intensity ratio and the initial moisture content, the increasing tendency of  $I_{90}/I_0$  ratio with



TABLE X

X-RAY DIFFRACTION PEAK INTENSITY RATIOS -  
STANDARD AASHO COMPACTION

(CuK $\alpha$  Radiation, KVP:40, MA:20, T.C: 1.0, CPS:1000)

Sample Number	Orientation Degrees	Bragg Angle $2\theta$ Degrees	Diffraction Intensity counts/10 sec.			Peak Intensity Ratio
			Peak	Mean Back-ground	Net	
A14-0-1-0	0	20.80	1272	509	763	0.6920
A14-0-1-90	90	20.80	1024	496	528	
A14-0-1-0	0	26.60	3062	452	2610	0.9164
A14-0-1-90	90	26.60	2851	459	2392	
A15-0-1-0	0	20.80	1048	483	565	0.8000
A15-0-1-90	90	20.80	916	464	452	
A15-0-1-0	0	26.60	2916	452	2464	0.8571
A15-0-1-90	90	26.60	2553	441	2112	
A16-0-1-0	0	20.80	974	490	484	1.1983
A16-0-1-90	90	20.80	1068	488	580	
A16-0-1-0	0	26.60	3445	460	2985	0.7102
A16-0-1-90	90	26.60	2567	447	2120	
A17-45-1-45	45	20.80	1036	499	537	0.8770
A17-45-1-135	135	20.80	1023	552	471	
A17-45-1-45	45	26.60	3207	431	2776	0.7460
A17-45-1-135	135	26.60	2511	440	2071	

TABLE XI

X-RAY DIFFRACTION PEAK INTENSITY RATIOS -  
MODIFIED AASHO COMPACTION

(CuK $\alpha$  Radiation, KVP:40, MA:20. T.C:1.0, CPS:1000)

Sample Number	Orientation Degrees	Bragg Angle $2\theta$ Degrees	Diffraction Intensity counts/10 sec.			Peak Intensity Ratio
			Peak	Mean Back-ground	Net	
B11-0-2-0	0	20.80	882	478	404	1.5767
B11-0-2-90	90	20.80	1117	480	637	
B11-0-2-0	0	26.60	3037	464	2573	0.9560
B11-0-2-90	90	26.60	2896	436	2460	
B14-45-1-45	45	20.80	1181	480	701	0.6262
B14-45-1-135	135	20.80	898	459	439	
B14-45-1-45	45	26.60	3084	430	2654	1.0388
B14-45-1-135	135	26.60	3172	415	2757	
B15-0-1-0	0	20.80	1109	502	607	0.6738
B15-0-1-90	90	20.80	886	477	409	
B15-0-1-0	0	26.60	3423	424	2999	0.7229
B15-0-1-90	90	26.60	2632	464	2168	
B16-0-1-0	0	20.80	1031	482	549	0.8214
B16-0-1-90	90	20.80	1006	555	451	
B16-0-1-0	0	26.60	2907	520	2387	0.9074
B16-0-1-90	90	26.60	2611	445	2166	

TABLE XI (continued)

B17-0-1-0	0	20.80	1014	511	503	
<hr/>						
B17-0-1-90	90	20.80	1696	499	1197	2.3797
<hr/>						
B17-0-1-0	0	26.60	2768	426	2342	
<hr/>						
B17-0-1-90	90	26.60	4939	469	4470	1.9086
<hr/>						
<hr/>						

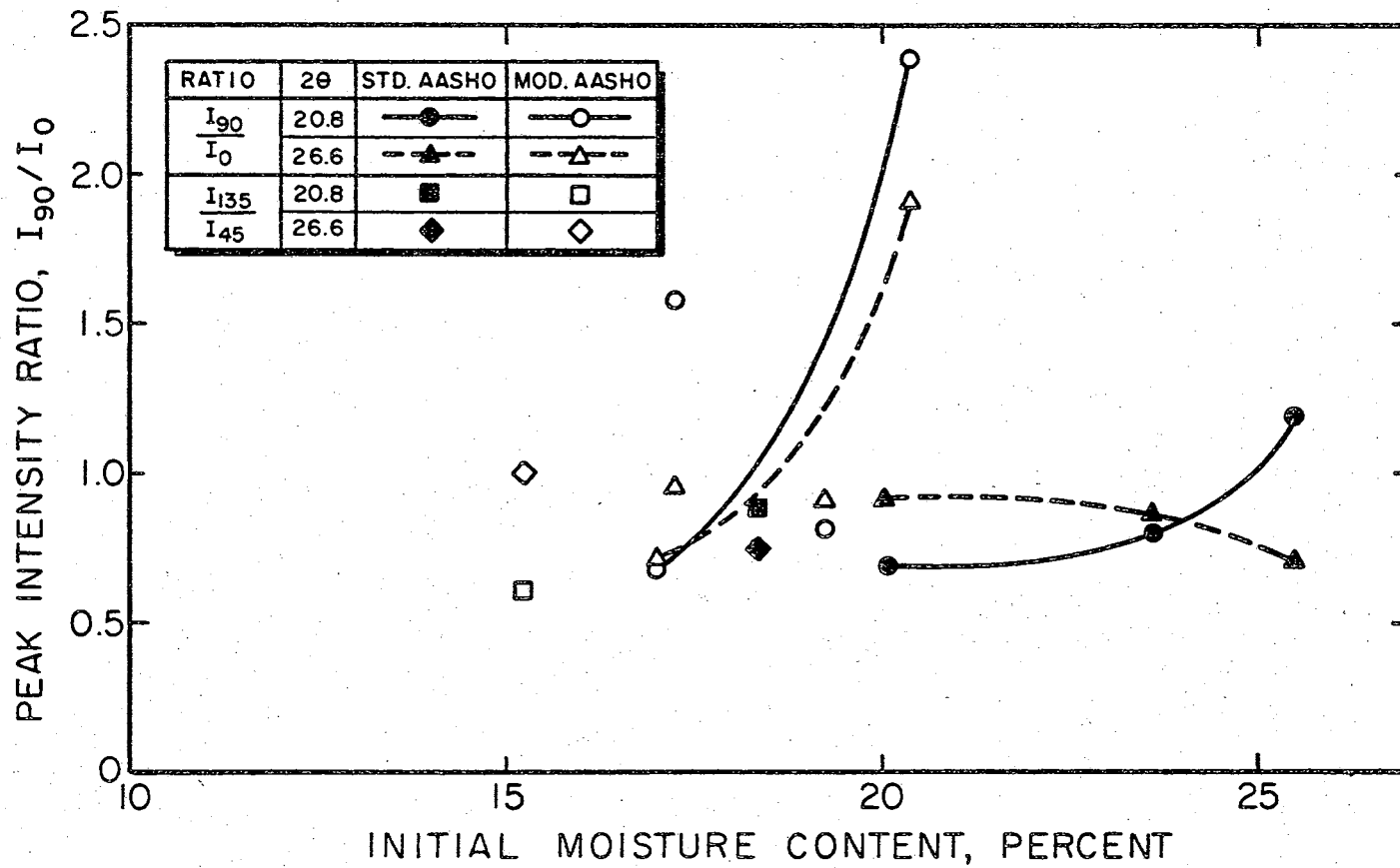


Figure 54. Relationship Between Initial Moisture Content and Peak Intensity Ratio.

increasing initial moisture content is nevertheless evident in Figure 54. It can be observed that this effect is more pronounced in Modified AASHO compaction in view of the greater compactive effort which tends to produce a more parallel particle orientation as compared to that in Standard AASHO compaction. For the oriented thin sections inclined at 45 and 135 degrees to the direction of compaction, the peak intensity ratio  $I_{135}/I_{45}$  was computed and this is also shown in Figure 54 against the corresponding initial moisture content. It is seen that the ratio  $I_{135}/I_{45}$  is approximately equal to unity for moisture contents at or near optimum for Standard and Modified AASHO thin sections and this suggests that the overall soil fabric is approximately the same on planes inclined at 45 and 135 degrees with the direction of compaction - a condition that is likely to result when the particles are either randomly distributed inside the compacted soil block or arranged in a parallel orientation normal to the compaction direction. However further study is required to investigate the variation of the  $I_{135}/I_{45}$  ratio at different initial moisture contents.

### Scanning Electron Microscope Study

#### Introduction

The Scanning Electron Microscope is a relatively new instrument, quite different from the conventional Transmission Electron Microscope both in regard to its principles and applications. Since its introduction in 1965, it has found extensive applications in the diverse fields of geology, clay mineralogy, metallurgy, semiconductor technology, biology and other areas involving surface studies.

In the scanning electron microscope, the sample under study is bombarded with a fine probe of electrons, on an area  $100 \text{ \AA}$  or less in diameter. The electron source is usually a heated hairpin tungsten filament. As the probe strikes only one point on the specimen at a time, data is accumulated from many points to build up a representation of an area of the sample. This is achieved by scanning the electron probe over an area of the sample in a raster pattern. A cathode ray tube is also scanned in synchronization with the electron beam and the intensity of the cathode ray tube is modulated in proportion to the intensity of one or another types of information generated by the impingement of the electron probe on the sample, and this results in a representative image of the area of the sample. The cathode ray tube display is generally recorded photographically, although it is also possible to record it on videotape or to directly computer-process it. The operating parameters such as the speed of scan, number of lines scanned etc., are selected to optimize the resulting image.

The equipment incorporates a sample stage, permitting tilt, rotation and translation of the sample to facilitate examination of the sample surface. Unlike the transmission microscope, changing magnification or specimen orientation in the scanning electron microscope does not require any change in focus. One of the most important features of the scanning electron microscope is its capability of providing a high magnification and depth of field, far exceeding those of an optical microscope. For the examination of rough surfaces, the scanning electron microscope is a powerful tool. The specimen preparation involves a shadowing technique in which the surface is coated with a thin film ( $100 - 500 \text{ \AA}$ ) of a heavy metal, to provide conductivity on an insulating

surface. When this coated surface is examined in the scanning electron microscope, the varying shadow film thickness causes differential scattering of electrons and reveals the gradation of the surface. Kimoto and Russ (1969) have provided a good introduction to scanning electron microscopy and discussed its wide applications in different fields.

#### Preparation of Test Specimens

In the scanning electron microscope the specimen is exposed to high vacuum, heating effects from electron absorption and charge effects from absorption and secondary emission of electrons. Instability of the specimen may, therefore, affect the final interpretation. Generally, soil fabric studies using the electron microscope will require dry specimens as there is a possibility of fabric disturbance in a moist specimen when it is subjected to a high vacuum prior to shadowing. Therefore, the method chosen for the preparation of test specimens should be one producing the least change in the conditions of the sample. Drying the specimen either at room temperature or in an oven is not desirable as the consequent shrinkage would result in fabric disturbance and the development of cracks. In view of these considerations, soil specimens in which the fabric has been preserved by some preliminary treatment appear to be best suited in studies concerning soil structure.

In this research, oriented test specimens which had previously been impregnated using standard impregnation procedures, were used. The impregnating material used (Epoxy plastic) might reduce the image contrast to some extent. However, it was believed that the electron micrographs would provide enough contrast to permit the study of the particle arrangement in the test specimens. To facilitate comparison of the

electron micrographs with the corresponding X-ray diffraction data, oriented test specimens belonging to the same compaction series as those used in diffraction analysis, were used in the scanning electron microscope study.

The orientation of the faces to be studied were accurately marked in these specimens and a record of their orientations relative to the direction of compaction was maintained. Fresh surfaces at the required orientations were fractured by tamping gently with a sharp edge. Great care was taken to see that the sharp edge did not pass through the fractured surface and alter the soil fabric. Two small soil cubes of about one centimeter side, were cut out of each of the test specimens. One cube contained a freshly fractured surface parallel to the direction of compaction and other contained a freshly fractured surface perpendicular to the direction of compaction. These soil cubes were mounted in the high vacuum-evaporator (Model: JEOLCO-JEE-4C of the main unit) and subjected to a high vacuum. The required vacuum was obtained in about 12 minutes, after which the freshly fractured surfaces were shadowed using a gold-palladium alloy wire as ionizing material. This shadowing permits greater contrast and three-dimensional effect on the particle surface of the sample.

In this investigation, 6 samples were prepared out of three oriented test specimens and all these samples were shadowed and studied in the scanning electron microscope. The test specimens for this study were cut from soil blocks compacted by Modified AASHO procedure.

#### Test Procedure

The scanning electron microscope, model. JSM-2 (manufactured by

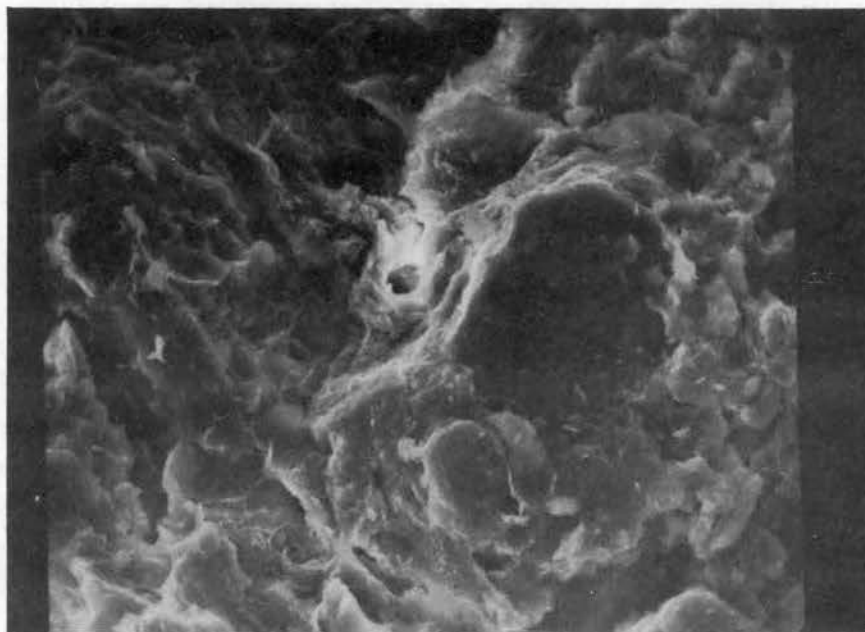


JEOLCO-Japan Electron Optics Laboratory Co., Ltd.), available in the Geology Department of the University of Oklahoma, Norman campus, was used in this investigation. The shadowed samples were mounted in the sample stage of the equipment and the coated surfaces were studied at different magnifications. The entire area of the surface was scanned by rotating the sample stage, and the surface features were studied from observations of the representative images formed on the fluorescent screen. Micrographs of the shadowed faces in fields which provided maximum contrast and relief effects of the surface features, were photographed at different magnifications, using the special camera attachment. These micrographs were used for further detailed study.

#### Data and Discussion

The scanning electron micrographs of faces parallel, perpendicular and at an inclination of 135 degrees to the direction of compaction, in the test specimens are shown in Figures 55 through 57.

Clays are essentially hydrous aluminum silicates and these have a layer lattice or sheet structure. Because of the variation in structure, composition and degree of order in the clay mineral groups, the morphological characteristics of the various mineral species vary widely. Electron micrographs of well crystallized kaolinite show well developed hexagonal flakes, frequently elongated in one direction. The edges are usually beveled and the flakes appear to be twinned. However in poorly crystallized kaolinites, the hexagonal boundary is not well developed, appearing crude and generally in association with smaller particles. Electron micrographs of montmorillonite exhibit broad undulating mosaic sheets. Often they appear as irregular flake-shaped aggregates,

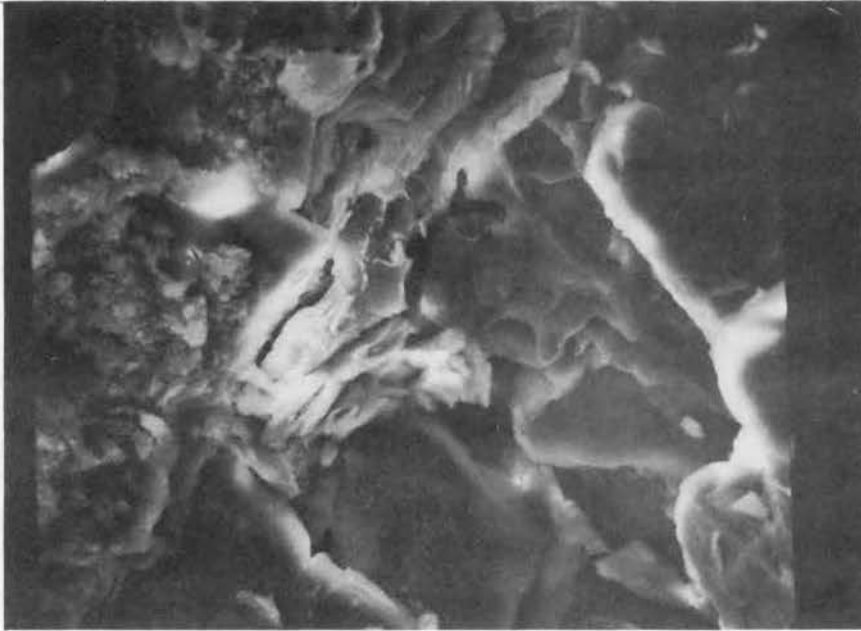


(a)

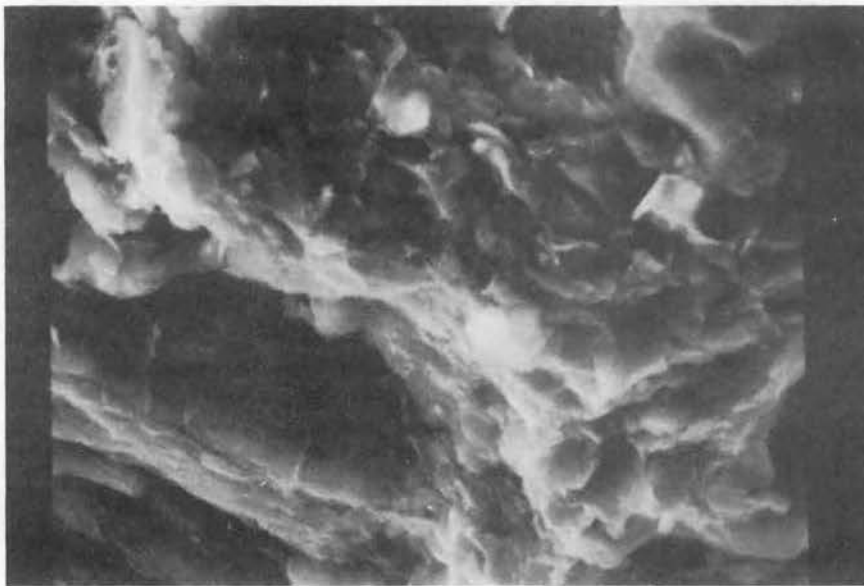


(b)

Figure 55. Electron Micrograph for Face Inclined at 135 Degrees to Compaction Direction in Specimen B 14- 45- 1: (a) 600X; (b) 1800X.

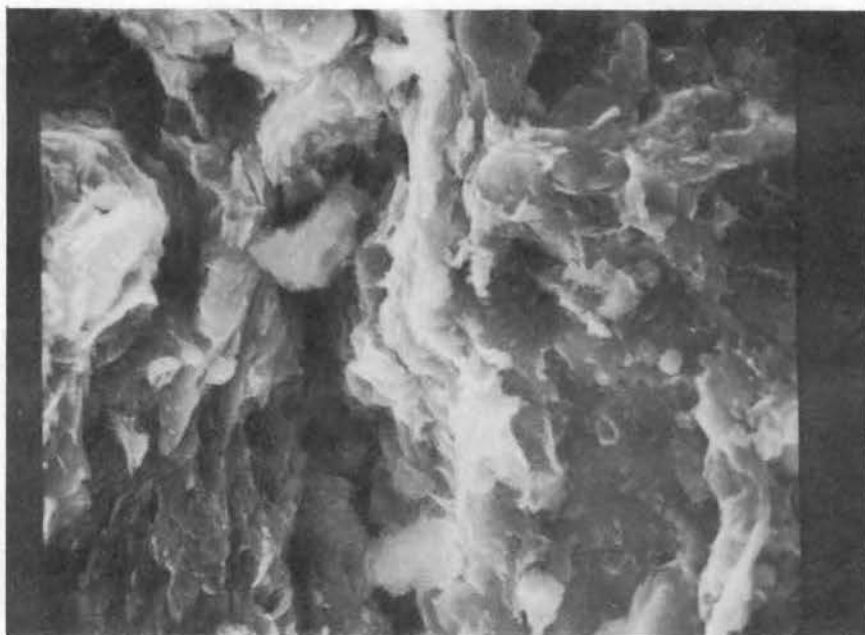


(a)



(b)

Figure 56. Electron Micrograph for Specimen B 15- 0- 1:  
(a) Face Parallel to Compaction Direction, 540X; (b) Face Perpendicular to Compaction Direction, 1440X.



(a)



(b)

Figure 57. Electron Micrograph for Specimen B 17- 0- 1:  
(a) Face Parallel to Compaction Direction, 1800X; (b) Face Perpendicular to Compaction Direction, 1200X.

sometimes with curled edges. The individual particles are too small to reveal clear boundaries, and they are seen generally as plate-like aggregates with a fuzzy appearance. Electron micrographs of illite show generally small, poorly defined flakes grouped together in irregular aggregates. Generally, electron micrographs of illite resemble those of montmorillonites except that they show larger and better defined edges.

As mentioned earlier, only impregnated samples were used in this study. The effect of the impregnating material, epoxy plastic, on the observed fabric pattern is not known. However it is believed that the plastic would tend to mask only the individual particles and reduce the contrast, without affecting the soil fabric. The electron micrographs in Figures 55 through 57, show predominantly irregular plate-like aggregates with curved outlines. The characteristic sheet-like pattern with fuzzy and undulating trend which persists in Figures 55 and 57, suggests the presence of montmorillonite mineral. Small, poorly defined and irregular aggregates might indicate illite. The electron micrographs do not generally show clear and well-developed hexagonal flakes of kaolinite although in some places (Figures 55 and 56) very poorly developed hexagonal flakes can be noticed. This is probably due to the presence of very poorly crystallized kaolinite mineral in the soil.

The object of this study was to investigate the degree of preferred particle orientation relative to the direction of compaction. As discussed in Chapter II, the degree of particle orientation attained during compaction is dependent on the molding moisture content, the mode of compaction and the compactive effort (Lambe, 1960). The average molding moisture contents of the specimens B 14-45-1, B 15-0-1 and B 17-0-1

are respectively 15.23%, 16.99% and 20.38%. The optimum moisture content for the soil using Modified AASHTO compaction procedure, is 14.5%. Therefore specimen B 14-45-1 represents a compaction state very near the optimum while specimen B 17-0-1 corresponds to a condition very much wet of optimum. Specimen B 15-0-1, also represents a compaction condition wet of optimum but it is intermediate between the two states represented by specimens B 14-45-1 and B 17-0-1.

The electron micrographs of specimen B 17-0-1 indicate that there is a very pronounced parallel particle arrangement in the face perpendicular to the compaction direction as compared to that for the face parallel to the direction of compaction (Figure 57). The slightly dipping edges of the stacked-up sheets seen in the micrographs, also indicate that the plate-like particles are arranged in a parallel orientation with their plate faces at right angles to the direction of compaction. As the water content of this specimen is much greater than optimum, there is increased dispersion of the particles which is reflected by a pronounced parallel particle arrangement.

The electron micrographs of specimen B 15-0-1 indicate features similar to those of specimen B 17-0-1, except that in this case the degree of parallel arrangement of particles is relatively less pronounced. Nevertheless parallel sheet configuration is clearly seen in isolated areas (Figure 56). The molding moisture content of specimen B 15-0-1 is less than that of B 17-0-1, and consequently specimen B 15-0-1 represents a less dispersed system compared to the specimen B 17-0-1. And this is reflected in the lesser degree of particle orientation in specimen B 15-0-1 compared to that in specimen B 17-0-1.

The electron micrographs of specimen B 14-45-1 shown in Figure 55, show the soil fabric along plane inclined at 135 degrees with the direction of compaction. A parallel sheet-like arrangement of particles is clearly seen in Figure 55, although it is somewhat less pronounced as compared to that in Figure 57. The characteristic 45-degree striations indicate stacked-up sheets intersecting the surface at an angle of about 45-degree and this corresponds to a parallel particle orientation normal to the direction of compaction. However the degree of particle orientation in specimen B 14-45-1 appears to be less than that of either specimen B 17-0-1 or B 15-0-1. As the water content of specimen B 14-45-1 is nearer to optimum and is less than that of B 15-0-1 and B 17-0-1, the observed low degree of particle orientation is probably due to an increased tendency towards a flocculent structure.

Previous studies have indicated that compaction tends to produce a parallel arrangement of the particles and that the degree of particle orientation is a function of the molding moisture content and compactive effort (Pacey, 1956., Lambe, 1960, and others). The results of this study are substantially in agreement with the established concepts of soil structure of compacted clays. However one interesting feature revealed in this study is that although compaction tends to produce a parallel orientation of particles, this orientational effect is evident only in isolated pockets or domains particularly with molding moisture content near optimum (and probably on the dry side of optimum also). The experimental data further indicate that the degree of particle orientation increases with an increase in the molding water content.

## CHAPTER IV

### GENERAL ANALYSIS

#### Introduction

As stated earlier the purpose of this study was to investigate the anisotropic swelling characteristics of compacted Permian clay and to correlate the observed swelling behavior with the soil fabric. To achieve these objectives, swelling tests were performed using the tri-axial swelling apparatus, and the particle orientation in the compacted soil was studied using X-ray diffraction techniques and scanning electron microscopy. The experimental results and detailed discussions were presented in Chapter III. An attempt will be made here to review briefly and correlate the results of the different phases of this investigation.

#### Swelling Characteristics

The magnitudes of the unit swelling of compacted soil, parallel and perpendicular to the direction of compaction were determined using oriented test specimens. The test data have indicated that the magnitudes of the unit vertical and horizontal swelling vary considerably for specimens cut at different orientations relative to the direction of compaction (Figures 30 through 35 and Tables VI and VII). Specimens whose molding water content was less swelled more and at a faster rate, than those compacted at higher water contents. In general, the water



intake of specimens during swelling was found invariably to exceed the total volume increase; and, for a constant water intake, Modified AASHO samples registered a greater total volume increase than Standard AASHO samples (Figure 36). Specimens with less initial degree of saturation swelled more than those with high initial degree of saturation although the final degree of saturation attained was approximately the same for both. The same effect was observed both for Standard and Modified AASHO samples.

The compactive energy has an influence on the swelling characteristics of compacted soil. In general Modified AASHO samples swelled more than Standard AASHO samples although Standard AASHO samples reached a higher final moisture content after swelling (Figures 39 and 40). The discrepancy between the measured unit swelling values of oriented specimens even corresponding to the same direction is clearly seen in the experimental results presented in Figure 30 through 35 and in Tables VI and VII. The reasons for this observed anomaly were discussed in Chapter III. It was shown that, in view of the possible structural variations in the oriented samples and experimental errors associated with the  $\epsilon_h$  values, the  $\epsilon_v$  values measured with dial gage, should be considered as most reliably representing the true swelling values. The relationships developed on this basis have shown that the unit swelling,  $\epsilon_o$ , parallel to the direction of compaction is generally greater than the unit swelling,  $\epsilon_{90}$ , perpendicular to it, both for Standard and Modified AASHO samples (Figures 44 and 45). The difference between the  $\epsilon_o$  and  $\epsilon_{90}$  values was greater for specimens compacted at water contents less than optimum than for those compacted wet of optimum. Statistical analysis of the relationship between the swelling ratio

( $\epsilon_o/\epsilon_{90}$ ) and the initial moisture content has revealed that the  $\epsilon_o/\epsilon_{90}$  value is generally greater than unity both for the Standard and Modified AASHO compaction in the range of the moisture contents tested (Figures 46 and 47). Also it is seen that  $\epsilon_o/\epsilon_{90}$  has a slightly decreasing tendency with increasing moisture content in the case of Standard AASHO compaction, while it indicates a definite increasing tendency with increasing initial moisture content for Modified AASHO compaction.

### Soil Structure

The structure of compacted soils was studied using X-ray diffraction technique and scanning electron microscopy. The diffraction patterns of oriented thin sections have revealed that the observed net diffraction intensities at 20.80 and 26.60 degree reflections are greater than those for a powder sample and this indicates preferred orientation of particles in the thin sections. Also the diffraction intensities for the thin section normal to the compaction direction were greater than those for the thin section parallel to the compaction direction, particularly for water contents very much wet of optimum (Figures 48 through 51). The experimental data presented in Figure 54 and Tables X and XI, have shown that the peak intensity ratio,  $I_{90}/I_o$ , corresponding to the 20.80 degree reflection shows generally an increasing trend with increasing moisture content of the soil from which the thin sections were made - the effect being more pronounced in the case of Modified AASHO compaction. A similar effect was noticed for the Modified AASHO compaction for the 26.60 degree reflection also, although it tends to decrease slightly with increasing moisture content for the Standard AASHO compaction. There is considerable evidence to indicate that

compaction tends to produce a parallel particle orientation normal to compaction direction and the degree of orientation increases with increase in molding water content and compactive effort (Pacey, 1956; Lambe, 1960 and others). The observed increase in the value of the peak intensity ratio with increasing molding water content should, therefore, be construed as a manifestation of the greater degree of particle orientation at higher water contents.

The limited diffraction data for the thin sections oriented at 45 and 135 degrees to the direction of compaction indicate that the magnitude of the peak intensity ratio,  $I_{135}/I_{45}$ , is approximately equal to unity for water contents at or near optimum. This probably indicates that the overall fabric on the 45 and 135 degree planes is approximately similar.

The scanning electron micrographs of faces in the compacted soil, parallel, perpendicular and at an angle of 135 degrees to compaction direction, indicate that there is a very pronounced parallel particle arrangement normal to compaction direction in samples compacted very much wet of optimum moisture content (Figure 57). For lower moisture contents this orientational effect was not only less pronounced but also was evident only in isolated pockets or domains, particularly in samples compacted at or near the optimum.

#### Effect of Soil Structure on Swelling

In order to study the effect of soil structure on the swelling characteristics of compacted soil, it is necessary to correlate the results of the swelling tests with the data obtained from fabric studies. The scanning electron micrographs indicate qualitatively the parallel

orientation of particles normal to compaction direction at moisture contents wet of optimum. In an attempt to correlate quantitatively the observed swelling behavior with the particle orientation, the relationship between the swelling ratio and the peak intensity ratio was studied and the results are shown in Figure 58. In this figure the swelling ratio,  $\epsilon_o/\epsilon_{90}$ , of the compacted soil is plotted against the peak intensity ratio,  $I_{90}/I_o$  (corresponding to the 20.80 and 26.60 degree reflections) of the oriented thin sections belonging to the same compaction series. As the degree of particle orientation is thought to be directly related to the compactive energy and as the peak intensity ratio is directly proportional to the degree of particle orientation, it is obvious that the peak intensity ratio reflects the effects of different compaction energy levels. Consequently no attempt was made in Figure 58 to differentiate the two compaction procedures used. It can be observed that the swelling ratio increases with increasing peak intensity ratio. The wide scatter of points near about  $I_{90}/I_o = 1$ , is probably due to the lesser degree of particle orientation associated with lower molding moisture contents (cf. Figures 55 and 56). It was shown earlier that the magnitudes of the unit swelling, parallel and perpendicular to the direction of compaction, decrease with increasing molding moisture contents (Figures 44 and 45). However, the swelling ratio ( $\epsilon_o/\epsilon_{90}$ ) appears to increase with increasing initial water contents for Modified AASHO compaction while for Standard AASHO compaction it shows a slightly decreasing tendency (Figures 46, and 47).

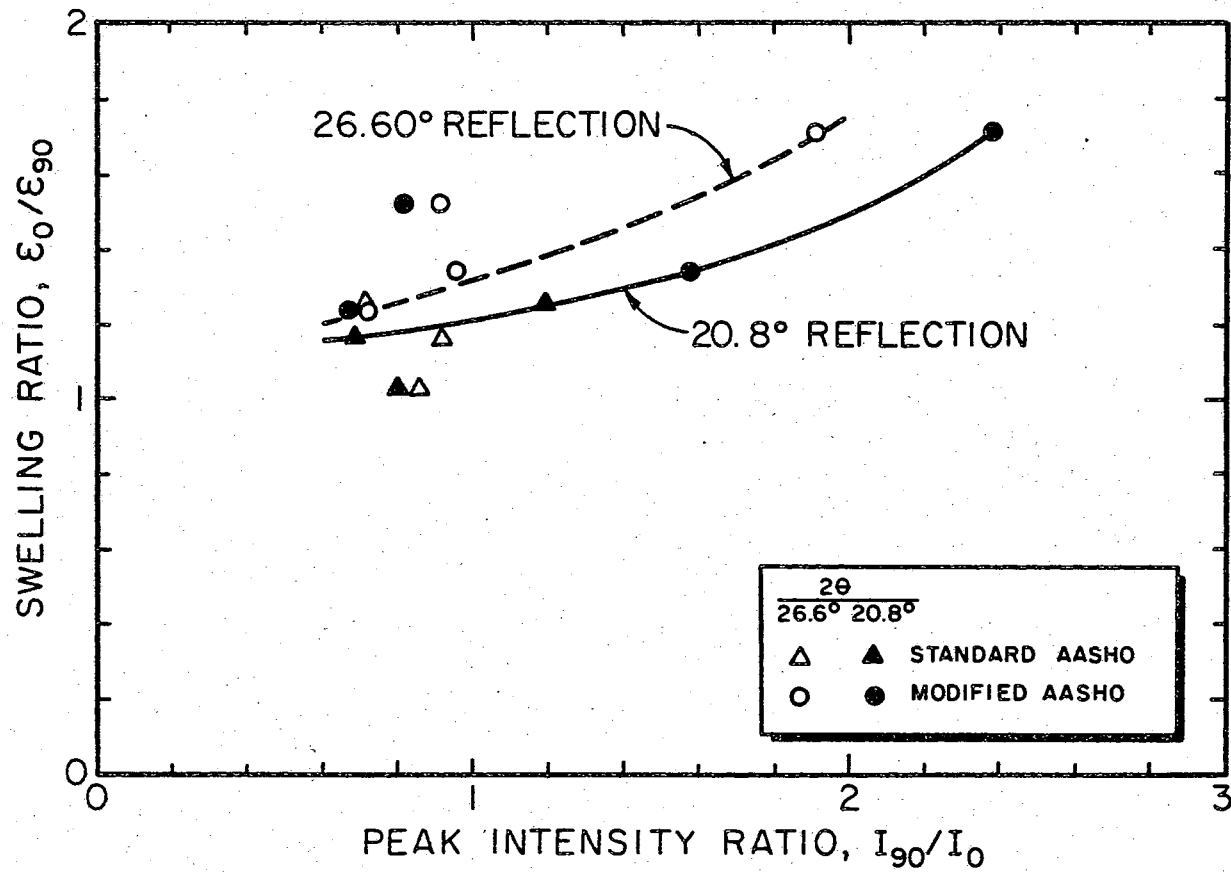


Figure 58. Relationship Between Swelling Ratio and Peak Intensity Ratio.

## CHAPTER V

### CONCLUSIONS AND RECOMMENDATIONS

#### Conclusions

The anisotropic swelling characteristics of compacted clay were studied in the triaxial swelling apparatus and the particle arrangement in the compacted soil was investigated using the X-ray diffractometer and the scanning electron microscope. Based on the experimental data, it is possible to arrive at the following conclusions:

1) The magnitude and the rate of swelling of compacted soil are dependent on the initial moisture content and the compactive effort. Samples whose molding water contents are less swell more and at a faster rate than those compacted at higher water contents, and this is true for samples compacted by both Standard and Modified AASHO procedures. Samples compacted by Modified AASHO procedure swell more than those compacted by Standard AASHO procedure.

2) The water intake by the soil during the swelling process invariably exceeds the total volume increase, for both Standard and Modified AASHO compaction. For a constant water intake, the samples compacted by Modified AASHO procedure swelled more and registered a greater volume increase than those compacted by Standard AASHO procedure.

3) Samples with a low initial degree of saturation swell more than those with high initial degree of saturation although the final degree of saturation attained is about the same for both. The final

degree of saturation is generally less than 100%. Also, samples compacted by Standard AASHO procedure reach a higher final moisture content after swelling than those compacted by Modified AASHO procedure.

4) Compacted soils are, in general, anisotropic with respect to swelling. The magnitude of unit swelling parallel to the direction of compaction ( $\epsilon_o$ ) is greater than the unit swelling perpendicular to the direction of compaction ( $\epsilon_{90}$ ), both for Standard and Modified AASHO compaction. For samples compacted dry of the optimum moisture content, the difference between the  $\epsilon_o$  and  $\epsilon_{90}$  values tends to be greater than for those compacted wet of the optimum.

5) There is an appreciable difference between the unit swelling values of oriented specimens even corresponding to the same direction. The unit horizontal swelling of a vertically cut sample differs from the unit vertical swelling of a horizontally cut sample. A similar anomaly is noticed between the unit vertical swelling of a vertically cut sample and the unit horizontal swelling of a horizontally cut sample. The reasons for the observed differences are believed to be due to individual structural variations in the oriented specimens and possible experimental errors associated with the measured horizontal unit swelling values.

6) The swelling ratio,  $\epsilon_o/\epsilon_{90}$  of the compacted soil is, in general, found to be greater than unity, for the range of moisture contents tested. The relationship between the swelling ratio and the initial moisture content of the compacted soil can be characterized by the following regression equations:

Standard AASHO compaction: ( $14.74\% \leq X \leq 25.50\%$ )

$$Y = -0.02437 X + 1.76675$$

Modified AASHO compaction: ( $13.54\% \leq X \leq 20.38\%$ )

$$Y = + 0.09266 X - 0.21268$$

where

$X$  = Initial moisture content, percent, and

$Y$  = Swelling ratio,  $\epsilon_o/\epsilon_{90}$ .

7) For Standard AASHO compaction, the swelling ratio tends to decrease slightly with increasing initial moisture content, probably due to soil disturbance caused by repeated penetrations of the hammer during compaction at higher water contents. However, in the case of Modified AASHO compaction, the swelling ratio shows a definite increasing trend with increasing initial moisture content and this is believed to be due to the greater degree of particle orientation resulting from the increased compactive effort used.

8) The peak intensity ratio,  $I_{90}/I_o$ , corresponding to the 20.80 and 26.60 degree reflections increases with increasing initial moisture content of the compacted soil from which the oriented thin sections were extracted. The increased peak intensity ratio appears to be due to the greater degree of orientation normal to the compaction direction at higher water contents. The peak intensity ratio,  $I_{135}/I_{45}$ , of thin sections at 45 and 135 degrees to the compaction direction, is found to be approximately equal to unity for initial moisture contents at or near the optimum.

9) The scanning electron micrographs of oriented faces in the compacted soil indicate that there is a pronounced parallel particle orientation normal to the compaction direction in specimens compacted



very much wet of the optimum moisture content. The degree of particle orientation is less in samples compacted at or near the optimum. Also this orientational effect is evident only in isolated pockets or domains, particularly with molding water contents at or near the optimum.

10) The swelling ratio,  $\epsilon_o/\epsilon_{90}$  increases with increasing peak intensity ratio,  $I_{90}/I_o$ . As the peak intensity ratio increases with increasing initial moisture content, it appears that the swelling ratio would, in general, increase with increasing initial moisture content (cf. item 7).

11) The use of filter strips along the sides of the test specimen in triaxial swelling tests tends to equalize the moisture distribution along its length. However even with the use of filter strips complete equalization of moisture content was not achieved.

12) The triaxial swelling apparatus is found to be satisfactory in studies concerning the swelling characteristics of soil. However, in view of the observed anomaly between the unit swelling values of oriented specimens and the experimental difficulties encountered in the measurement of the  $\epsilon_h$  values from the saran tube readings, some modifications of the apparatus appear necessary.

#### Recommendations for Further Research

In this investigation an attempt has been made to study the anisotropic swelling characteristics of compacted Permian clay and to correlate the observed swelling behavior with the particle orientation. The experimental results have established the swelling and structural anisotropy of compacted soils and have indicated the influence of particle orientation on the swelling characteristics. However, much

additional research is necessary to gain a complete understanding of the anisotropic swelling behavior and its relation to soil structure. The following are some suggestions which might prove useful in future research:

- 1) Investigation of the anisotropic swelling characteristics of remolded soils using other methods of compaction and pure clay minerals.
- 2) Quantitative evaluation of the fabric variations in compacted soil on planes at different orientations relative to the direction of compaction.
- 3) Correlation of the swelling anisotropy with the structural anisotropy for soils compacted by different compaction procedures.
- 4) Development of instrumentation for investigating three-dimensional swelling anisotropy in soils.

## A SELECTED BIBLIOGRAPHY

- Abelev, Yu. M., V. S. Sazhin, and E. S. Burov. "Deformational Properties of Expansive Soils." Proceedings, 3rd Asian Regional Conference on Soil Mechanics and Foundation Engineering, Vol 1, Haifa, Israel (1967), pp. 57-59.
- Azaroff, L. V. Elements of X-ray Crystallography. New York: McGraw-Hill Book Company, 1968, 610 p.
- Baracos, A., and M. Bozozuk. "Seasonal Movements in Some Canadian Clays" Proceedings, 4th International Conference on Soil Mechanics and Foundation Engineering, Vol. 1, London (1957), pp. 264-268.
- Barber, E. S. Discussion of "Engineering Properties of Expansive Clays" by W. G. Holtz and H. J. Gibbs, Transactions, ASCE, Vol. 121 (1956) pp. 669-673.
- Bolt, G. H. "Analysis of the Validity of the Gouy-Chapman Theory of the Electric Double Layer". Journal of Colloid Science, Vol. 10 (1955), pp. 206-218.
- \_\_\_\_\_. "Physico-Chemical Analysis of the Compressibility of Pure Clays." Geotechnique, Vol. 6 (1956), pp. 86-93.
- Bozozuk, M., and K. N. Burn. "Vertical Ground Movements Near Elm Trees" Geotechnique, Vol. 10 (1960), pp. 19-32.
- Brindley, G. W. "An X-ray Method for Studying Orientation of Micaceous Minerals in Shales, Clays and Similar Material". The Mineralogical Magazine, Vol. 30, No. 220 (1953), pp. 71-78.
- Bruijin, C. M. A. De. "Swelling Characteristics of Transported Soil Profile at Leeuhof Vereeniging (Transvaal)." Proceedings, 5th International Conference on Soil Mechanics and Foundation Engineering, Vol. 1, Paris (1961), pp. 43-49.
- Campagna, N. A. "Fabric of Consolidated and Sheared Kaolinite". (Unpublished S.M. Thesis, Massachusetts Institute of Technology, Cambridge, Massachusetts, 1967).
- Casagrande, A. "The Structure of Clay and Its Importance in Foundation Engineering". Boston Society of Civil Engineers, Contributions to Soil Mechanics, (1925-1940), pp. 72-125.

Cullity, B. D. Elements of X-ray Diffraction. Reading, Massachusetts: Addison-Wesley Publishing Company, Inc., 1956, 514 p.

Dapples, E. C., and J. F. Rominger. "Orientation Analysis of Fine-Grained Clastic Sediments: A Report of Progress". Journal of Geology, Vol. 53 (1945), pp. 246-261.

Dawson, R. F. "Movement of Small Houses Erected on an Expansive Clay Soil". Proceedings, 3rd International Conference on Soil Mechanics and Foundation Engineering, Vol. 1, Switzerland (1953), pp. 346-350.

\_\_\_\_\_. "Modern Practices Used in the Design of Foundations for Structures on Expansive Soils". Colorado School of Mines Quarterly, Vol. 54, No. 4 (1959), pp. 67-87.

De Graft-Johnson, J. W. S., H. S. Bhatia, and M. D. Gidigasu. "The Consolidation and Swell Characteristics of Accra Mottled Clays". Proceedings, 3rd Asian Regional Conference on Soil Mechanics and Foundation Engineering, Vol. 1, Haifa, Israel (1967), pp. 75-80.

Fost, R. B. "Development of Equipment for Clay Swelling Tests". (Unpublished M. S. Thesis, Oklahoma State University, Stillwater, Oklahoma, 1962).

Greco, E. M. "Stabilization of Clay With 4-Tert-Butylpyrocatechol". (Unpublished M. S. Thesis, Oklahoma State University, Stillwater, Oklahoma, 1964).

Grim, R. E. "Physico-Chemical Properties of Soils: Clay Minerals". Journal of the Soil Mechanics and Foundations Division, ASCE, Vol. 85, No. SM 2, Proc. Paper 1998 (1959), pp. 1-17.

\_\_\_\_\_. Clay Mineralogy. 2nd Edition. New York: McGraw-Hill Book Company, Inc., 1968, 596 p.

Gupta, S. N., B. N. Gupta, and K. P. Shukla. "Physico-Chemical Properties of Expansive Clays in Relation to Their Engineering Behavior". Proceedings, 3rd Asian Regional Conference on Soil Mechanics and Foundation Engineering, Vol. 1, Haifa, Israel (1967) pp. 84-89.

Ho, M. M. K. "The Effect of Swelling on Swelling Pressure". Proceedings, 3rd Asian Regional Conference on Soil Mechanics and Foundation Engineering, Vol. 1, Haifa, Israel (1967), pp. 90-93.

Holtz, W. G., and H. J. Gibbs. "Engineering Properties of Expansive Clays". Transactions, ASCE, Vol. 121 (1956), pp. 641-663.

Holtz, W. G. "Expansive Clays-Properties and Problems". Colorado School of Mines Quarterly, Vol. 54, No. 4 (1959), pp. 89-117.

- Jennings, J. E. "The Heaving of Buildings on Desiccated Clays". Proceedings, 3rd International Conference on Soil Mechanics and Foundation Engineering, Vol. 1, Switzerland (1953), pp. 390-396.
- Kerr, P. F. "Attapulugus Clay." The American Mineralogist, Journal of the Mineralogical Society of America, Vol. 22 (1937), pp. 534-550.
- \_\_\_\_\_. Discussion of "Physico-Chemical Properties of Soils: Clay Minerals" by R. E. Grim, Journal of the Soil Mechanics and Foundations Division, ASCE, Vol. 85, No. SM 2, Proc. Paper 2010 (1959), pp. 73-78.
- Kimoto, S., and J. C. Russ. "The Characteristics and Applications of the Scanning Electron Microscope." American Scientist, Vol. 57, No. 1 (1969), pp. 112-133.
- Klug, H. P., and L. E. Alexander. X-ray Diffraction Procedures for Polycrystalline and Amorphous Materials. New York: John Wiley and Sons, Inc., 1954, 716 p.
- Komornik, A., and M. Livneh. "The Effect of Anisotropy on Swelling of a Compacted Clay." Proceedings, 3rd Asian Regional Conference on Soil Mechanics and Foundation Engineering, Vol. 2, Haifa, Israel (1967), pp. 181-185.
- Ladd, C. C. "Mechanisms of Swelling by Compacted Clay." Highway Research Board Bulletin 245 (1959), pp. 10-26.
- Lambe, T. W. "The Structure of Inorganic Soil". Proceedings, ASCE, Vol. 79, Separate No. 315 (1953), pp. 1-49.
- \_\_\_\_\_. "Compacted Clay-Structure and Engineering Behavior". Transactions, ASCE, Vol. 125 (1960), pp. 681-756.
- Lambe, T. W., and R. V. Whitman. "The Role of Effective Stress in the Behavior of Expansive Soils" Colorado School of Mines Quarterly, Vol. 54, No. 4 (1959), pp. 33-61.
- \_\_\_\_\_. Soil Mechanics. New York: John Wiley and Sons, 1969, 553 p.
- Langmuir, I. "Repulsive Forces Between Charged Surfaces in Water, and the Cause of the Jones-Ray Effect". Science, Vol. 88 (1938), pp. 430-432.
- Liu, P. C. "Some Swelling Characteristics of Compacted and Undisturbed Clays." (M.S. Thesis, Oklahoma State University, Stillwater, Oklahoma, 1964).
- Low, P. F. Discussion of "Physico-Chemical Properties of Soils: Ion Exchange Phenomena", by A. W. Taylor, Journal of the Soil Mechanics and Foundations Division, ASCE, Vol. 85, No. SM 2, Proc. Paper 2010 (1959), pp. 79-89.

Martin, R. T. "Research on the Physical Properties of Marine Soils".  
M.I.T. Research Report, R 62-42, Soils Publication, No. 127 (1962).

"Quantitative Fabric of Consolidated Kaolinite". M.I.T.  
Research Report, R 65-47, Soils Publication, No. 179 (1965).

Marshall, C. E. "The Orientation of Anisotropic Particles in an  
Electric Field". Transactions, Faraday Society, Vol. 26 (1930),  
pp. 173-189.

"Clays as Minerals and Colloids". Transactions, Ceramics  
Society (England), Vol. 30 (1931), pp. 81-96.

McDowell, C. "The Relation of Laboratory Testing to Design for Pave-  
ments and Structures on Expansive Soils". Colorado School of Mines  
Quarterly, Vol. 54, No. 4 (1959), pp. 127-153.

Means, R. E. "Buildings on Expansive Clay". Colorado School of Mines  
Quarterly, Vol. 54, No. 4 (1959), pp. 1-31.

Mitchell, J. K. "The Fabric of Natural Clays and its Relation to  
Engineering Properties." Proceedings, Highway Research Board,  
vol. 35 (1956), pp. 693-713.

Morgenstern, N. R., and J. S. Tchalenko. "The Optical Determination of  
Preferred Orientation in Clays and Its Application to the Study of  
Microstructure in Consolidated Kaolin, I and II." Proceedings of  
the Royal Society, A, Vol. 300 (1967), pp. 218-234 and 235-250.

Morris, P. O. "A Comparison Between the Actual and the Potential Verti-  
cal Displacement of the Ground Surface at Various Locations at the  
New Town of Elizabeth, South Australia". Proceedings, 3rd  
Australian-New Zealand Conference on Soil Mechanics and Foundation  
Engineering, Australia (1960), pp. 39-42.

Nuffield, E. W. X-ray Diffraction Methods. New York: John Wiley and  
Sons, Inc., 1966, 409 p.

O'Brien, N. R. "Origin of Pennsylvanian Underclays in the Illinois  
Basin." Geological Society of America Bulletin, Vol. 75, No. 3,  
(1964), pp. 823-832.

Olphen, H. Van. An Introduction to Clay Colloid Chemistry. New York:  
Interscience Publishers, 1963, 304 p.

Ozkol, S. "Swelling Characteristics of Permian Clay." (Unpublished  
Ph.D. Thesis, Oklahoma State University, Stillwater, Oklahoma  
1965).

Pacey, J. G., Jr., "The Structure of Compacted Soils". (M.S. Thesis,  
Massachusetts Institute of Technology, Cambridge, Massachusetts,  
1956).

- Parcher, J. V., and P. C. Liu. "Some Swelling Characteristics of Compacted Clays." Journal of the Soil Mechanics and Foundations Division, ASCE, Vol. 91, No. SM 3, Proc. Paper 4316 (1965), pp. 1-17.
- Parcher, J. V., and R. E. Means. Soil Mechanics and Foundations. Columbus, Ohio: Charles E. Merrill Publishing Company, 1968, 573 p.
- Potter, P. E., and R. F. Mast. "Sedimentary Structures, Sand Shape Fabrics and Permeability, I." Journal of Geology, Vol. 71 (1963) pp. 441-471.
- Quigley, R. M.; and C. D. Thompson. "The Fabric of Anisotropically Consolidated Sensitive Marine Clay". Canadian Geotechnical Journal, Vol. 3, No. 2 (1966), pp. 61-73.
- Ranganatham, B. V., and B. Satyanarayana. "A Rational Method of Predicting Swelling Potential for Compacted Expansive Clays". Proceedings, 6th International Conference on Soil Mechanics and Foundation Engineering, Vol. 1, Toronto, Canada (1965), pp. 92-96.
- Rose, C. W. Agricultural Physics. First Edition. New York: Pergamon Press Ltd., 1966, 226 p.
- Rosenqvist, I. Th. "Physico-Chemical Properties of Soils: Soil-Water Systems". Journal of the Soil Mechanics and Foundations Division, ASCE, Vol. 85, No. SM 2, Proc. Paper 2000 (1959), pp. 31-53.
- Ross, C. S., and E. V. Shannon. "Minerals of Bentonite and Related Clays, and Their Physical Properties". Journal of American Ceramics Society, Vol. 9 (1926), pp. 77-96.
- Salas, J. A. J., and J. M. Serratosa. "Foundations on Swelling Clays". Proceedings, 4th International Conference on Soil Mechanics and Foundation Engineering, Vol. 1, London (1957), pp. 424-428.
- Scott, R. F. Principles of Soil Mechanics. Reading, Massachusetts: Addison-Wesley Publishing Company, Inc., 1963, 550 p.
- Seed, H. B., and C. K. Chan. "Compacted Clays-Structure and Strength Characteristics." Transactions, ASCE, Vol. 126 (1961), pp. 1343-1425.
- Seed, H. B., J. K. Mitchell and C. K. Chan. "Studies of Swell and Swell Pressure Characteristics of Compacted Clays" Highway Research Board Bulletin, 313 (1961), pp. 12-39.
- Seed, H. B., R. J. Woodward and R. Lundgren. "Prediction of Swelling Potential for Compacted Clay." Journal of the Soil Mechanics and Foundations Division, ASCE, Vol. 88, No. SM 3, Proc. Paper 3169 (1962). pp. 53-87.

- Silverman, E. N., and T. F. Bates. "X-ray Diffraction Study of Orientation in the Chattanooga Shale". American Mineralogist, Vol. 45 No. 1 (1960), pp. 60-68.
- Sloan, R. L., and T. R. Kell. "The Fabric of Mechanically Compacted Kaolin". Clays and Clay Minerals, 14th Conference Proceedings, Pergamon Press, New York (1965), pp. 289-296.
- Taylor, A. W. "Physico-Chemical Properties of Soils: Ion Exchange Phenomena". Journal of the Soil Mechanics and Foundations Division, ASCE, Vol. 85, No. SM 2, Proc. Paper 1999 (1959), pp. 19-30.
- Terzaghi, K. "The Influence of Elasticity and Permeability on the Swelling of Two-Phase Systems". Colloid Chemistry by Jerome Alexander (Editor), Vol. 3 (1931), pp. 65-88.
- Tice, J. A. "Fabric of Compacted Kaolinite". (Unpublished M.S. Thesis, Massachusetts Institute of Technology, Cambridge, Massachusetts, 1967).
- Trollope, D. H., and C. K. Chan. "Soil Structure and Step-Strain Phenomenon". Journal of the Soil Mechanics and Foundations Division, ASCE, Vol. 86, No. SM 2, Proc. Paper 2431 (1960), pp. 1-39.
- Tschebotarioff, G. P. "A Case of Structural Damages Sustained by One-Storey High Houses Founded on Swelling Clays." Proceedings, 3rd International Conference on Soil Mechanics and Foundation Engineering, Vol. 1, Switzerland (1953), pp. 473-476.
- Tsytoovich, N. A., Yu. K. Zaretsky and Z. G. Ter-Martirosyan. "Problems of Soil Swelling on Wetting." Proceedings, 3rd Asian Regional Conference on Soil Mechanics and Foundation Engineering, Vol. 1, Haifa, Israel (1967), pp. 120-123.
- Ward, W. H. "Soil Movement and Weather". Proceedings, 3rd International Conference on Soil Mechanics and Foundation Engineering, Vol. 1, Switzerland (1953), pp. 477-482.
- Ward, W. H., S. G. Samuels and M. E. Butler. "Further Studies of the Properties of London Clay". Geotechnique, Vol. 9 (1959), pp. 33-58.
- Warkentin, B. P., and M. Bozozuk. "Shrinkage and Swelling Properties of Two Canadian Clays", Proceedings, 5th International Conference on Soil Mechanics and Foundation Engineering, Vol. 1, Paris (1961) pp. 851-855.
- Williamson, W. O. "The Fabric, Water Distribution, Drying-Shrinkage, and Porosity of Some Shaped Discs of Clay". American Journal of Science, Vol. 245 (1947), pp. 645-662.



Willis, W. O., D. R. Nielsen and J. W. Biggar. "Water Movement Through Acrylic Plastic." Proceedings, Soil Science Society of America, Vol. 29 (1965), pp. 636-637.

Wooltorton, F. L. D. "A Preliminary Investigation Into the Subject of Foundations in the Black Cotton and Kyatti Soils of the Mandalay District, Burma." Proceedings, 1st International Conference on Soil Mechanics and Foundation Engineering, Vol. 3, Cambridge, Massachusetts (1936), pp. 242-256.

\_\_\_\_\_. "Movements in the Desiccated Alkaline Soils of Burma" Proceedings, ASCE, Vol. 76, No. 1 (1950), pp. 63-69.

Yong, R. N. "The Swelling of a Montmorillonite Clay at Elevated Temperatures". Proceedings, 3rd Asian Regional Conference on Soil Mechanics and Foundation Engineering, Vol. 1, Haifa, Israel (1967) pp. 124-128.

Yong, R. N., and B. P. Warkentin. Introduction to Soil Behavior. New York: The Macmillan Company, 1966, 451 p.

Youssef, M. S., A. A. Sabry and M. M. Tewfik. "Substantial Consolidation and Swelling of Clay Cause Two Interesting Cases of Serious Damage to Hospital Buildings in Egypt." Proceedings, 4th International Conference on Soil Mechanics and Foundation Engineering, Vol. 1, London (1957), pp. 462-466.

APPENDIX A

DERIVATION OF EXPRESSIONS FOR THE  
ANALYSIS OF SWELLING TEST DATA

## INTRODUCTION

All the swelling tests in this investigation were performed using the triaxial swelling apparatus. Cylindrical soil specimens cut in different orientation, out of soil blocks compacted by Standard and Modified AASHO procedures were used. The observational data during the swelling tests included the vertical swelling recorded by dial gage, the linear displacement of the air-water interface in the saran tube corresponding to the volumetric displacement of chamber water due to the radial swelling, and the amount of water absorbed by the soil as recorded by the drop in water level of the reservoir and which was measured with a sensitive micrometer screw. The derivation of the various expressions that were used in the analysis of the swelling test data, are given below.

## ASSUMPTIONS

1. The swelling in the horizontal or radial direction is uniform and is constant along the length of the specimen. That is, the cross section of the specimen after swelling is perfectly circular and has the same area along its length.
2. There is no loss of water due to absorption by Plexiglas components of the apparatus, saran tube and through the various connections.
3. The physical properties of the chamber fluid remain constant during the duration of test.
4. Idealized conditions exist during the test for the free swelling of the specimen.

## DERIVATION OF EXPRESSIONS

Unit Swelling in the Vertical Direction

As the dial gage registers directly the swelling in the vertical direction, the unit swelling in the vertical direction ( $\epsilon_v$ ), is given by:

$$\epsilon_v = \frac{\Delta H}{H} \quad (1)$$

or, expressing  $\epsilon_v$  as a percentage,

$$\epsilon_v = \frac{\Delta H}{H} \times 100 \quad (2)$$

where  $\Delta H$  = Swelling in the vertical direction, and

$H$  = Initial height of the specimen.

Unit Swelling in the Horizontal or Radial Direction

A soil specimen, when allowed to absorb water, will continue to swell until equilibrium is reached between the pore water pressure and the repulsive and other attractive forces in the electric double layer around the clay particles.

At any instant during the swelling process, if  $\Delta H$  and  $\Delta r$  are respectively the magnitudes of swelling in the vertical and radial directions of a cylindrical specimen (Figure 59), then the total volume increase ( $\Delta V$ ) can be written as:

$$\Delta V = \pi(r+\Delta r)^2 (H+\Delta H) - \pi r^2 H \quad (3)$$

However, in the triaxial swelling test, only the volume increase contributed by the swelling in the radial direction, is measured by the

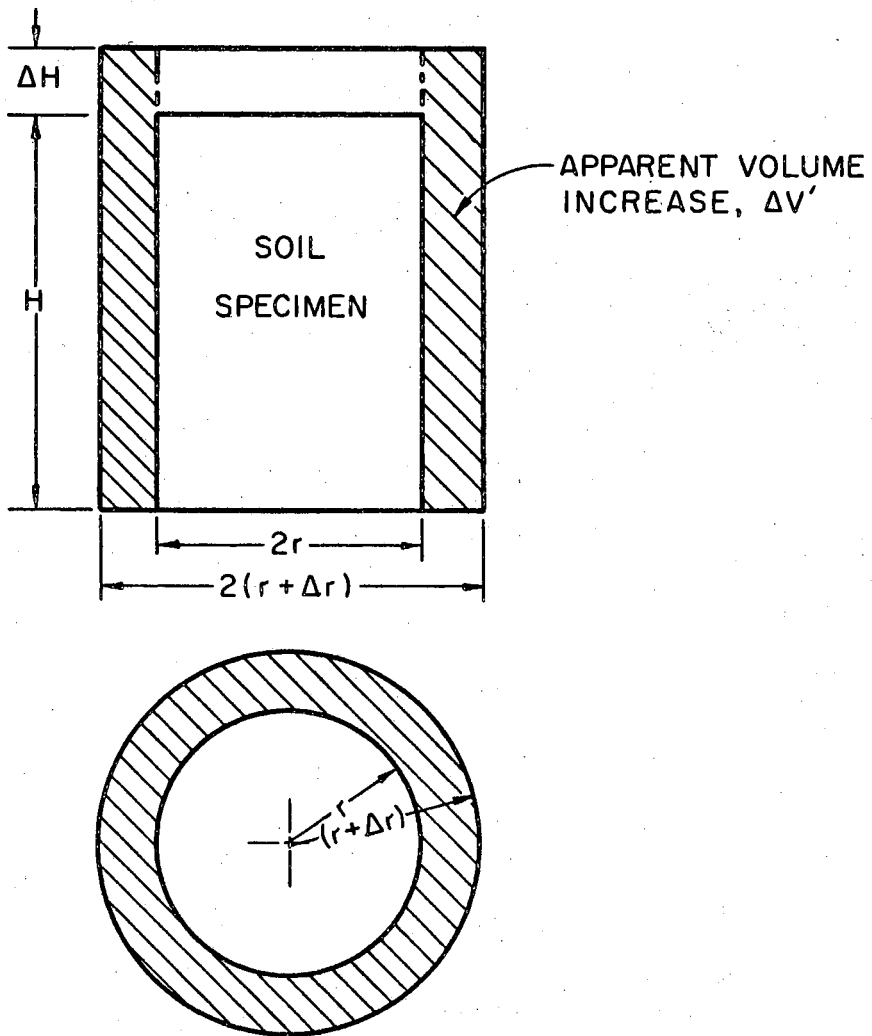


Figure 59. Swelling of a Cylindrical Soil Specimen.

sarantube, because the design of the apparatus prevents the total volume increase from being registered. Considering only this apparent volume increase ( $\Delta V'$ ) (shown shaded in Figure 59), we have:

$$\Delta V' = 2\pi\left(r + \frac{\Delta r}{2}\right) \Delta r (H + \Delta H) = C \cdot \Delta R$$

Where  $C$  = Capacity per unit length of the saran tube, and

$\Delta R$  = Linear displacement of water in the saran tube.

$$\text{i.e. } \pi(H + \Delta H)(\Delta r)^2 + 2\pi r(H + \Delta H)(\Delta r) - C \cdot \Delta R = 0$$

But

$$\epsilon_v = \frac{\Delta H}{H} \quad \text{and} \quad \epsilon_h = \frac{\Delta r}{r}$$

$$\therefore \pi H(1 + \epsilon_v)\epsilon_h^2 + 2\pi H(1 + \epsilon_v)\epsilon_h - \frac{C \cdot \Delta R}{r^2} = 0$$

$$\epsilon_h^2 + 2\epsilon_h - \frac{C \cdot \Delta R}{\pi r^2 H(1 + \epsilon_v)} = 0$$

Solving this quadratic equation, we obtain:

$$\epsilon_h = \sqrt{1 + \frac{C \cdot \Delta R}{\pi r^2 H(1 + \epsilon_v)}} - 1 \quad (4)$$

This is the required expression for the horizontal swelling, expressed as a ratio.

If  $\epsilon_v$  and  $\epsilon_h$  are expressed as percentages, then:

$$\epsilon_h = 100 \left[ \sqrt{1 + \frac{C \cdot \Delta R}{\pi r^2 H(1 + 0.01 \epsilon_v)}} - 1 \right] \quad (5)$$

Expanding the term under the radical sign, as a Binomial series:

$$\epsilon_h = 100 \left[ \left\{ 1 + \frac{1}{2} \frac{C \cdot \Delta R}{\pi r^2 H (1 + 0.01 \epsilon_v)} - \frac{1}{8} \left( \frac{C \cdot \Delta R}{\pi r^2 H (1 + 0.01 \epsilon_v)} \right)^2 + \dots \right\} - 1 \right]$$

If we neglect all the higher powers of

$$\frac{C \cdot \Delta R}{(\pi r^2 H)(1 + 0.01 \epsilon_v)}$$

we can write:

$$\epsilon_h = \frac{C \cdot \Delta R}{2\pi r^2 H (1 + 0.01 \epsilon_v)} \times 100 \quad (6)$$

It can be observed that the equation (6) is exactly the same approximate expression given by Parcher and Liu (1965).

This approximate expression overestimates the value of  $\epsilon_h$  by less than 3 percent (Parcher and Liu, 1965). However, it is considered desirable in this investigation to use the accurate expression for  $\epsilon_h$ , as given by equations (4) and (5).

### Volumetric Swelling

The total volume increase ( $\Delta V$ ) which the specimen undergoes during swelling is, by equation (3):

$$\begin{aligned} \Delta V &= \pi(r + \Delta r)^2(H + \Delta H) - \pi r^2 H \\ &= \pi r^2 \Delta H + (2\pi r + \pi \Delta r) \Delta r (H + \Delta H) \end{aligned}$$

Incorporating the unit swelling  $\epsilon_v$  and  $\epsilon_h$ , we get:

$$\Delta V = \pi r^2 H \epsilon_v + 2\pi r^2 H \left(1 + \frac{\epsilon_h}{2}\right) \epsilon_h (1 + \epsilon_v)$$

$$\Delta V = \pi r^2 H \left[ \epsilon_v + \epsilon_h (1 + \epsilon_v)(2 + \epsilon_h) \right]$$

Therefore the volumetric swelling ( $\eta$ ), which is defined as the ratio of the total volume increase to the initial volume of the specimen, is given by:

$$\eta = \epsilon_v + \epsilon_h (1 + \epsilon_v)(2 + \epsilon_h) \quad (7)$$

Expressing  $\epsilon_v$  and  $\epsilon_h$  and  $\eta$  as percentages,

$$\eta = \epsilon_v + 2 \epsilon_h (1 + 0.01 \epsilon_v)(1 + 0.005 \epsilon_h) \quad (8)$$

### Swell-Intake Ratio

The triaxial swelling apparatus permits the accurate measurement of the quantity of water absorbed by the soil specimen during the swelling process and this is accomplished by observing the position of water level in the reservoir by means of a micrometer screw.

If ( $\Delta a$ ) is the drop in the water level of the reservoir, then the water intake of the specimen =  $\pi R_c^2 (\Delta a)$  where

$$R_c = \text{Radius of the reservoir.}$$

It has been established that the total volume increase which a soil undergoes during swelling is always less than the actual water intake. To serve as a check on the accuracy of the swelling tests and as well as to investigate the swelling and water intake characteristics, the swell-intake ratio, which is defined as the ratio of the total volume increase to the water intake, is computed for all the tests, using the following relationship:



$$\text{Swell-Intake Ratio} = \frac{\pi r^2 H [\epsilon_v + \epsilon_h (1 + \epsilon_v)(2 + \epsilon_h)]}{\pi R_c^2 (\Delta a)} \quad (9)$$

Expressing  $\epsilon_v$  and  $\epsilon_h$  as percentages.

$$= \frac{\pi r^2 H}{100} \frac{[\epsilon_v + \epsilon_h (1 + 0.01\epsilon_v)(2 + 0.01\epsilon_h)]}{\pi R_c^2 (\Delta a)} \quad (10)$$

### Swelling Ratio

One of the main objectives of this investigation is to study the relationship between the measured swelling parallel and perpendicular to the direction of compaction. To accomplish this, a series of swelling tests were conducted using specimens cut vertically and horizontally out of the Proctor mold.

The swelling ratio, as defined in this study, is the ratio of the unit swelling parallel to the direction of compaction to the unit swelling in the perpendicular direction (Figure 42).

Stated symbolically,

$$\text{Swelling Ratio} = \frac{\epsilon_0}{\epsilon_{90}} \quad (11)$$

This expression represents the swelling ratio for the compacted soil block, as obtained in the Proctor mold during laboratory compaction.

However, when the test specimens are considered individually, the ratio of the unit vertical swelling ( $\epsilon_v$ ) to the unit horizontal or radial swelling ( $\epsilon_h$ ) has significance only with reference to their orientations. For example, ( $\epsilon_v/\epsilon_h$ ) ratio for a vertically-cut specimen (denoted as  $(\epsilon_v)_o/(\epsilon_h)_o$ ) will be different from the ( $\epsilon_v/\epsilon_h$ ) ratio of a

horizontally-cut specimen (denoted as  $(\epsilon_v)_{90}/(\epsilon_h)_{90}$ ).

Considering the orientations of test specimens with reference to the direction of compaction, one might anticipate that the ratios:

$$(\epsilon_v)_o/(\epsilon_h)_o, (\epsilon_h)_{90}/(\epsilon_v)_{90}, (\epsilon_v)_o/(\epsilon_v)_{90} \text{ and } (\epsilon_h)_{90}/(\epsilon_h)_o$$

computed from the swelling test data of specimens cut at right angles to each other, essentially represent the swelling ratio,  $(\epsilon_o/\epsilon_{90})$  of the compacted soil block (Figure 42).

This will not be generally true in view of the variations in the particle arrangement produced by the compactive effort used. This aspect is considered in detail in Chapter III.

APPENDIX B

EXPRESSIONS FOR THREE-DIMENSIONAL  
ANISOTROPIC SWELLING

## PROBLEM

To derive expressions for the swelling ratios in the case of three-dimensional anisotropic swelling of soil.

## DERIVATION

Consider a rectangular prism of soil whose dimensions in the direction of the three coordinate axes are respectively  $x$ ,  $y$ , and  $z$ . (Figure 60). Let  $\Delta x$ ,  $\Delta y$ , and  $\Delta z$  be respectively the amount of swelling along  $x$ ,  $y$ , and  $z$  axes.

Then the total volume increase,  $\Delta V$ , can be written as:

$$\Delta V = xyz [(1+\epsilon_x)(1+\epsilon_y)(1+\epsilon_z)-1] \quad (1)$$

where  $\epsilon_x$ ,  $\epsilon_y$ , and  $\epsilon_z$  are respectively the unit swelling along  $x$ ,  $y$ , and  $z$  axes.

The volumetric swelling,  $\eta$ , which is the ratio of the total volume increase to the initial volume, is given by:

$$\eta = \frac{\Delta V}{V} = (1+\epsilon_x)(1+\epsilon_y)(1+\epsilon_z)-1 \quad (2)$$

This expression will be useful to evaluate the value of  $\eta$ , provided  $\epsilon_x$ ,  $\epsilon_y$ , and  $\epsilon_z$  are known or directly measurable. Alternately, we can compute the unit swelling in any one direction, if the values of the unit swelling in the other two directions and the volumetric swelling are determined experimentally. However, as in the case of triaxial swelling test, if the unit swelling in one direction and the volume increase contributed by the swelling in the plane perpendicular to it are measured, then equation (1) requires modification as follows:

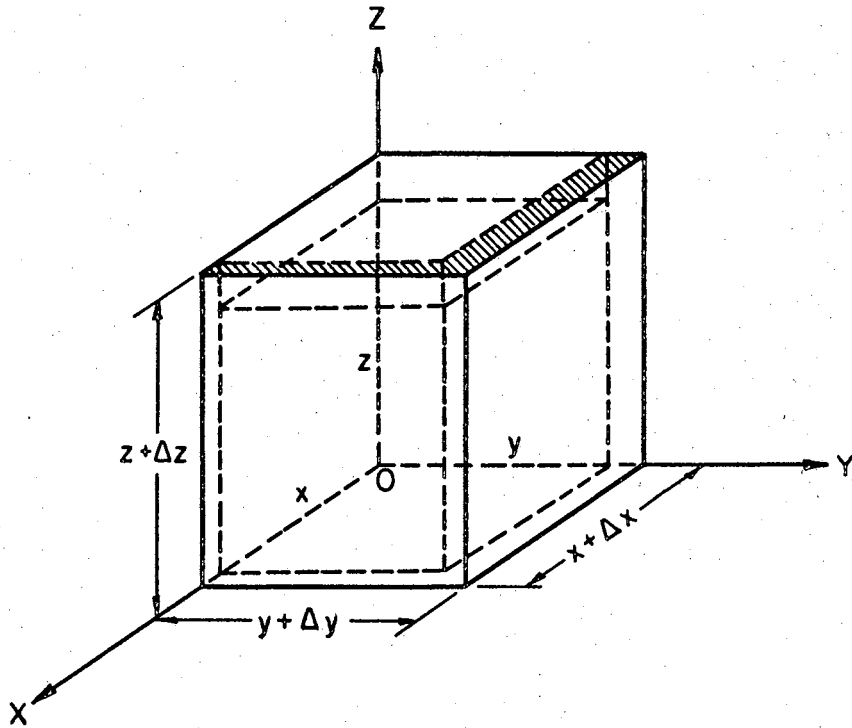


Figure 60. Schematic Representation of Three-Dimensional Anisotropic Swelling of Soil.

Considering the volume increase in the xy-plane only, we can write:

$$(\Delta V)_{xy} = xyz (1+\epsilon_x)(1+\epsilon_y)(1+\epsilon_z) - xyz(1+\epsilon_z)$$

or

$$(1+\epsilon_z)(\epsilon_x + \epsilon_y + \epsilon_x \epsilon_y) = \frac{(\Delta V)_{xy}}{xyz} = K_1 \quad (3)$$

where  $K_1$  can be considered as a constant.

By similar reasoning, considering the volume increases in the yz and zx-planes, we have:

$$(1+\epsilon_x)(\epsilon_y + \epsilon_z + \epsilon_y \epsilon_z) = \frac{(\Delta V)_{yz}}{xyz} = K_2 \quad (4)$$

and

$$(1+\epsilon_y)(\epsilon_z + \epsilon_x + \epsilon_z \epsilon_x) = \frac{(\Delta V)_{zx}}{xyz} = K_3 \quad (5)$$

Denoting  $\epsilon_x/\epsilon_z$  and  $\epsilon_y/\epsilon_z$  as  $\alpha$  and  $\beta$  respectively, equations (3) through (5) become:

$$(1+\epsilon_z)(\alpha\epsilon_z + \beta\epsilon_z + \alpha\beta\epsilon_z^2) = K_1$$

$$(1+\alpha\epsilon_z)(\beta\epsilon_z + \epsilon_z + \beta\epsilon_z^2) = K_2$$

$$(1+\beta\epsilon_z)(\epsilon_z + \alpha\epsilon_z + \alpha\epsilon_z^2) = K_3$$

Rearranging and solving for  $\alpha$  and  $\beta$ , we obtain:

$$\alpha = 1 + \frac{(K_1 - K_2)}{\epsilon_z} \quad (6)$$

$$\beta = 1 + \frac{(K_1 - K_3)}{\epsilon_z} \quad (7)$$

In the above expressions,  $K_1$ ,  $K_2$  and  $K_3$  are the apparent volumetric swelling corresponding to the swelling in the xy, yz, and zx-planes and they can be determined from the experimentally found values of volume increase and the initial volume of the soil specimen.

If three specimens are cut parallel to the three coordinate axes and are tested independently in the triaxial swelling apparatus, then, knowing the value of  $\epsilon_z$ , which is measured directly by dial gage, and the values of  $(\Delta V)_{xy}$ ,  $(\Delta V)_{yz}$  and  $(\Delta V)_{zx}$ , which are found by the displacement of water in the saran tube, one can, using the equations (6) and (7), evaluate the ratios  $\alpha$  and  $\beta$ . For cylindrical specimens:

$$\alpha = \frac{\epsilon_x}{\epsilon_z} = 1 + \frac{1}{\epsilon_z} \left[ \frac{C.(\Delta R)_{xy}}{\pi r_1^2 H_1} - \frac{C.(\Delta R)_{yz}}{\pi r_2^2 H_2} \right] \quad (8)$$

$$\beta = \frac{\epsilon_y}{\epsilon_z} = 1 + \frac{1}{\epsilon_z} \left[ \frac{C.(\Delta R)_{xy}}{\pi r_1^2 H_1} - \frac{C.(\Delta R)_{zx}}{\pi r_3^2 H_3} \right] \quad (9)$$

where

$C$  = Capacity of saran tube, per unit length,

$r_1, r_2, r_3$  = Radii of specimens,

$H_1, H_2, H_3$  = Heights of specimens, and

$(\Delta R)_{xy}, (\Delta R)_{yz}, (\Delta R)_{zx}$  = Displacements of air-water interface in the saran tube corresponding to the swelling in the xy, yz, and zx-planes.

As  $\epsilon_x$ ,  $\epsilon_y$ , and  $\epsilon_z$  are directly measured during the swelling tests, these can be compared with the values of the unit swelling obtained by equation (8) and (9) which involve the saran tube readings and thus, the accuracy of the testing procedure can be checked.

The swelling ratios, in the case of three-dimensional anisotropic swelling, are defined as:

$$S_{zx} = 1/\alpha \quad \text{and} \quad S_{zy} = 1/\beta$$

Therefore from equations (8) and (9), we can write:

$$S_{zx} = \frac{\epsilon_z}{\epsilon_x} = \frac{\epsilon_z}{\epsilon_z + (K_1 - K_2)} \quad (10)$$

$$S_{zy} = \frac{\epsilon_z}{\epsilon_y} = \frac{\epsilon_z}{\epsilon_z + (K_1 - K_3)} \quad (11)$$

where

$$K_1 = \frac{C \cdot (\Delta R)_{xy}}{\pi r_1^2 H_1}$$

$$K_2 = \frac{C \cdot (\Delta R)_{yz}}{\pi r_2^2 H_2} \quad , \text{ and}$$

$$K_3 = \frac{C \cdot (\Delta R)_{zx}}{\pi r_3^2 H_3}$$

### Corollary

1) If it is assumed that the unit swelling the xy-plane is the same in all directions and is equal to  $\epsilon_h$ , then for a cylindrical specimen of radius  $r$  and height  $H$ , we can, from equation (3), write:

$$(1 + \epsilon_z)(\epsilon_h + \epsilon_h + \epsilon_h^2) = \frac{(\Delta V)_{xy}}{xyz} = \frac{C \cdot \Delta R}{\pi r^2 H}$$

$$\epsilon_h^2 + 2 \epsilon_h - \frac{C \cdot \Delta R}{(\pi r^2 H)(1 + \epsilon_z)} = 0$$



Solving this quadratic equation for  $\epsilon_h$ , we have:

$$\epsilon_h = \sqrt{1 + \frac{C \cdot \Delta R}{(\pi r^2 H)(1 + \epsilon_z)}} - 1$$

This is the same accurate expression derived for the conditions assumed in the triaxial swelling test (Appendix A).

Also, neglecting the second order term of  $\epsilon_h$ , we get:

$$\epsilon_h = \frac{C \cdot \Delta R}{2\pi r^2 H(1 + \epsilon_z)}$$

where

$\epsilon_h$  = unit horizontal or radial swelling, and

$\epsilon_z$  = unit vertical swelling along z-axis

(equal to  $\epsilon_v$ ).

It may be noted that the above expression is exactly the same approximate relation given by Liu (1964) and Parcher and Liu (1965).

2. Also, if

$$K_1 > K_2, \epsilon_z / \epsilon_x < 1 \quad S_{zx} < 1$$

$$K_1 < K_2, \epsilon_z / \epsilon_x > 1 \quad S_{zx} > 1$$

$$K_1 = K_2, \epsilon_z / \epsilon_x = 1 \quad S_{zx} = 1$$

The same results follow for  $S_{zy}$  also.

3. If  $K_1 = K_2 = K_3$ , then it follows  $\epsilon_x = \epsilon_y = \epsilon_z$  and this corresponds to the perfectly isotropic case. Therefore  $S_{zx} = S_{zy} = 1$ .

VITA

2

Venkatraman Srinivasan

Candidate for the Degree of

Doctor of Philosophy

Thesis: ANISOTROPIC SWELLING CHARACTERISTICS OF COMPACTED CLAY

Major Field: Engineering

Biographical:

Personal Data: Born in Portonovo, Madras, India, December 16, 1933, the son of Venkatraman and Rajalakshmi.

Education: Graduated from Board High School, Portonovo, Madras, India, in 1949; received the Bachelor of Engineering degree from the Annamalai University, Madras, India, with a major in Civil Engineering, in October, 1955; received the Master of Science degree from the University of Madras, Madras, India, with a major in Civil Engineering, in September, 1962; completed requirements for the Doctor of Philosophy degree at Oklahoma State University, Stillwater, Oklahoma, in July, 1970.

Professional Experience: Junior Engineer, Highways Department, Madras, India, 1955-1958 and 1961-1964; Assistant Lecturer, College of Engineering, Madras, India, 1958-1960; Junior Town Planner, Town Planning Directorate, Madras, India, 1964-1965; Assistant Engineer (Soil Research), Highways Research Station, Madras, India, 1965-1966; Graduate Teaching Assistant, School of Civil Engineering, Oklahoma State University, Stillwater, Oklahoma, 1967-1970; Engineer, McClelland Engineers, Inc., Houston, Texas, Summer, 1968.

Professional Societies: Associate Member, American Society of Civil Engineers; Associate Member, The Society of Sigma Xi.